OAK RIDGE NATIONAL LABORATORY

operated by

UNION CARBIDE CORPORATION

for the

U. S. ATOMIC ENERGY COMMISSION

ORNL-RSIC-36

SHIELDING AGAINST INITIAL RADIATIONS from NUCLEAR WEAPONS

Lorraine S. Abbott

RADIATION SHIELDING INFORMATION CENTER

ORNL-RSIC-36

Contract No. W-7405-eng. 26

Neutron Physics Division

SHIELDING AGAINST INITIAL RADIATIONS FROM NUCLEAR WEAPONS
(A State-of-the-Art Report on Shield Design Techniques)

Lorraine S. Abbott

This work supported by
U. S. CORPS OF ENGINEERS, OMAHA DISTRICT,
Omaha, Nebraska,
and
DEFENSE NUCLEAR AGENCY
under Subtask PB-052

JULY 1973

OAK RIDGE NATIONAL LABORATORY
Oak Ridge, Tennessee 37830
operated by
UNION CARBIDE CORPORATION
U.S. ATOMIC ENERGY COMMISSION

PREFACE

In the Fall of 1971, representatives from the Omaha District of the U. S. Corps of Engineers, Omaha, Nebraska, contracted with Oak Ridge National Laboratory for a chapter on the state of the art of nuclear weapons initial radiation shielding which was to be included in a larger publication. The proposed publication, tentatively titled as "State-of-the-Art Evaluation of the Vulnerability and Hardness Analysis for Ballistic Missile Defense Facilities," was being sponsored by the Office of the Chief of Engineers and administered by the U. S. Army Engineer Waterways Experiment Station of the U. S. Corps of Engineers at Vicksburg, Mississippi. Because the publication was to be directed to non-nuclear engineers, it was requested that the shielding chapter include an introduction to the subject and that no undefined nuclear terminology be employed.

In preparing the chapter, the writer relied on the technical reviews of several individuals acquainted with the field, and several major changes were introduced before the final chapter, published here as RSIC-36, was completed. In particular, a few sample problems requested by and supported by the Defense Nuclear Agency were included, and it is under the auspices of DNA, with the permission of the Corps of Engineers, that this separate publication is made. Although the primary purpose of the chapter is to assist engineers first becoming acquainted with the field of weapons radiation shielding, the chapter also represents a summary of most of the work published on the subject prior to November, 1972, and for this reason DNA proposed that it also be made available to long-time participants in the field through a general RSIC distribution.

The reader is forewarned that the cutoff date given in the preceding paragraph is important. A recent emphasis on "sensitivity" studies is mentioned here only briefly, and the potential impact of such studies is becoming increasingly apparent. They are designed to reveal the sensitivity of the quantity being calculated, such as dose, to variations in the cross sections used in the calculation. The cross sections found to have the most influence will then be studied in greater detail than those found to be less important, and the uncertainties associated with the calculated quantities will be reduced more rapidly. Related studies to optimize the calculational techniques employed for certain classes of problems will also reduce the errors on the calculated quantities. The promising success of this approach indicates that a state-of-the-art report on weapons radiation shielding a few years hence will reflect a noticeably improved situation for the shield designer.

May 1973

ACKNOWLEDGEMENTS

The author of this chapter, a technical writer and editor in the Neutron Physics Division of Oak Ridge National Laboratory, wishes to acknowledge that it was primarily through her work as an editor of the Defense Nuclear Agency's *Weapons Radiation Shielding Handbook* that she has gained an overview of this subject. In particular she has profited from numerous discussions with another Handbook editor, H. Clyde Claiborne of ORNL, and from study of the material provided by several of the Handbook authors, especially P. N. Stevens of the University of Tennessee and L. G. Mooney, M. B. Wells, and W. E. Selph of Radiation Research Associates, Inc. She has also received invaluable guidance from Charles E. Clifford, who for many years has directed ORNL's experimental and theoretical weapons radiation shielding research program, including calculations subcontracted to RRA to generate data for the Handbook.

With respect to this final document, the author expresses especial gratitude to D. K. Trubey of the ORNL Radiation Shielding Information Center, to Captain Dean Kaul of the Defense Nuclear Agency, and to E. A. Straker of Science Applications, Inc., for their technical reviews of the entire manuscript during various stages of its writing. If this document accomplishes its purpose of acquainting non-nuclear engineers with radiation shielding design, then these three individuals should be given much of the credit. On the other hand they should not be held responsible for misinterpretations, some of which could have been introduced after their reviews were completed.

Several other persons have been generous with their time. J. K. Dickens of ORNL reviewed Sections 1.0 - 5.0; L. G. Mooney of RRA reviewed Sections 9.0 - 10.0; and F. G. Perey and R. W. Roussin of ORNL reviewed Section 11.0. V. R. Cain, F. R. Mynatt, J. V. Pace, D. E. Bartine, and W. W. Engle, all of ORNL, willingly provided information and advice in various areas, and Virginia Glidewell, also of ORNL, improved the readability of the manuscript by uncovering many inconsistencies and errors as she typed the numerous drafts.

Finally, the support of Carl J. Distefano, John Smart, and Ronald G. Dodson of the U. S. Corps of Engineers, Omaha District, is acknowledged and greatly appreciated.

TABLE OF CONTFNTS

BLANK PAGE

ABSTRACT

Neutrons and gamma rays released by in-air detonations of nuclear weapons undergo various types of interactions with the surrounding environment, some of which result in additional radiations being born at points far removed from the original burst location. In the absence of adequate weapons test data, designers of shields to attenuate the initial radiations (those born within the first minute) must rely on information gained from "transport" calculations performed on large electronic computers. In such calculations the detonation and surrounding materials, including the proposed shielded structure, are mocked up as accurately as is possible and practicable, and the intensities of the radiations reaching specified locations within the structures are computed. Such calculations are extremely difficult and very time-consuming, and much of the shielding research effort during the past decade has been devoted to the development of adequate transport methods and of the necessary input data that describe neutron and gamma-ray interactions in the pertinent materials. A major result has been the successful application of the discrete ordinates and Monte Carlo transport methods to a limited number of weapons radiation shielding problems. This report, which includes an elementary description of weapons radiations and their interactions, summarizes these problems and points out both their uses and their limitations.

1.0 INTRODUCTION

It is well known that the energy released in a nuclear weapons detonation is due either to the fission process or to the fusion process. In the fission process the nucleus of a uranium or plutonium atom is split into two or more parts, while in the fusion process the nuclei of two hydrogen atoms are fused together. Accompanying both these reactions, as well as subsequent reactions that occur during a detonation, is the emission of several types of nuclear radiations that are biologically harmful and also capable of interfering with the operation of critical equipment. Many of the radiations are immediately absorbed in the surrounding environment, however, and only two types have a high probability of reaching personnel or equipment sufficiently protected to survive a nuclear blast. These are the subatomic particles known as neutrons and the electromagnetic radiations known as gamma rays.

A radiation shield designer views a nuclear detonation as the sudden release of neutrons and gamma rays within a volume that expands rapidly and eventually encompasses the region he is interested in protecting. Insofar as possible, he must predict the number of neutrons and gamma rays produced within that volume, their points of birth, their times of birth, the energies with which they are born, and the paths they follow. The results of such predictions are then used to determine what shielding is necessary to keep radiation exposures at given locations within tolerable limits.

The discussion that follows is intended to be a guide to engineers who without a background of nuclear physics must consider the effects of nuclear weapons radiations on the integrity and usefulness of various types of structures. It begins with an elementary description of the physical characteristics of neutrons and gamma rays and their possible interactions with matter. It continues with a brief summary of the methods most frequently used to calculate the penetration of neutrons and gamma rays through the atmosphere and into shielded structures. Finally, it gives some examples of how these methods have been applied to particular structures that are assumed to be in the vicinity of low-altitude bursts.

BLANK PAGE

Unfortunately, the examples presented here do not reflect the application of a comprehensive engineering shield design method. No method of general applicability is yet available, and it is not clear that one will be forthcoming in the near future. However, calculations performed to date have given considerable insight into the overall problem of the interaction of radiations with the atmosphere and ground, as well as with structural materials. In some cases a sufficient number of calculations have been carried out to provide parametric data for certain types of structures exposed to specific in-air detonations, and the engineer will find these data helpful in making rough estimates of the amount of radiation that will penetrate into similar structures under similar conditions. However, when the design of a structure has progressed to the point that specifications for the radiation shield must be fixed, then in all probability a full-scale calculation should be performed by persons experienced in using the techniques. Hopefully the following discussion will acquaint the structure designer with the many factors that must be considered in radiation shield design and will aid him in determining the best approach to his particular problem.

2.0 WEAPONS RADIATIONS

It is stated in the introduction that of the several types of radiations produced by a nuclear weapons detonation, only neutrons and gamma rays present a radiation shielding problem. The nature of these radiations and their origins are described in this section. For reference, a summary listing of the various radiation components contributing to the total neutron and gamma-ray environments is provided in Table 1, and their corresponding energies are given in Table 2.

2.1. Neutrons

Neutrons are electrically neutral subatomic particles having a rest mass of 1.008665 atomic mass units (amu), where 1 amu = 1.66043×10^{-24} gram.[a] Neutrons in combination with positively charged protons of slightly smaller mass form the nuclei of atoms around which negatively charged electrons orbit. A proton has a mass of 1.00727 amu, and an electron a mass of 1.00727/1847 amu. The nuclei of all the isotopes of a given element contain the same number of protons, which is called the atomic number of the element. The isotopes differ from one another by the number of neutrons contained in their nuclei, the combined number of neutrons and protons being the mass number of the isotope. For example, each uranium isotope has 92 protons in its nucleus, but the particular uranium isotope having an atomic mass of 235 has only 143 neutrons, whereas the uranium isotope having an atomic mass of 238 has 146 neutrons.[b]

When a nucleus is split by the fission process, two or more neutrons in the original nucleus are promptly freed. Similarly, when two nuclei are fused together in the most common fusion reactions, one or two neutrons from the original nuclei are not required by the new nucleus. Outside a

---

[a] The 1.66×10^{-24} gram for 1 amu is based on 1/12th the mass of a neutral atom of the most abundant isotope of carbon (C^{12}).

[b] It follows that isotopes of different elements may have the same mass numbers (for example, uranium 239 and plutonium 239).

Table 1. Components of Radiation Released in Nuclear Weapons Bursts

Radiation Component	Time Emitted After Initiation of Explosion*
Prompt fission and fusion neutrons	<~0.75 μsec
Delayed fission neutrons	<1 min
Fission gamma rays	<~0.75 μsec
Inelastic-scattering gamma rays	
From weapon	<~1 μsec
From air	<~10 μsec
From ground	<~10 μsec
From structure	<~10 μsec
Gamma rays from charged-particle reactions	
From weapon	<~1 μsec
From air	<~10 μsec
From ground	<~10 μsec
From structure	<~10 μsec
Capture gamma rays	
From weapon	<~1 μsec
From air	Few msec to 0.2 sec
From ground	Few msec to 0.2 sec
From structure	Few msec to 0.2 sec
Fission-product gamma rays	
Early-time	~0.2 sec to 1 min
Residual	1 min to many years
Activation gamma rays	
Early-time	~0.2 sec to 1 min
Residual	1 min to many years

*1 μsec = one-millionth of a second = 10^{-6} sec; 1 msec = one-thousandth of a second = 10^{-3} sec.

Table 2. Approximate Energies of Radiation Components Released in Nuclear Weapons Bursts

Radiation Component	Energy Range[a]	Most Probable Energy[a]
Fusion neutrons	~14 MeV	~14 MeV
Prompt fission neutrons	0–18 MeV	1 MeV
Delayed fission neutrons	0--~0.6 MeV	<0.5 MeV
Fission gamma rays	0.02–10.5 MeV	7 MeV (avg. total)[b]
Inelastic-scattering gamma rays		
From nitrogen	0.7–7 MeV	1.622, 2.312, 5.105 MeV
From oxygen	2–7 MeV	6.13, 6.92, 7.12 MeV
From elements in ground and structure[c]	0–8 MeV	1–4 MeV
Gamma rays from charged-particle reactions		
From nitrogen	0–7 MeV	
From oxygen	~3.5 MeV	~3.5 MeV
From elements in ground and structure	<2 MeV	<2 MeV
Capture gamma rays		
From nitrogen	1.5–11 MeV	4–7.5 MeV, 10.83 MeV
From oxygen	*b*	*d*
From elements in ground and structure	0–>9 MeV	
Fission-product gamma rays	0–6 MeV	<2.5 MeV 0.7 MeV (avg.)
Activation gamma rays	0–2 MeV	~1.25 MeV

[a]MeV = million electron volts, where 1 eV is the energy gained by a particle of unit electric charge when accelerated by an electrostatic potential of 1 volt; 1 eV = 1.6020×10^{-12} erg.

[b]Average total energy of all gamma rays emitted per fission.

[c]Based on fission neutron interactions; fusion neutrons may produce higher energy gamma rays.

[d]Negligible contribution.

nucleus, a neutron has a half-life[c] of only about 13 min, disintegrating into a proton, an electron, and a neutrino.[d] The proton and electron, because of their positive and negative charges respectively, are stopped by the electrical fields associated with atoms. The neutrino, possessing no charge, is highly penetrating but so unlikely to interact with any material that it can be disregarded. Thus neutrons emitted from a weapon create a shielding problem only so long as they remain neutrons. This is small comfort, however, since 13 min is many orders of magnitude longer than the time required for a neutron to travel the distances with which shield designers are concerned.

The speed of a neutron is proportional to the square root of its energy.[e] Neutrons emitted in the fission process have a spectrum of energies that extend to as high as approximately 10 MeV; however, less than 0.1% have energies greater than 10 MeV and the most probable energy is just under 1 MeV. The neutron speed averaged over the fission spectrum is about 1.4×10^9 cm/sec (8500 miles/sec). Neutrons emitted in the most common fusion process have an approximately uniform energy of 14 MeV, with an average speed of 5×10^9 cm/sec, which is considerably faster than that of the fission neutrons. At these speeds neutrons that pass unimpeded between the nuclei of the air or some other medium will reach locations on the order of a mile from the center of the detonation within an infinitesimal fraction of a second. Even most of those neutrons that follow a random path by repeatedly bouncing against nuclei can travel a mile in extremely short times. As a result, neutrons produced by a nuclear weapon are not in evidence within the vicinity of the burst at times greater than a second, and actually do not cause damage *directly* for times greater than a few milliseconds. The number of neutrons that appear within those few milliseconds is extremely large, however, and

---

[c] The additional time required for one-half of the neutrons at any given time to disintegrate (or decay).

[d] A neutrino has a mass one-thousandth of that of an electron; that is, it has a mass of (1.00727/1847)/1000 amu.

[e] This proportionality does not hold if the velocity of the neutron approaches the velocity of light.

as we shall see later they have an indirect effect that extends over longer periods.

A general idea of the number of neutrons produced by an in-air detonation can be obtained by considering a 1-kiloton weapon that utilizes the fission process alone. (The Hiroshima and Nagasaki weapons were nominally 20-kiloton fission weapons.) As pointed out above, with each fission two or more "prompt" neutrons are freed. In order to maintain the chain reaction, an average of at least one of the neutrons must itself induce a fission in the next generation of fissions, the "left-over" neutrons being either absorbed in the weapon materials or emitted into the atmosphere. In a 1-kiloton fission weapon, about 15×10^{22} fissions occur in roughly 55 generations over a period totalling 0.25 to 0.75 μsec.[f,1,2] But over 99% of the fissions occur during the last five generations, the largest fraction in the last generation. Since with the last generation the chain reaction ceases, all the neutrons from this generation are either absorbed in the weapon materials or emitted into the atmosphere. If it is assumed that one-half of the total number of fissions occur in the last generation and that an average of one neutron per fission escapes the weapon (which may or may not be good assumptions), then the last generation of a 1-kiloton weapon would eject about 7.5×10^{22} neutrons into the atmosphere.[g] Simple extrapolation indicates how higher yield weapons would produce numbers of neutrons that are many orders of magnitude higher.

Kukhtevich et al.[3] estimate that a 1-kiloton uranium bomb "liberates" approximately 2.3×10^{23} neutrons and a 1-kiloton plutonium bomb liberates 3×10^{23} neutrons. These numbers are based on the simple expression $N(\nu - 1)$, where N is the number of fissions per kiloton (that is, 15×10^{22}) and ν is the number of neutrons produced per fission for the particular

---

[f] Detonation times are sometimes given in terms of "shakes," a shake being equivalent to 10^{-8} sec.

[g] Some authors have reported a much higher percentage of neutron absorption in the weapon materials.

isotope used. For ^{235}U and ^{233}U, $\nu = \sim 2.5$ and for ^{239}Pu, $\nu = \sim 3$. The "-1" in the expression accounts for the maintenance of the fission chain. In their use of the word "liberate" they make no allowances for the attenuation of neutrons by the weapons materials.

Another source of neutrons from a fission weapon which should be mentioned is the source due to delayed neutrons. These are fission neutrons that may be emitted for as much as a minute following the initiation of the explosion. Since they comprise less than 1% of the total number of neutrons and have mean energies of less than 0.5 MeV, they usually are not considered in a weapons radiation shielding calculation. On the other hand, their relative contribution could be larger than might first be guessed since they are emitted after the weapon has disintegrated and consequently will undergo essentially no attenuation in the weapon materials.

2.2. Gamma Rays

Gamma rays are electromagnetic radiations (energy waves) and therefore have no mass. Unlike neutrons, which travel at various speeds, gamma rays travel at the constant speed of light, as do other forms of electromagnetic radiations (X rays, visible light, radio waves, etc.). The speed of light is 3×10^{10} cm/sec (186,000 miles/sec), which is approximately 23 times faster than the average speed of fission neutrons.

In nuclear physics, two different theories have been offered to describe electromagnetic radiations. According to classical theory, they consist of a continuous flow of energy, but this description is inadequate for explaining many nuclear phenomena. Another more satisfactory theory, called quantum theory, describes electromagnetic radiations as discrete bundles of energy of size $h\nu$, where h (Planck's constant) is equal to 6.624×10^{-27} erg/sec and ν is the wave frequency. Each bundle is referred to as a photon. Those photons that are gamma rays have the greatest wave frequencies, on the order of 10^{17} to 10^{21} per second, and the shortest wave lengths, 10^{-6} to 10^{-11} cm, which correspond to energies from about

1 keV (thousand electron volts) to 12 MeV. It is the energy of a gamma ray that determines how it interacts with nuclei or atoms. (Gamma rays and X rays have an overlapping energy region in which they are indistinguishable. They differ primarily with respect to their origins, gamma rays arising largely from nuclear processes and X rays from electronic processes.)

Gamma rays produced by a nuclear weapon arise from a number of reactions, some of which continue at times long after the original detonation and at points considerably removed from the original detonation. This is in contrast to the birth of neutrons, which, being due entirely to the fission and fusion processes,[h] are emitted within the confines of the weapon (or weapon debris, in the case of delayed neutrons).

2.2.1. Fission Gamma Rays

In a nuclear weapon that utilizes fission -- as all do to some extent -- the first group of gamma rays emitted are those released by the fissioning nuclei. The numbers and energies of the fission gamma rays produced by the different fissionable isotopes of uranium and plutonium are not well established, but at least two sets of experiments[4,5] have indicated that the energy spectra of gamma rays for all the isotopes are very similar and are independent of the energy of the neutron causing the fission. Experiments[6,7] which determined the spectrum of gamma rays produced by the fission of ^{235}U by thermal (low-energy) neutrons have shown that an average of about eight gamma rays are emitted per fission and that their combined energies average about 7 MeV. Their individual energies range from approximately 0.01 to 10 MeV.

Fission gamma rays, like fission neutrons, are emitted within the confines of the weapon before it disintegrates (within less than a microsecond). If the simple formula applied above to estimate the production

---

[h] This is not strictly true since some neutrons are produced by subsequent reactions; their relative number is so small, however, that for all practical purposes they can be ignored.

of neutrons from a 1-kiloton weapon were used to estimate the production of fission gamma rays, then the 7.5×10^{22} fissions occurring in the last generation would produce a total of 6×10^{23} fission gamma rays having a spectrum of energies between about 0.01 and 10 MeV. Most of the important gamma rays are in the energy region from 1 to 4.5 MeV.

What fraction of the fission gamma rays escape into the atmosphere depends entirely on the weapon design. It is known that a large number of fission gamma rays are attenuated by the weapon materials, and it will be apparent in other sections of this chapter that this attenuation plus the prominence of gamma rays arising from several other sources tend to minimize the importance of the fission gamma rays. Kukhtevich et al.[3] flatly state that "the contribution of fission gamma radiation during a nuclear explosion can be ignored," citing an example in which the fission gamma rays were attenuated by a factor of 1000 in the weapon materials.

Fission gamma rays should not be completely discounted, however. Attenuating the 6×10^{23} fission gamma rays by a factor of 1000 would still mean that 6×10^{20} gamma rays are emitted into the atmosphere. While this may be a small number compared with the total number of gamma rays produced by the various sources, these gamma rays are all emitted in an extremely short time interval and for some situations may contribute the highest pulse of radiation produced by the weapon. This would be important when damage to sensitive components of electronic systems is being considered.

2.2.2. Inelastic-Scattering Gamma Rays

The second group of gamma rays produced by a weapon consists of "inelastic-scattering" gamma rays. The term "inelastic-scattering" refers to a type of nonfission neutron-nucleus interaction that is accompanied by the instantaneous release of gamma rays (see Section 4.2.2). Inelastic scatterings can occur with most nuclei, including those comprising both the fueled and nonfueled components of the weapon itself. Because neutrons

that become involved in inelastic scatterings are high-energy neutrons, a fission or fusion neutron undergoing an inelastic scattering has spent little if any time in travel or in prior interactions. As a result, inelastic-scattering gamma rays are produced within the weapon during the same time interval as the neutrons (within less than a microsecond). The number and energies of the gamma rays so produced are dependent on the weapon design, and to a large extent on the fission/fusion ratio of the weapon. The higher the fusion fraction, with the concomitant increase in the number of high-energy neutrons produced in the weapon, the greater the probability that inelastic-scattering gamma rays will be produced within the weapon.

Inelastic-scattering gamma rays are also produced within the atmosphere, in the ground, and in structural materials. Because of the speeds of the neutrons undergoing such interactions, they will have occurred within approximately 10^{-5} sec following the initiation of the detonation. Thus within an extremely short time interval, inelastic-scattering gamma rays are born throughout a large volume surrounding the detonation point. Traveling at the speed of light, some of these gamma rays, particularly those produced in or near the weapon, create high pulses of radiation that can overlap with the pulse produced by the fission gamma rays. For predominantly fission weapons, inelastic-scattering gamma rays, like fission gamma rays, may not be important to the total accumulated effect. For fusion weapons, however, they may be the major gamma-ray component of the accumulated effect.

Much current research is directed toward determining the numbers and energies of gamma rays produced when neutrons scatter inelastically with the nuclei of various isotopes. Orphan and Hoot[8] and Dickens and Perey,[9,10] among others, have made measurements of the gamma rays produced in nitrogen and oxygen by inelastic scattering and have observed discrete gamma rays with energies from about 0.7 to 7 MeV for nitrogen and from about 2 to 7 MeV for oxygen. In general, the experiments of Orphan and Hoot cover neutron energies from about 5 to 16 MeV and those of Dickens and Perey cover neutron energies from 5 to 11 MeV. Three strong inelastic-

scattering gamma rays are well established for both elements, those for nitrogen having energies of 1.622, 2.312, and 5.105 MeV and those for oxygen having energies of 6.13, 6.92, and 7.12 MeV. The nitrogen production is, of course, the most important because of the greater abundance of nitrogen in the atmosphere.

Dickens has made similar measurements of gamma-ray production for four elements that can be found in the ground and/or structural materials: Si, Al, Fe, and Na.[11-14] Again high-energy inelastic-scattering gamma rays are detectable up to 7 or 8 MeV, but they are not produced in as great a number as in oxygen and nitrogen.

A series of experiments described by Maerker and Muckenthaler[15] indicate that of the secondary gamma rays produced in 13 different materials[i] by the interaction of fission neutrons with energies above 1 MeV, more than 94% of the total yield corresponds to gamma rays having energies between 1 and 4 MeV. For materials with mass numbers greater than about 45, the percentage is about 97%. In nearly all the materials, however, gamma rays with energies up to 6 or 7 MeV were detected. (It should be kept in mind when considering these data that the mean energy of the neutrons producing these gamma rays is considerably lower than the 14-MeV neutrons produced in the fusion reaction.)

2.2.3. Gamma Rays Produced by Charged-Particle Reactions

Another possible source of gamma rays that can be attributed to the interaction of high-energy neutrons with nuclei is charged-particle reactions. In these reactions a neutron enters the nucleus and a charged particle, such as a proton or an alpha particle,[j] emerges. In some cases the charged particle is accompanied by a gamma ray. If such

[i] Na, Al, Si, S, K, Ca, Ti, Fe, stainless steel, Ni, Cu, Zn, and Ba.

[j] An alpha particle consists of two protons and two neutrons (the same as a helium nucleus).

a reaction occurs within the weapon, then the resulting gamma rays, like the inelastic-scattering gamma rays, are emitted during the same time interval as the fission gamma rays (that is, within a microsecond). Similarly, charged-particle reactions may produce gamma rays within the atmosphere and in ground and structural materials, in which case they join the inelastic-scattering gamma rays in broadening a high pulse of radiation within approximately 10^{-5} sec following the initiation of the detonation.

Charged-particle ($n,p\gamma$ and $n,\alpha\gamma$) reactions can produce gamma rays in nitrogen[9] with energies up to 7 MeV and in oxygen[10] with energies of $\sim$ 3.5 MeV. However, the neutron energies required for the reactions are about 6 MeV for nitrogen and 8 MeV for oxygen, which are considerably higher than those required for inelastic scatterings. Because of this, gamma rays produced by charged-particle reactions in the atmosphere are not considered too important. Obviously their importance increases as the fusion fraction increases.

Gamma rays produced by charged-particle reactions in the ground and structural materials are even less important. In aluminum[12] and silicon,[11] for example, the resulting gamma rays have energies less than 2 MeV, the reaction again requiring neutron energies on the order of 6 MeV.

2.2.4. Capture Gamma Rays

Following the production of the fission and inelastic-scattering gamma rays, together with those from the charged-particle reactions, another source of gamma rays begins to play a prominent role. This source is also produced by a type of nonfission neutron-nucleus interaction which results in the capture of the neutron by the nucleus and the simultaneous emission of one or more gamma rays that are not in this case accompanied by the emission of a particle. These gamma rays are commonly referred to as radiative-capture of simply capture gamma rays.

The neutrons most likely to be captured are low-energy neutrons that travel at much slower speeds than the high-energy neutrons producing inelastic-scattering gamma rays. Thus on the average, capture reactions occur at later times than inelastic-scattering reactions, and the resulting gamma rays appear in later time intervals. They also appear over a longer time, since many neutrons that originate at high energies slow down through a period of time by repeated scatterings until they are ultimately captured.

Many different types of nuclei can give birth to capture gamma rays; therefore, capture gamma rays, like inelastic-scattering gamma rays, can be born throughout a large volume surrounding the detonation point. In general, capture gamma rays are responsible for most of the radiation present during the period from a few milliseconds following the detonation until about 0.2 sec after the detonation, and in some cases can be very important to the total accumulated effect of a weapon detonation. In fact, in some radiation transport calculations of the "free-field" radiation doses produced by predominantly fission weapons, gamma rays produced by neutron capture in the nitrogen of the atmosphere have been the only gamma rays considered other than fission-product gamma rays (see Section 9.3).

Investigations of the production of capture gamma rays in various materials have been underway for many years, with most of the effort centered on the lowest energy neutrons, called "thermal" neutrons because they are in thermal equilibrium with the atoms (or molecules) of the medium in which they are present. The most probable energy of thermal neutrons in room-temperature media is 0.025 eV. Particular attention has been given to the production of gamma rays by the capture of thermal neutrons in nitrogen. These gamma rays range in energy from about 1.5 MeV to about 11 MeV, with those between 4 and 7.5 MeV, together with a 10.83-MeV gamma ray, being the most promiment. The production of gamma rays by the capture of thermal neutrons in oxygen is insignificant and can be ignored.

A second series of experiments described by Maerker and Muckenthaler[16] shows that in some cases the gamma rays produced by the capture of low-

energy neutrons in 14 different materials[k] that might be included in ground or structural materials have energies exceeding 9 MeV (see Table 3). This becomes particularly important if the material producing the gamma ray has been used in a structure. Iron, nickel, and copper, for example, have high probabilities of producing gamma rays with energies above 7 MeV.

It has generally been assumed that for a given material the capture of neutrons having energies higher than thermal energy would produce approximately the same spectrum of gamma rays as would be produced by thermal neutrons, but in recent years it has been shown that this is not always a good assumption. Following studies by Yost and Solomito,[17] plus others, it is conceded that capture gamma-ray production data should be established as a function of neutron energy but for all practical purposes this has not yet been accomplished. For the case of highly optimized reactor shields it is essential that research yielding these data be pursued, but insofar as weapons radiation shielding is concerned, contributions by capture gamma rays produced by neutrons with energies higher than thermal energy may not be important.

2.2.5. Fission-Product Gamma Rays

A fifth source of gamma rays produced by weapons detonations is from the fission products -- the smaller isotopes formed when a heavy fissionable isotope is split into two or more parts. While some of these isotopes are stable, most are radioactive, and as they decay to stable isotopes, they emit beta rays (electrons) that are usually accompanied by gamma rays. The beta rays are stopped very close to their origin, but the gamma rays have the same penetrating characteristics as those produced by other sources.

The spatial distribution of fission-product gamma rays differs from those of the other gamma-ray sources. While fission gamma rays are given

[k] The 13 listed in footnote *i* plus Cl.

Table 3. Gamma Rays Produced by the Capture of Thermal Neutrons in Various Materials[a]

Gamma-Ray Energy (MeV)	Number of Photons Produced per 100 Thermal-Neutron Captures													
	Na (23)[b]	Al (27)	Si (28)	S (32)	Cl (35)	K (39)	Ca (40)	Ti (48)	Fe (56)	SS[c]	Ni (58)	Cu (63)	Zn (68)	Ba (138)
1–1.5[d]	14.8	18.6	15.3	1.7	45.2	35.0	20.9	83.8	5.0	14.5	6.3	17.8	52.1	63.4
1.5–2.0	11.9	10.4[e]	0	3.1	45.4	25.6	79.6	25.7	15.0	9.7	2.2	12.3	30.5	34.6
2.0–2.5	26.9	13.1	23.0	43.9	14.3	37.2	41.5	3.6	3.9	6.1	2.2	7.2	25.4	34.3
2.5–3.0	47.6	20.5	4.6	22.8	19.3	23.5	14.3	5.0	6.0	4.4	3.1	8.6	18.2	24.3
3.0–3.5	14.2	15.9	5.4	29.4	12.3	16.7	7.9	6.2	9.2	7.4	2.0	8.7	22.8	17.6
3.5–4.0	34.0	14.3	76.6	3.0	9.1	23.2	13.5	4.6	3.5	3.7	1.6	7.8	13.8	16.0
4.0–4.5	6.4	16.1	0.8	7.0	6.5	20.2	19.4	0.7	7.2	5.8	1.1	10.4	14.4	28.1
4.5–5.0	2.65	17.6	70.3	15.3	9.0	7.7	6.6	9.5	3.3	3.2	1.3	4.2	13.9	12.6
5.0–5.5	2.2	6.8	6.4	61.9	3.4	16.2	2.5	0.4	1.0	3.5	3.4	8.7	12.4	7.6
5.5–6.0	5.9	2.8	0.2	3.9	11.7	17.3	12.1	1.0	9.9	9.4	4.3	1.8	10.4	9.5
6.0–6.5	21.5	6.0	12.2	0.4	26.2	0.95	40.0	33.1	10.1	7.5	4.2	4.9	7.4	4.0
6.5–7.0		2.2	0.8	1.0	18.3	2.15		56.0	0.5	4.1	11.2	10.3	13.1	1.0
7.0–7.5		0.7	9.7	1.0	12.4	0.45		0.9	5.5	8.5	2.9	13.5	5.4	{2.0}
7.5–8.0		32.4	0	3.5	10.0	5.65		0.18	50.6	33.6	10.4	42.8	14.1	
8.0–8.5			2.2	0.5	0			0.32	{0.8}	3.6	7.6		1.0	0.3
8.5–9.0				2.0	3.2			0		12.2	{48.0}		0.1	0.4
≥9.0								0.21	3.3	3.7			1.2	0.4
% BE[f]	89	95	104	94	108	96	100	106	95	96	92	101	105	91

[a]From Maerker and Muckenthaler, ref. 16.
[b]Mass number of most plentiful isotope in parentheses.
[c]Type 304 stainless steel.
[d]The lower limit of this energy interval varies slightly for the different materials.
[e]Does not include the 1.78-MeV gamma rays in Si^{28} following a β-decay of Al^{28}.
[f]Percent of binding energy of the naturally occurring isotope in the sample that is accounted for by the measured spectrum down to zero energy; contributions from photons with energies below approximately 1 MeV not included.

off almost instantaneously from what might be considered a "point" in space, and inelastic-scattering and capture gamma rays are produced over more or less fixed volumes during relatively short time intervals, fission-product gamma rays are emitted over long periods of times (some for years) and they are produced within a volume that is constantly changing in size and shape.

The fission products are usually assumed to be distributed evenly in the weapon debris; however, the validity of this assumption has not been established. For low-altitude detonations the debris (fireball) is approximately spherical immediately following the burst and then undergoes a transition to a toroidal shape (see Section 9.4). At early times the fission-product gamma rays are emitted directly from the cloud of weapon debris as it begins to rise. Later the fission products themselves

begin to fall toward the ground. In the absence of wind, the radioactive debris would be expected to settle in a circular pattern around ground zero. In the presence of a constant wind, the settling patterns would be elliptical in the downwind direction.

Since the fission-product gamma rays are emitted after the weapon has broken apart, they are not significantly attenuated in the weapons material, and those originating in the outer edges of the debris cloud can escape into the atmosphere without passing through any weapons materials. Also at the time some of these gamma rays are being emitted, the shock wave has developed, pushing air away from the detonation center. If the shock wave extends beyond the position of interest, then there will be less air to attenuate the fission-product gamma rays than there was to attenuate the gamma rays produced at earlier times.

After about 0.2 sec, most of the radiation produced by a weapons detonation is due to the fission products. Kukhtevich et al.[3] estimate that during the first minute following an explosion the "quantities" of gamma radiation due to fission products is 100 times greater than that due to the prompt fission gamma rays. This may be quoted from Glasstone,[1] however, who said that during the first minute fission-product gamma rays *plus the nitrogen-capture gamma rays* contribute 100 times more to the total nuclear radiation received at a given point than do the fission gamma rays.

The fission products consist of a mixture of a large number of different radioactive isotopes. Crocker and Conners[18] list a total of 186. The energies of the earliest gamma rays emitted by these isotopes are reported by Engle and Fisher[19] to be as high as 6 MeV for the fission of ^{235}U, ^{238}U, or ^{239}Pu. In general, however, the energies are much lower. Jaeger,[20] apparently quoting Stehn and Clancy,[21] says that the average energy of fission-product gamma rays is 0.7 MeV, and that no more than a dozen of the isotopes emit gamma rays with energies above 2.5 MeV. He further states that the total energy emitted as fission-product gamma rays is 7 MeV per fission, with most of it emitted within 30 min. This is to be compared with a total of 8.4 MeV per fission (with a mean energy of 2 MeV)

reported by Kukhtevich et al.[3] and (5.7 ± 0.7) MeV per fission reported by Maienschein, Peelle, Zobel, and Love.[22] The latter number is specified for a time period between 1 and 10^8 sec and for gamma-ray energies between 0.3 and 5.0 MeV. In an earlier paper, Zobel and Love[23] had reported a total of 3.233 MeV/fission for the time period between 1.25 and 1600 sec, a number based on the emission of gamma rays in the quantities and with the energies shown in Table 4.

Table 4. Fission-Product Gamma Rays Emitted Between 1.25 and 1600 sec*

Average Gamma-Ray Energy (MeV)	Photons per Fission	Energy (MeV) per Fission
0.395	0.747	0.295
0.815	1.225	0.998
1.37	0.452	0.619
1.96	0.235	0.461
2.9	0.198	0.575
4.25	0.067	0.285
Total	2.924	3.233

*From Zobel and Love, ref. 23.

2.2.6. Activation Gamma Rays

The last group of gamma rays to be considered as a weapons radiation source are those known as "activation" gamma rays. These are gamma rays emitted from the nuclei of isotopes that have become radioactive because of exposure to the fission or fusion neutrons. The reactions producing the activation gamma rays (also referred to as "induced activity") are the neutron-capture and charged-particle reactions. As pointed out in Sections 2.2.3 and 2.2.4, these two reactions result in the instantaneous emission of gamma rays. If after the emission of these early gamma rays the nucleus remains radioactive, activation gamma rays are emitted at later times.

Many isotopes are susceptible to activation, including essentially all the constituents of the weapon and surrounding environment. Thus the radioactive cloud is not due to fission products alone, but also includes activated weapon debris. And, depending on the size of the weapon and its relative location to the ground, the cloud may have picked up radioactive ground materials. Finally, the soil and structural materials remaining in the vicinity of the burst may be radioactive. It is the gamma rays from the stationary materials, together with those emitted from the materials that fall from the cloud, that make an area radioactive and uninhabitable for a period of time after a detonation has occurred.

Although the number of different activated isotopes that might appear in the cloud or be left in the area of the burst is very large -- Crocker and Wong[24] list 77 isotopes -- only a few are considered to be important in weapons radiation shielding. These are in general limited to the activated weapons materials, which will be determined by the design of the weapon, and to the isotopes appearing in the ground and in structural materials. For ground the most important isotopes are ^{24}Na, ^{28}Al, and ^{56}Mn, which emit the gamma rays listed in Table 5. Silicon, which comprises about 28% of the earth's crust, also becomes activated, but it mostly gives off beta rays and only infrequently emits a gamma ray. Reinforced concrete usually contains these same activants, plus ^{59}Fe, which emits 1.10- and 1.30-MeV gamma rays. Other activants that may be present are ^{65}Ni, which emits 1.12- and 1.49-MeV gamma rays; ^{64}Cu, which emits 1.34-MeV gamma rays; ^{65}Zn, which emits 1.12-MeV gamma rays; ^{60}Co, which emits 1.17- and 1.33-MeV gamma rays; and ^{40}K, which emits a 1.46-MeV gamma ray. The potassium isotope arises from the decay of ^{40}Ca in the concrete and is extremely long lived (halflife of 1.3×10^9 years), so that continuous exposure of personnel to activated concrete may create an operations problem.

Compared to gamma rays from other sources, activation gamma rays contribute very little to the total radiation environment produced by a weapon. Kukhtevich et al.[3] estimate that if it is assumed that one-half of all the neutrons emitted from a plutonium bomb are absorbed in the soil and if it is further assumed that the soil offers no attenuation to the resulting

Table 5. Important Activation Gamma Rays from the Ground

Isotope	Gamma-Ray Energy (MeV)
^{24}Na	1.38
	2.76
^{28}Al	1.78
^{56}Mn	0.82
	1.77
	2.06

activation gamma rays, the total energy radiated by the soil would still be a factor of 14 lower than that emitted by the fission products. Because of this, activation gamma rays are usually neglected in weapons radiation shielding calculations. This could not be done, of course, if the weapon were a purely fusion weapon, in which case all the radioactive materials in the cloud would consist of activated weapons materials and activated environmental materials picked up in the burst.

3.0 DISTINCTION BETWEEN INITIAL AND RESIDUAL RADIATIONS

From the foregoing discussion it is obvious that radiations from a given detonation may continue to be emitted for years but that those emitted approximately in coincidence with the detonation are by far the most concentrated in space and time. When the protection of locations in the near-vicinity of the burst is of concern, it is this latter group of radiations, identified as *initial* radiations, that must be considered. Somewhat arbitrarily, and very conservatively, a time limit of 1 min has been assigned to initial radiations, with all radiations appearing after 1 min being called *residual* radiations.

With these time limits it is clear that all neutrons produced by a weapon are initial radiations. Fission gamma rays, inelastic-scattering gamma rays, capture gamma rays, and gamma rays from charged-particle reactions are also unquestionably initial radiations. Fission-product gamma rays, however, fall in both categories, with those emitted during the first minute referred to as "early-time" fission-product gamma rays. Activation gamma rays similarly fall into both categories.

Initial radiations are sometimes incorrectly referred to as "prompt" radiations. Prompt radiations are actually components of initial radiation. Although in some contexts prompt radiations are thought to be those radiations emitted directly in the fission or fusion process, they actually include all radiations emitted from the weapon itself. Some writers have coupled the definition of prompt radiations with a 1-sec time limit, but this should not be done since gamma rays produced outside the weapon would then be included. The term "prompt" is often used interchangeably with the term "primary" when the radiations produced within the weapon are being contrasted with "secondary" radiations produced outside the weapon. (The only secondary radiations of concern in shielding calculations are the secondary gamma rays produced by neutron interactions.)

The terms "residual radiation" and "fallout radiation" are also frequently confused. If only the radiation dispersed by the radioactive

cloud is considered, both terms are equally applicable, but fallout does not include radioactive materials left near ground zero (that is, materials activated by the burst but not picked up in the cloud).

A listing of the various initial and residual radiations is given in Table 6. Shielding studies for the two categories are carried out separately, usually by unrelated groups. From the military viewpoint, the initial radiations are usually of overriding importance and it is this category that is emphasized in this chapter. How many of the various initial radiation sources are treated in a particular shielding study depends on the study itself. As has already been pointed out, for some situations, particularly for a well-shielded location, the damage from some of the sources will be negligible and need not be considered.

Table 6. Components of Initial and Residual Radiations

Initial Radiations (Emitted within 1 min after detonation)
Prompt fission and fusion neutrons (produced in weapon)
Delayed neutrons (emitted from weapon debris)
Prompt (primary) gamma rays (produced in weapon)
Fission gamma rays
Inelastic-scattering gamma rays produced in weapon
Gamma rays from charged-particle reactions in weapon
Capture gamma rays produced in weapon
Environmental (secondary) gamma rays (produced outside weapon)
Inelastic-scattering gamma rays produced in air, ground, and structural materials
Gamma rays produced by charged-particle reactions in air, ground, and structural materials
Capture gamma rays produced in air, ground, and structural materials
Early-time fission-product gamma rays (emitted from debris cloud)
Early-time activation gamma rays
From activated weapons residue (emitted from debris cloud)
From activated environmental materials picked up in cloud
From activated environmental materials not picked up in cloud
Residual Radiations (Emitted at times >1 min after detonation)
Fallout radiation
Gamma rays emitted by fission products distributed by cloud
Gamma rays emitted by activated weapons residue distributed by cloud
Gamma rays emitted by activated environmental materials distributed by cloud
Gamma rays from activated materials not picked up in cloud (in vicinity of burst)

4.0 INTERACTIONS OF NEUTRONS WITH MATTER

4.1. Neutron Cross Sections

A neutron can interact with the nuclei of the materials comprising the weapon and the surrounding environment in several different ways. The probability that one particular type of interaction will occur is expressed in terms of the "cross section" for that interaction, the cross section being a function of the neutron energy and the material. A "microscopic" cross section, usually denoted by the symbol σ, can be regarded as the *effective* area (not related to the actual area) that a single target nucleus presents to an oncoming neutron. The larger the effective area, the greater the probability that the interaction will occur. The units for the microscopic cross section are cm^2/atom, or barns/atom, where 1 barn = 10^{-24} cm^2. A "macroscopic" cross section, denoted by Σ, is simply the product of the nuclide density N (atoms/cm^3) and σ (cm^2/atom). Thus Σ is expressed in units of cm^{-1} and can be interpreted as the probability of a neutron interaction per unit distance of neutron travel.

Cross sections for neutron interactions are classed either as elastic and nonelastic cross sections or as scattering and absorption cross sections. The groupings in the two classifications are somewhat different, but in either case they add to give a total cross section for the probability that a neutron of a given energy will interact with a particular type of nucleus in some way. The individual cross sections making up the total are referred to as "partial" cross sections. The interrelationship of the partial cross sections in the two separate classification schemes is shown in Fig. 1. If the elastic versus nonelastic classification is used, it is because the distinction being made is between those interactions in which the nucleus undergoes an internal change either in energy and/or in structure (nonelastic events) and those in which no such changes occur. If the scattering versus absorption classification is used, the distinction being made is between those interactions in which the interacting neutron (or its substitute) emerges from the collision (scattering events)

ORNL-DWG 72-7980

(a)

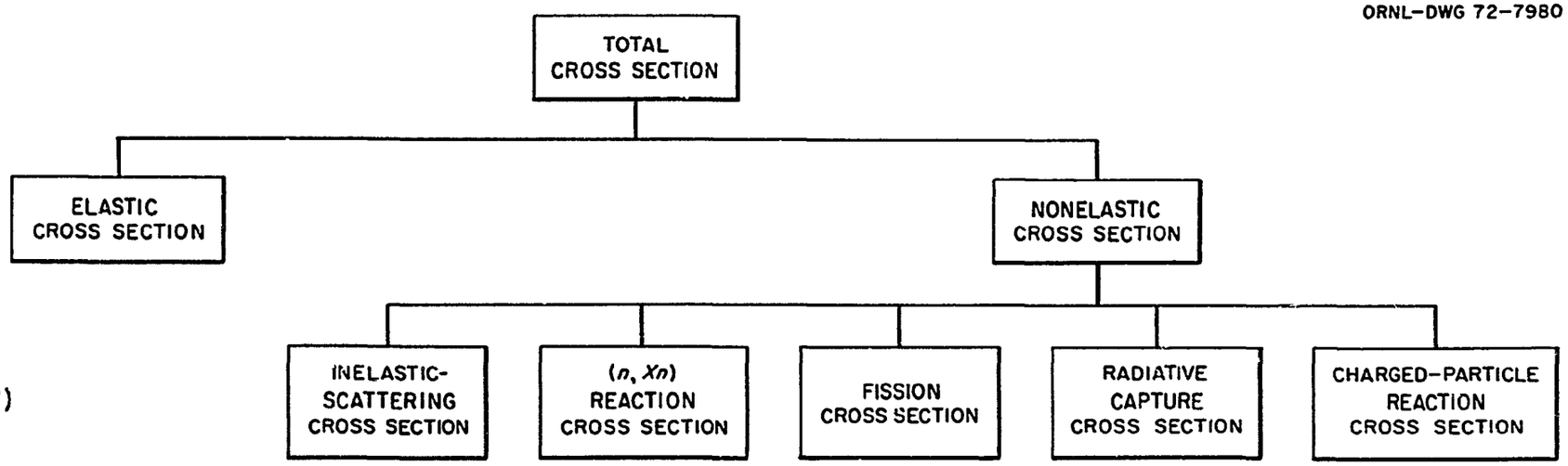

(b)

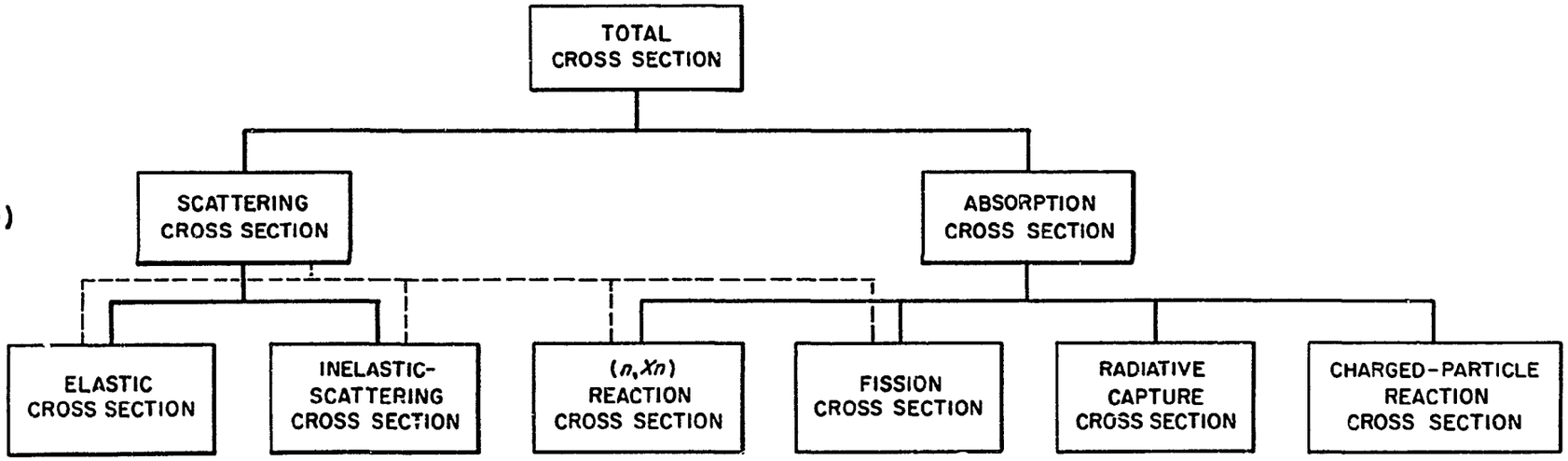

Fig. 1. Interrelationship of Neutron Interaction Cross Sections. Neutron cross sections are categorized either as (*a*) elastic and nonelastic cross sections or as (*b*) scattering and absorption cross sections. Occasionally all interactions in which neutrons leave the nucleus are classified as scattering interactions, in which case the four processes bracketed by the dashed lines would be considered scatterings.

and those interactions in which the interacting neutron disappears (absorption events). In scattering events the nucleus retains its identity, whereas in absorption events the product nucleus (or nuclei) differs from the target nucleus either in atomic mass or in atomic number. Because of the change of the target nucleus to that of another isotope, absorption processes are frequently referred to as *reactions* rather than *interactions*.

Neutron cross sections are the essential input to the neutron transport calculations required for shield design and the subject of a vast amount of basic research, both experimental and theoretical. Since neutron cross sections vary with the neutron energy, sometimes drastically, the number of different cross sections that can be determined even for one type of interaction for a single isotope is essentially unlimited. Moreover, cross sections are frequently given as a function of the angle at which a particle leaves an interaction (either the original neutron or a new particle produced in the interaction), in which case they are called "differential" cross sections and the units are barns/atom per steradian.

Because the number of cross sections used in transport calculations must be kept to some reasonable limit, the entire energy range of the neutrons for a particular problem (usually from 0 to 15 MeV) is divided into energy groups and a single cross section is used for each group. Depending on the number of groups used, the cross sections are referred to as "multigroup" cross sections or as "point" cross sections, the latter because some of the energy intervals are so narrow that they can be thought of as representing a point in the energy range.

In discussing the groups used for the neutron energies, it has become common practice to classify those for neutron energies above about 0.1 MeV as being fast or high-energy groups and those for energies below 0.1 MeV as low-energy groups. The lowest energy group is often designated as the thermal group as described in Section 2.2.4. The term "intermediate" is sometimes used for the energy range from about 1 eV to 0.1 MeV. These classifications are used in discussing the various neutron interactions in the following paragraphs.

4.2. Neutron Interaction Processes

4.2.1. Elastic Scattering

Elastic scattering can be viewed as the collision of two perfectly elastic spheres. In this process the target nucleus gains *kinetic* energy (not internal energy) from the neutron, and the neutron is deflected from its original course. By repeated elastic scatterings a neutron can be slowed in energy so that it is much more likely to enter into another type of reaction that will ensure its disappearance. Elastic scattering, referred to as the (n,n) interaction, is especially effective as an attenuating mechanism for high-energy neutrons in light elements, particularly hydrogen. It is much less effective in heavy elements. To illustrate this point, Jaeger[20] (p. 39) pointed out that a neutron with an initial energy of 2 MeV could be reduced to thermal energy by undergoing approximately 20 successive elastic scatterings against hydrogen nuclei whereas more than 2000 successive elastic scatterings against uranium nuclei would be required.

For elastic scattering to be taken into account exactly in shielding calculations for weapons radiation, the differential cross sections for the interaction must be known over the neutron energy range from 0 to 15 MeV for all the elements in the weapon, in the atmosphere, and in the structural materials used for buildings. Needless to say, the cross-section technology has not yet been developed to this extent.

4.2.2. Inelastic Scattering

Inelastic scattering is an interaction that can be thought of as a temporary capture and subsequent ejection of the neutron by the nucleus. When the capture occurs, some of the neutron's kinetic energy is absorbed by the nucleus (that is, the nucleus becomes "excited"), so that when the incident neutron, or its substitute, leaves the collision it is with a change in direction and with a reduction in energy equal to the energy taken on by the nucleus. The nucleus then usually returns to a

stable state by emitting promptly one or more gamma rays, the sum of whose energies is always less than the kinetic energy of the incident neutron. This interaction is referred to as the $(n,n'\gamma)$ interaction, and the product nucleus has the same identity as the target nucleus.

For inelastic scattering to be possible, the neutron must have an energy of at least 1 MeV for light nuclei and about 100 keV for heavy nuclei. In general, the lighter elements emit the highest energy gamma rays; however, a few heavy elements (the so-called "magic" nuclei) behave like light nuclei insofar as inelastic scattering is concerned.

Detailed inelastic-scattering cross sections, together with information on the concomitant production of secondary gamma rays, are only now becoming available for many elements (see Section 11.0).

4.2.3. Charged-Particle Reactions

In charged-particle reactions the neutron is absorbed by the target nucleus, which then de-excites itself by emitting a proton, deuteron, triton, or alpha particle, all of which are positively charged and therefore do not present shielding problems. Occasionally the charged-particle emission is accompanied by a gamma ray or neutron [such as $(n,p\gamma)$ or (n,np) reactions]. Charged-particle reactions are most probable for neutrons with energies in the MeV range; however, an important charged-particle reaction insofar as shielding is concerned is that of low-energy neutrons with the boron-10 isotope. When the ^{10}B nucleus captures a low-energy neutron, it emits an alpha particle, together with a gamma ray of only 0.5 MeV, and so this isotope can be added to shields to suppress the production of high-energy capture gamma rays at points close to the location requiring protection. Another important charged-particle reaction for low-energy neutrons is the (n,p) reaction in nitrogen which, unlike the $(n,p\gamma)$ reaction, is not accompanied by gamma rays. If it were not for the (n,p) reaction in nitrogen the production of gamma rays by neutron interactions in the air would create a much greater problem.

4.2.4. Radiative Capture

In the neutron interaction (or *re*action) called radiative capture the neutron is absorbed by the nucleus it strikes, and the excited compound nucleus immediately begins de-exciting through the emission of one or more gamma rays. The gamma rays given off promptly are the capture gamma rays discussed in Section 2.2.4; those emitted at later times, if any, are activation gamma rays. The total energy of all the gamma rays given off by one nucleus is the sum of the kinetic energy of the neutron that entered into the reaction plus an additional amount of energy, called the binding energy, which a nucleus releases when it takes on an additional neutron. For nuclei with atomic weights greater than about 15, the binding energies vary between 7 and 9 MeV.

Radiative capture, while desirable for removing neutrons from a radiation field, presents one of the greatest problems encountered in shield design. Because the neutrons most likely to be captured are those of low energy, neutrons that lose energy by successive scatterings in a medium have an increasing probability of being captured. At the same time they may be scattering toward the location the shield designer is interested in protecting. It is entirely possible that captures will occur *at* that location, causing gamma rays to be produced at points where no shielding is left to absorb them.

Although capture cross sections as a function of energy have been established in considerable detail for a number of elements, except for thermal neutrons the corresponding secondary gamma-ray production cross sections are extremely tentative (see Section 11.0).

4.2.5. Fission and (n,Xn) Reactions

The fission reaction, described in Section 2.1, is unimportant in the neutron transport calculations of shielding studies unless depleted uranium is used as a shield material, in which case high-energy neutrons will cause the ^{238}U isotope to fission, producing two or three neutrons per

fission. Cross sections for this interaction are included in the calculations if appropriate.

Another process which may or may not be considered in shielding calculations is the process whereby one neutron is captured by a nucleus and two, sometimes three, neutrons are emitted [(the $(n,2n)$ and $(n,3n)$ reactions], as well as an occasional gamma ray. In general the neutron energy has to be very high, greater than 10 MeV, for this interaction to occur; however, for a few isotopes the process is possible with lower energy neutrons, notably hydrogen-2, lithium-6, boron-9, bismuth-209, thorium-232, and uranium-238. Certain isotopes of beryllium and tungsten may also multiply the neutron population.

5.0 INTERACTIONS OF GAMMA RAYS WITH MATTER

5.1. Gamma-Ray Cross Sections

Gamma rays can interact with matter in a number of different ways, and as is the case for neutrons (see Section 4.1), the probability that a particular type of interaction will occur is expressed in terms of the cross section for that interaction. As for the neutron cross section, the units for the microscopic gamma-ray cross section (σ) are cm^2 or barns, but since some gamma-ray interactions are with the electrons surrounding a nucleus instead of with the nucleus itself, the cross section for some interactions is given as barns/electron rather than as barns/nucleus or barns/atom.

Although a number of different gamma-ray interactions are possible, three interactions are so dominant that all others are usually ignored in shielding calculations. The three processes are identified as the photoelectric effect, pair production, and Compton scattering, and their respective microscopic cross sections add to give the total microscopic cross section for the probability that a gamma ray of a given energy will in some way interact with a particular type of atom:

$$\sigma_t = \sigma_{PE} + \sigma_{PP} + Z\sigma_C \quad ,$$

where σ_{PE} and σ_{PP} are the photoelectric and pair-production cross sections per atom and σ_C is the Compton scattering cross section per electron. Z is the atomic number, which specifies the number of electrons orbiting around the nucleus. (In an electrically neutral atom, the number of electrons is the same as the number of protons in the nucleus.)

The macroscopic cross section for gamma rays is referred to as the linear absorption coefficient (or linear attenuation coefficient). It is denoted by the sumbol μ but has the same definition and units as the symbol Σ used for neutrons. That is, μ is equivalent to σN, where N is the nuclide density (atoms/cm^3), and its units, like those of Σ, are cm^{-1}.

Another quantity that describes the probability of gamma-ray interactions is the mass attenuation coefficient, which is the linear absorption coefficient divided by the material density (μ/g).

Gamma-ray cross sections are required as input in any shielding calculation in which the transport of gamma rays is considered, whether they be the gamma rays emitted from the weapon or secondary gamma rays produced by the various neutron interactions. As in the case for neutrons, the number of cross sections used in a calculation is usually kept to a reasonable limit by dividing the energy range into intervals (energy groups) and allowing a single cross section to represent each interval.

5.2. Gamma-Ray Interaction Processes

5.2.1. Photoelectric Effect

The gamma-ray interaction known as the photoelectric effect results in the disappearance of the photon and therefore is an absorption process. It is not the nucleus of the atom that absorbs the gamma ray, however, but rather one of the electrons orbiting the nucleus. Following the absorption, the electron leaves the atom with a kinetic energy equal to the original gamma-ray energy minus the energy required to wrench the electron from its orbit (the electron's binding energy). The void left in the orbital shell is filled with an electron from an outer shell, and the difference in the binding energies of the two shells is emitted from the atom as softer electromagnetic radiations (fluorescent X rays) that do not create a radiation shielding problem, primarily because they in turn become involved in the photoelectric effect.

The photoelectric process is not possible with a free electron, and neither is it possible with an electron in an atomic orbit if the energy of the incident gamma ray greatly exceeds the electron's binding energy. Thus the cross section for the interaction in a given material increases rapidly with decreasing gamma-ray energy. The cross section also increases

with the atomic number Z, but even in high-density shields the photoelectric effect is dominant only for gamma-ray energies less than 1 MeV.

5.2.2. Pair Production

Pair production is a second process whereby a gamma ray disappears with the subsequent emission of electromagnetic radiations of lower energy. An intervening step is the conversion of some of the gamma-ray energy into a pair of particles -- an electron and a positron -- which have identical masses but opposite charges. The pair production process cannot occur except within the electrical field surrounding a charged particle. Since the charge of a nucleus is considerably larger than that of, say, one of its electrons, the process has a greater probability of occurring in an electrical field associated with a nucleus than elsewhere.

For a gamma ray to enter into a pair production process in the electrical field around a nucleus, it must have an energy greater than 1.02 MeV, that being the amount of energy required to produce the masses of the electron and positron pair ($E = 2\, m_e c^2 = 1.02$ MeV, where m_e is the mass of an electron or positron and c is the velocity of light). Any additional energy is utilized as kinetic energy by the two particles. Upon losing its kinetic energy, the positron interacts with an ordinary electron and both are converted to energy which is given off as two 0.51-MeV photons. Because of their origin, these photons are referred to as annihilation radiations.

The probability that pair production will occur increases with the gamma-ray energy and with the atomic number of the material. For gamma-ray energies above about 5 MeV and materials with atomic numbers above about 30 it is the dominant attenuating process.

Because the 0.51-MeV annihilation photons are relatively low in energy, they are sometimes ignored in shielding calculations; however, in the most detailed calculations they are treated as an additional gamma-ray source.

5.2.3. Compton Scattering

The process known as Compton scattering is an interaction of a gamma ray with an electron, resulting in a transfer of some of the gamma ray's energy to the electron and a change in the gamma-ray direction (similar to the inelastic scattering of a neutron with a nucleus). In all cases the electron is considered to be an independent agent, even when it is bound in an atom since it is the outer loosely bound electrons that are most likely to be involved and their binding energies are negligibly small compared to the energies of the gamma rays. Correspondingly, the cross section for Compton scattering is given on a per electron basis and must be multiplied by the atomic number to obtain a cross section for a given material.

For materials with high atomic numbers Compton scattering is the dominant interaction for gamma rays with energies between 1 and 5 MeV; for materials with low atomic numbers it is the dominant interaction for gamma rays of all energies. The energy loss suffered by the gamma ray increases with an increasing scattering angle (the angle between the original and scattered directions of the gamma ray) and with an increasing original energy. For example, a 0.01-MeV gamma ray scattered at 180 deg loses less than 5% of its energy, whereas a 5-MeV gamma ray loses 95% of its energy. However, the probability that a 5-MeV gamma ray will undergo a 180-deg scattering is quite small, whereas the probability that a 0.01-MeV gamma ray will suffer a 180-deg scattering is as high as that for a 20-deg scattering. That is not to say that the differential cross sections for all scattering angles are equal for low-energy gamma rays. Actually they drop from their highest values at small angles to a minimum at 90 deg and then increase again to 180 deg. This behavior is exhibited for gamma-ray energies up to about 0.5 MeV, although the increase in the cross section at 180 deg becomes less pronounced with an increasing gamma-ray energy and disappears at about 0.6 MeV. For higher gamma-ray energies the cross section decreases rapidly with an increasing scattering angle to the extent that large-angle scattering of MeV gamma rays can be assumed to be nonexistent, a characteristic which is used to great advantage in shield designs. Regardless of the initial energy, the

maximum energy of any gamma ray scattered 180 deg is 0.253 MeV. At 90 deg the maximum energy is 0.51 MeV and at 60 deg it is 1.02 MeV.

5.2.4. Relative Importance of the Three Gamma-Ray Interactions

From the preceding discussion it can be deduced that for a given gamma-ray energy the microscopic cross section for each of the three gamma-ray interactions increases with an increasing atomic number (Z) of the material. Thus the total macroscopic cross sections for gamma rays of all energies will increase with Z and with the density of the material they are traversing. For a given material, the total cross section will be highest for low gamma-ray energies, decreasing with increasing energy to a minimum and then increasing with increasing energy. This behavior results from the variations of the three partial cross sections with energy; that is, the cross section for pair production increases with energy while the cross sections for the other two processes decrease with energy. It is to be pointed out, however, that for all materials the cross sections are smooth functions of both the material and the gamma-ray energy, making gamma-ray attenuation amenable to interpolation. This is in contrast to neutron cross sections, which exhibit large variations with both the material and the particle's energy.

6.0 METHODS FOR CALCULATING THE TRANSPORT OF WEAPONS RADIATION

Theoretically the amount of weapons radiation penetrating to a specified position within a particular structure can be calculated exactly by applying to the weapons-structure system an equation well-known as the Boltzmann transport equation.[1] The basis of the Boltzmann transport equation is that the net storage of particles in a volume, such as a small volume surrounding a point of interest in the structure, is set equal to the number of particles that have entered the volume minus the number of particles that have left the volume. In other words, the equation is a bookkeeping process, but a bookkeeping process so refined that it keeps track of the directions and energies with which the particles enter and leave the volume, as well as the times in which they enter and leave. Thus the general behavior of the radiation particles within the system is described in terms of seven-dimensional phase space, the seven dimensions including the usual three spatial coordinates (x, y, and z), two direction-defining angles, the particle energy, and the time. To say it another way, with a complete solution of the Boltzmann transport equation for a given problem, one would know from the instant of detonation the total number of radiation particles reaching various locations in the system at all times, together with the energies with which they arrive and the directions in which they are traveling.

Two types of input are required for the Boltzmann transport equation: a description of the geometrical arrangement of the materials in the system; and the cross sections for all types of particle interactions within those materials. If it is not already apparent that truly exact solutions of the Boltzmann transport equation are not physically possible, we need only consider what these two input requirements entail. For example, a complete description of the geometrical arrangement of the materials would begin with a description of the weapon itself. It would require an inti-

---

[1] So named because of its similarity to an expression obtained by L. Boltzmann in connection with the kinetic theory of gases.

mate knowledge of the weapon design so that the location of all the materials in the weapon could be specified in the calculation. It would also require a knowledge of the variation of the geometrical arrangement of these materials during the time period that the weapon is breaking apart. The description would continue with details of the surrounding atmosphere, including the variation of its density with height above the ground and with time following the detonation. Finally, the description would include the ground and the structure itself, including any irregularities in the structure such as entranceways or air gaps between abutting components.

Obviously an exact description of the geometrical arrangement is not presently feasible, and even if it were, the immense amount of detail that would be required in the corresponding cross sections would preclude the possibility that an exact solution could be obtained. Such cross-section detail is never available and if available could not be used because of limitations in the size and speed of electronic computers. It is easy to see that the amount of cross-section data needed would be essentially infinite when one recalls that the microscopic cross section for a particular type of neutron interaction in a given material may vary radically with the neutron energy. Thus for the interaction to be considered exactly in a calculation, cross sections for each material in the system would have to be input for every point in the energy range. These in turn would have to be given for all angles in which the particle emerging from each interaction might be directed. The situation is thus impossible even without considering the gamma-ray interaction cross sections and gamma-ray production cross sections also required.

For the foregoing reasons, solutions can be obtained only for approximate forms of the Boltzmann transport equation and over the years much effort has been directed toward developing "transport methods" which will solve the approximate forms for systems of increasing complexity. For weapons shielding calculations this has been particularly difficult since shield penetration problems are inherently more complex than the reactor or weapons criticality problems for which most of the transport methods were initially developed. Whereas in criticality calculations it

is the average behavior of the overall particle population that is of concern, in shielding calculations it is the behavior of a relatively few unusual particles that is of concern. For example, if a shield has an attenuation factor of 10^{-10}, which many practical shields do, then only one out of every 10^{10} particles entering the shield is successful in penetrating its full thickness. Unfortunately these unusual particles are usually high-energy particles whose interaction mechanisms are the least understood because they are difficult to produce in abundant quantities under laboratory conditions and therefore are less amenable to experimental investigation than are the lower energy particles.

The several transport methods that have been developed for solving approximate forms of the Boltzmann transport equation include the spherical harmonics, invariant embedding, kernel, diffusion, moments, discrete ordinates, and Monte Carlo methods, all of which are described briefly by Stevens and Trubey in Chapter 3 of the *Weapons Radiation Shielding Handbook*.[25,m] Most of these methods have served as the basis for digital computer programs that can be applied to various classes of shielding problems, but of these only the computer codes based on the discrete ordinates method and the Monte Carlo method can rigorously treat initial weapons radiation in complex geometries.[n]

---

[m] The *Weapons Radiction Shielding Handbook* is prepared and issued in chapter form at the Oak Ridge National Laboratory for the Defense Nuclear Agency (formerly Defense Atomic Support Agency), with calculations and manuscript preparation for several of the chapters subcontracted by ORNL to Radiation Research Associates, Inc. The chapters are edited by L. S. Abbott, H. C. Claiborne, and C. E. Clifford and are identified either as DASA-1892 or DNA-1892 with subnumbers. Several of the chapters are referred to throughout this document.

[n] The moments method is also a rigorous method and has been used successfully in studies of the penetration of residual radiation through shield materials[26,27] and in calculations of the penetration of initial weapons radiation through the atmosphere.[28] It is limited to problems that can be represented by infinite homogeneous media, however, and therefore cannot be applied to multidimensional and multi-material shields without approximate correction factors.

This section is therefore limited to a discussion of these two methods and the geometries and cross sections used with them.

6.1. Geometries Used with Transport Methods

The simpler the geometry that can be used to describe a problem the faster (and cheaper) the calculation. The simplest geometries are one-dimensional geometries: those in which only one of the three spatial coordinates has finite specifications. An example is a slab having a specified thickness but an infinite height and an infinite width (commonly referred to as an infinite slab). Another is a sphere having a finite radius and spherically symmetric materials. Another is a circular cylinder having a finite radius, an infinite height, and circularly symmetric materials (referred to as an infinite cylinder).

In many calculations employing one-dimensional geometries the medium through which the particles are transported is assumed to consist of a single material; however, the number of materials used in one-dimensional geometries is limited only by the transport method and/or the size of the calculation. An infinite slab can consist of several consecutive layers of different materials and a sphere or infinite cylinder can consist of several concentric shells of different materials.

In theory the radiation emitted into the atmosphere surrounding a weapon could be calculated by representing the weapon as spherical concentric shells; however, in practice consideration of the behavior of the particles within the weapon has been universally excluded from radiation transport calculations performed for shield design. The reasons are that the calculation would be too large, the weapons vary too much in design, and, perhaps even more to the point, calculations of the production of radiation within the weapon itself are traditionally outside the province of the shield designer. Rather he relies on the weapon designer to provide him with a description of the radiation source. Moreover, he assumes that the effect of the weapons materials on the numbers and energies of the radiations produced has already been taken into account. This being true,

he can ignore the fact that the source is actually distributed throughout a volume and can assume that all the radiation from the weapon is emitted from a single point located at the weapon's center. He thus avoids inputting into the calculation either the weapon geometry or the cross sections for interactions within the weapon. In this technique the difference between the distance from the weapon's center to the point of interest and the distance from the weapon's surface to the point of interest is neglected, but for the large distances involved the results are not significantly altered and the use of a point source in all weapons radiation shielding calculations has become common practice.

A number of one-dimensional calculations of the transport of weapons radiation through a homogeneous atmosphere have been made using the point source in spherical geometry. In addition, the infinite-slab geometry has been used for calculations of the penetration of weapons radiation through a slab (or slabs), in which case the source is taken to be an infinite-plane source that has developed because of a detonation at some distance away. Such a geometry is applicable, for example, for calculating the penetration of radiation through one wall of a structure since the wall thickness is its most important parameter.

One-dimensional geometries are particularly efficient for calculations covering large distances in the atmosphere or large shield thicknesses since they require a minimum of computer storage and computational time. However, they are inadequate for many situations, one being the calculation of the radiation that might be transported from an in-air weapon burst to a position on the ground. Particle interactions within the ground will affect the energies and numbers of particles at positions above and on the ground, and in order for these interactions to be considered a minimum of two space dimensions is required. An example of a two-dimensional geometry is a circular cylinder having both a finite radius and a finite height; another is a parallelepiped having one infinite and two finite dimensions. The cylinder is the geometry usually applied for "air-ground" weapons radiation calculations, its upper section composed of air and its lower section composed of ground. The point source is located in the air on the cylinder

axis. This is a much larger problem than the one-dimensional spherical problem since the particle behavior must be determined not only as a function of the distance along the radius of the cylinder, but also as a function of the distance along the axis. As a result the distances that can be covered in any one calculation are limited by the computer storage capacity. The radial distances, frequently referred to as ground ranges, can be extended by coupling the calculations in space -- a technique in which the results for the outer space boundary of one calculation are used as the source for an inner boundary in a second calculation, etc. When this is done the calculations are overlapped[29] ("bootstrapped") to compensate for the effects of a vacuum following the outer boundary in each preceding calculation of the series.

Obviously some weapons-structure systems cannot be adequately described in toto unless three space dimensions are used. However, describing the entire problem in three dimensions can frequently be circumvented by dividing the system into parts, each of which is described by the simplest possible geometry. Techniques for doing this are discussed later in this paper.

6.2. Preparation of Cross-Section Input

It was pointed out in Section 4.1 that the number of cross sections used in a particular calculation is kept to some reasonable limit by dividing the energy range covered by the source particles into energy intervals (or groups) and using a single average cross section to represent each group. Depending on the number of groups used, the cross sections are referred to as multigroup cross sections or as point cross sections, some of the energy intervals for the latter being sufficiently narrow that they can be thought of as representing points in the energy range.

For gamma rays the preparation of either multigroup or point cross sections is relatively simple, since the gamma-ray interactions vary smoothly with energy for $E > 0.1$ MeV. For neutrons, however, the preparation of cross-section sets is much more difficult, and one can be confident that a good grouping has been used only if sufficient information is available both on the source neutron energy spectrum and on the pertinent inter-

action processes so that the cross-section grouping can be tailored to the problem. Consider, for example, the case in which the cross section for a neutron interaction in a given material is very high at some particular energy; thus the probability that neutrons of that energy will successfully penetrate a shield comprised of that material is very low. At the same time the cross sections for neutrons with energies immediately below and immediately above that particular energy are very low; thus the probabilities that these neutrons will successfully penetrate the shield are very high. If all these neutrons were assigned to the same energy group and a linearly averaged cross section used, then neutrons that would actually be "streaming" through the shield would be treated in the calculation as having interactions and their effect will be underestimated. This can be avoided either by using a finely structured cross-section grouping or by sufficiently weighting the cross section within an energy group in the averaging process to account for the large differences in the cross sections over the group. Of course proper weighting depends on the detail with which the cross sections are known, on the transport method used for the calculation, and on the size of the problem.

The sensitivity of neutron transport calculations to the manner in which cross sections are treated has spawned a burgeoning cross-section preparation technology separate from that of determining the physical values of the differential cross sections themselves. The aim of this technology is to process the basic cross-section data for a given calculation so that they will most nearly simulate the average behavior in the real situation. As already pointed out, the same basic cross sections averaged differently do not necessarily give the same transport results. For codes that use multigroup cross sections the energy groups can be made quite broad, and it becomes particularly important that the cross section for each group be properly weighted. The number of groups is limited only by the computer capacity, however, and not even by that if a series of calculations are run and coupled in energy. [Coupling sequential calculations in energy does not require that they be overlapped as does coupling them in space (see above), but other disadvantages exist and the technique is used infrequently.]

A number of computer codes have been developed to generate multigroup cross sections. Codes commonly used are XSDRN[30] and SUPERTOG,[31] which generate neutron multigroup cross sections, and MUG[32] and GAMLEG,[33] which generate gamma-ray multigroup cross sections. Another code, called POPOP4,[34] combines the neutron interaction cross sections with gamma-ray yield data for those neutron interactions and then produces secondary gamma-ray production cross sections. The three different types of cross sections can be processed by a fourth code, called the Sample Coupling Code,[35] to produce "coupled" neutron and gamma-ray cross sections. With the coupled cross sections, neutron transport and gamma-ray production and transport can all be treated simultaneously, which is a relatively new development in transport calculations. Until coupled cross sections became available, the transport of the neutrons and primary gamma rays had to be calculated separately and the production and transport of secondary gamma rays constituted a third problem.

The trend toward using coupled cross sections has naturally resulted in the development of systems of interfaced computer codes to automate the process of obtaining coupled multigroup cross sections. One such system, identified as AMPX,[36] is now under development at Oak Ridge National Laboratory.

It should be pointed out that the preparation of cross sections for transport codes is increasingly involving "sensitivity" transport calculations to locate non-obvious energy regions or interactions that affect the results disproportionately. These in turn frequently must be checked against carefully designed experiments.

It should also be pointed out that the treatment of the particle direction following an interaction is unique to the transport method employed and is limited by the amount of scattering data available. To date, neutron elastic scattering and gamma-ray Compton scattering are the only interactions for which anisotropic scattering is treated in the transport methods. All other interactions are treated as resulting either in isotropic scattering or in the isotropic emission of secondary particles.

r example, neutrons emitted in fission, neutrons scattered inelastically, and secondary gamma rays produced by neutron interactions are assumed to be emitted isotropically. High-energy neutrons involved in inelastic interactions actually scatter anisotropically, and as more data on this process become available, it will be treated more accurately in the calculations. Thermal neutrons may also scatter anisotropically from certain nuclei or molecules, but this effect should not be too important in shielding calculations.

6.3. The Discrete Ordinates Transport Method

The discrete ordinates transport method is a numerical integration technique that yields highly differential results for the entire system simultaneously. The term "discrete" derives from the fact that the calculation specifies the number of particles traveling in discrete directions. The most common discrete ordinates method is often referred to as the discrete ordinates S_n method with the numerical value of n specifying the number of solid-angle segments representing the directions. The discrete ordinates method normally uses multigroup cross sections, and to date it is limited to one and two space dimensions.

As is indicated in the above description of the Boltzmann transport equation, the system being calculated is divided into finite space cells and the calculation maintains a balance between particle gains and losses for each space cell. For a given energy group the gains are the number of particles within that group that enter the space cell plus the number of particles that enter the energy group by downscattering in energy within the cell from higher energy groups. The losses are the number of particles within the energy group that leave the cell plus the number of particles within the cell that leave the energy group. Those that leave the energy group have been either absorbed within the cell or downscattered to lower energy groups. (Upscatterings to higher energy groups are also possible, but usually only downscatterings are treated in shielding calculations, which is the reason that calculations coupled in energy need not be overlapped, as pointed out in Section 6.3.)

With the origin (source) of the particles specified and the boundary conditions set, the calculation begins with the highest energy group and sweeps through all lower-energy groups and all space cells in the system for all particle directions. Several sweeps (iterations) are required before the results converge to give the number of particles from the high-energy group at the source that have entered each space cell, together with their resulting energies and directions. The procedure is repeated for each energy group in decreasing order. The results are presented for space points located at the centers of the space cells and are taken to be the means of the number of particles within the given energy group at opposing faces of the cells.

The method of discrete ordinates was originated in the mid-1940's[37,38] for criticality calculations using one-dimensional slab geometry and other simplifying assumptions. Not until 1955[39] was it extended to spherical and cylindrical geometries and not until after the mid-1960's was it possible to overcome several basic shortcomings that prevented it from being seriously considered for deep-penetration shielding problems.[40] One major difficulty was due to the fact that in shields the number of particles decreases rapidly with distance, and an unreasonably fine cell mesh was required in order for the average number of particles obtained from opposing cell faces to be realistic. This problem is now circumvented by repeating the calculations for these regions with less accurate methods and substituting the results in the primary calculation. Another difficulty resulted from the assumption in the original method that all particles scatter isotropically. In order to allow anisotropic scattering without making the excessive computer storage demands that would be required if all possible combinations of directional change and energy group transfer were considered, a technique was developed to approximate the angular dependence of each group-to-group transfer by a Legendre series, which fortunately requires only a low-order expansion for most problems. Other difficulties that have been alleviated have been associated with exceptionally long computer times required to treat particle scattering within an energy group and with oscillations in the results corresponding to finite directions in two-dimensional problems. Even with these improvements, however, discrete

ordinates calculations as they are performed today would not be possible had the development of computers not progressed so much during the last several years.

Since 1965 several computer codes based on the discrete ordinates method have been developed for application to shielding calculations. Among these are the DTF-IV code developed by Lathrop;[41] the TWOTRAN code developed by Lathrop and Binkley;[42] and the ANISN code,[43] the DOT code,[44] and the TDA code[45] developed by Engle and Mynatt. The DTF-IV and ANISN codes are limited to one-dimensional geometries and the TWOTRAN and DOT codes to two-dimensional geometries. The TDA code is a version of ANISN that gives time-dependent results.

All these codes can be obtained from the Radiation Shielding Information Center at Oak Ridge National Laboratory.

6.4. The Monte Carlo Transport Method

The Monte Carlo method is a numerical procedure based on statistical theory and is the only method by which the Boltzmann transport equation can be solved rigorously in three dimensions. Devised by von Neumann and others in the mid-1940's, it may be thought of either as solving an integrodifferential equation in a strict mathematical sense or as following individual particles in an analog sense. The individual particles are followed as they execute "random walks"[o] through the system, the steps of the walk consisting of a series of flights between interactions. Each interaction results either in a change in the particle's energy and direction or in its disappearance, depending on whether the particle scatters from the nucleus or is absorbed by it. The positions at which the interactions occur and the results of the interactions are determined from a range of possibilities by sets of random numbers -- hence the name Monte Carlo.

---

[o] The classical definition of the actual distance covered by a random walk is that it is comparable to the distance between a drunk and a light pole after the drunk has taken 100 steps away from the pole.

The premise of the Monte Carlo method is that if enough particles are followed, that is, if enough particle histories are generated, then the fraction of particles reaching a given location will be a reliable estimate of the fraction reaching that location in a real case involving a much larger particle population. The major difficulty in applying the Monte Carlo method to shielding calculations has been that enough histories for a reliable estimate is too many histories, and even with the fast computers available today, straightforward (analog) Monte Carlo calculations often consume too much time. Consider again the example of the shield which has an attenuation factor of 10^{-10}. In the real situation only about one out of 10^{10} particles would penetrate to the location of interest, which means that the number of histories followed would have to be many times 10^{10} particles.

In order to reduce the number of histories and yet obtain a reliable answer, much effort has been expended during the last decade in developing techniques for biasing the interaction probability distributions so that the particles sampled are those most likely to reach the positions of interest. At the same time the sampled particles must be properly weighted by correction factors so as to maintain a "fair game."[p] One of the techniques, called Russian roulette, consists in killing off particles whose energies or directions make it highly improbable that they will reach the position of interest and at the same time increasing the weights of the survivors so that they represent the "killed" particles as well as themselves. Another technique is to stretch the path length (actually increase the probability of a longer path) between collisions of those particles that have favorable directions and energies. Still another is to disallow the termination of a history by absorption of the particle; instead the absorption is taken to be a scattering process with the weight of the particle reduced by the ratio of the absorption cross section to the total cross section.

---

[p] To say it more mundanely, the dice must be loaded. But they must be loaded in such a way that the answer obtained with the loaded dice is the same answer that would be obtained with unloaded dice *if* enough tosses were made.

To employ biasing techniques, the user must have some knowledge of which particle energies and directions and which spatial regions in the system will be important to the answer. Much of this knowledge can be gained from experience, or it can be obtained by running parts of the problem and examining the results. A more sophisticated method applied in recent years, especially to difficult problems, is to obtain an "importance function" from a solution of the adjoint problem, which is equivalent to the transport problem solved backwards. In the adjoint problem the path whereby a particle has reached a particular position is traced in the reverse direction, and the interactions that directed that course of travel are determined. Thus the source particles important to the answer are identified. Obviously the adjoint solution should be obtained with some approximation, since to solve the backward problem precisely would obviate a forward solution. Usually the adjoint problem is solved by the discrete ordinates method with a one-dimensional approximation of the geometry.

Several Monte Carlo transport codes have been developed for specific purposes, frequently for particular geometries. Others have been developed for general geometries and thus can be applied to many more problems but require considerable adaptation to each problem. Among this latter group is the well-known 05R system developed by R. R. Coveyou and others[46] for neutron transport calculations. An improved version of this code, identified as 06R, yields time-dependent results. Another general system is the OGRE system developed by Penny et al.[47] for gamma-ray transport calculations. The SAM series of codes[48] can be used for either neutron or gamma-ray transport. All of these codes require point cross sections, as do most Monte Carlo codes, but a more recent code, the MORSE code developed by Straker et al.,[49] uses multigroup cross sections. Thus, like the discrete ordinates codes, it can handle neutron transport and secondary gamma-ray production and transport simultaneously. It also can yield time-dependent results.

All these codes, plus other Monte Carlo codes, can be obtained from the Radiation Shielding Information Center at Oak Ridge National Laboratory.

6.5. Coupled Transport Methods

The advent of Monte Carlo codes that can utilize the same multigroup cross sections as discrete ordinates codes will logically lead to the development of hybrid methods that can handle weapons shield systems of any size and geometry in the most efficient manner possible. With such methods a problem can be divided into one-, two-, and three-dimensional segments, and the best technique applied to each segment. The output from one part will then be used as the input for the next. Thus the problem will be solved by coupling the discrete ordinates and Monte Carlo transport methods using their respective geometries but always using the same cross-section input. With this technique, three-dimensional geometries will be limited to "have-to" regions, and the overall computing time may be greatly reduced.

Some coupled transport problems have already been performed at ORNL both in reactor shield studies and in weapons shield studies (see Section 10.0), but the interfacing of the methods has not been refined to the extent that it can be said that hybrid methods are generally available. Work is now in progress on a general program called DOMINO[50] which will automatically couple DOT two-dimensional calculations for cylindrical geometry with MORSE three-dimensional calculations. In addition, one hybrid method is already obtainable from the Radiation Shielding Information Center (the DOT-DASH code[51]). Other hybrid systems will no doubt be added in the future. In the meantime, weapons radiation shielding problems continue to be performed by dividing them into their simplest components, as will be apparent in some of the illustrations given in Section 10.0.

7.0 ASSUMPTIONS AND TECHNIQUES USED IN RADIATION TRANSPORT CALCULATIONS

Traditionally calculations of the penetration of weapons radiation into a shielded structure are divided into at least two parts: (1) a calculation of the free-field environment (the radiation that is transported through the atmosphere to the outer surface of the structure); and (2) a calculation of the penetration into the structure. The second calculation can be performed properly only if the results from the first specify the number of neutrons and gamma rays incident on the various structure surfaces, together with their energies and angles of incidence. If time-dependent results are needed to obtain information on peak pulses of radiation, then the results must also specify the time intervals in which the radiations arrive.

Early attempts (circa 1945 to 1955) to establish the free-field radiation environment produced by weapons detonations were based almost entirely on data obtained during weapons tests. While such tests yielded valuable information on total radiation exposures and effects, they gave very little data that could be used as a basis for determining the character of the radiations producing those effects. In fact, at the time atmospheric tests were being performed, few persons had realized that the energies and directions of the incident radiations were required for shield design; moreover, the experimental techniques and instrumentation were not yet sufficiently advanced to obtain the information in that detail. Thus the measurements that are available from weapons tests can at best be used only for gross comparisons with calculated results that have been obtained by the transport methods developed subsequently (see Section 6.0).

Calculations of radiation environments produced by nuclear weapon detonations have covered a gamut of conditions and assumptions that are still being refined.[52] The first free-field calculations were limited to the case of a burst in an infinite homogeneous medium of air (constant air density). More recently it has become possible to consider the presence of the ground below the air burst (see Section 6.1 on "Geometries"),

but even in these cases a constant air density is normally used, the assumption being that for burst altitudes important to structure design the effect of air density variations with burst height is negligible. Using a constant air density excludes consideration of variations in the density due to the blast wave, but this effect is not important for neutrons or gamma rays emitted directly from the weapon since they will have been transported before the air is disturbed by the blast wave. The blast wave may have some effect on the spatial distribution of capture gamma rays produced in the atmosphere, but in the capture gamma-ray calculations performed to date variations in the spatial distribution have not been considered. The blast wave will definitely affect the distribution of fission-product gamma rays, and for that and other reasons special techniques have been developed to calculate fission-product gamma-ray transport (see Section 9.4).

In spite of the advances that have been made in the calculational methods, several simplifying assumptions regarding the description of the weapon have remained necessary. As was pointed out in Section 6.1, the use of a point source is essential and justifiable. A second assumption is that the source radiations are emitted instantaneously from the point source rather than over a finite period of time. Since neither the transmutation of the nuclei in the medium to other nuclei nor changes in the locations of the nuclei are considered in the calculations, the assumption of an instantaneous source does not affect the results so long as the quantity of interest is proportional to the total radiation reaching any given location.[q]

Another common assumption is that the source radiations are emitted isotropically from the point source. With this assumption, the geometric attenuation of the radiation will reduce the number of particles per unit area reaching a location at a distance R from the source such that it can-

[q] Even if the transmutation effects and changes in the locations of the nuclei were considered, they probably would not substantially alter the total amount of radiation reaching a given location. In particular, the movement of the nuclei would be so slight as to be essentially undetectable.

not exceed the total number given off at the burst point divided by $4\pi R^2$. (The material attenuation produced by interactions would of course effect a further reduction.) The isotropic assumption is a good assumption only if the weapon is spherically symmetric. If a particular weapon is known to emit radiation asymmetrically, then the worst situation should be the case calculated. (One investigation of the effects of asymmetric emission was conducted by McGregor and Straker.[53])

The energies of the neutrons or gamma rays given off by the point isotropic instantaneous sources have been represented in the calculations in two different ways. When the energy spectrum of a weapon is known and information on that particular weapon is needed, the spectrum is divided into discrete energy intervals and all energy intervals are treated in the same calculation. While the energies and directions of the particles arriving at the position of interest will be deducible from the results, a correlation between the original energies of the source particles and the energies and directions of the incident radiations cannot be obtained. If information on the transport of source radiation of specific energies is desired, then separate calculations must be performed for each energy interval or for monoenergetic sources representing each energy interval. In many cases the separate calculations are performed with no particular weapons spectrum in mind, but the source energies are chosen so that they cover all energies that would be present in any weapon. In addition to allowing the various radiation components contributing to the total effect to be isolated and studied, this procedure provides sets of "transport data" for individual source energies that can be weighted and folded together to obtain corresponding results for a particular weapon emitting particles with a spectrum of energies.

In applying sets of transport data that have been calculated for monoenergetic sources to particular weapons, it must be remembered that the transport data apply only for the conditions under which they were obtained -- that is, for the same air density, the same burst height, and the same compositions of the air and ground. If other conditions are to be assumed for the weapons detonation, then corrections must be introduced in the calculations.

A correction for any difference in the air densities is made by adjusting ranges in the two media with the scaling law

$$R_2 = R_1(\rho_1/\rho_2) \quad ,$$

where R_1, R_2 (in cm) and ρ_1, ρ_2 (in g/cm^3) are the ranges and densities in atmospheres 1 and 2 respectively. This expression specifies that at range R_1 in the medium having density ρ_1 the same number of grams per square centimeter will exist as at range R_2 in the medium having a density ρ_2. Thus the dose at range R_1 in medium 1 will have undergone the same material attenuation (through interactions) as the dose at range R_2 in medium 2, in which case the dose at R_2 in medium 2 can be obtained from the dose at R_1 in medium 1 if an additional correction is made for the difference in the geometric attenuation resulting from the change in ranges. The geometric correction is made with the scaling law

$$D(R_2) = D(R_1) \times (R_1/R_2)^2 \quad ,$$

where $D(R_1)$ is the density-corrected dose and $D(R_2)$ is the dose at the range desired.

Use of these scaling laws is illustrated by the following sample problems:

Prob. A

At what range from a point source in an atmosphere with a density of 1.27 mg/cm^3 would the material attenuation of radiation be the same as that at a range of 1150 m in an atmosphere with a density of 1.11 mg/cm^3?

$$R_2 = 1150 \text{ m } (1.11/1.27)$$
$$= 1010.2 \text{ m.}$$

Prob. B

Given that the material attenuation at a range of 1010.2 m from a point source in medium 2 is the same as that at a range of 1150 m in medium 1, and given that the dose at the 1150-m range in medium 1 is 1.2×10^4 rads, what is the dose at the 1010.2-m range in medium 2?

$$D(R_2) = (1.2 \times 10^4 \text{ rads}) \ (1150/1010.2)^2$$
$$= 1.554 \times 10^4 \text{ rads.}$$

A word of caution: These scaling laws do not simply adjust the doses at a given range for different atmospheric densities, and neither do they adjust the doses for a given atmospheric density to different ranges.

Corrections for differences in the burst height are not nearly so clear cut, and this particular facet of free-field calculations is still receiving considerable attention. In general, however, for ranges beyond about 600 m it can be assumed that the results obtained for an infinite-air medium represent an upper limit and that for a given slant range the dose on the air-ground interface decreases with decreasing burst height because of absorption of particles in the ground. For positions close to ground zero, however, the ground appears to act more as a reflector than as an absorber, in which case the dose would be increased above that for an infinite medium. The ground also affects the energy and angular distributions of the incident radiations (see discussion in Sections 9.2 and 9.3).

Effects due to differences in the constituents in the air would be expected to be negligible and thus are usually ignored. Effects due to differences in ground composition also are usually ignored; however, when the radiations of concern are secondary gamma rays and the point of interest is near the ground, the number of gamma rays produced increases with increasing water content in the ground owing to the capture of thermal neutrons in hydrogen. To date this effect has not been sufficiently investigated for correction factors to be offered.

8.0 RESPONSE FUNCTIONS APPLIED TO TRANSPORT DATA

The data obtained from the many radiation transport calculations performed over the years vary in the degree of detail in which they are presented. The most useful results are given as particle fluences (number of particles per unit area) and particle fluxes (number of particles per unit area per unit time) as functions of both the energies and the angles of the incident particles at the positions of interest. With the proper conversion factors, or response functions, these fluences and fluxes can be converted to various quantities that are related to damage induced in exposed materials. (In the case of free-field calculations, it can be assumed that with the large distances involved, the field of incident particles at some particular range does not vary over a given surface, e.g., over the side of a building.)

The two basic mechanisms by which radiation creates damage in materials are ionization and atomic displacement. The damage induced by ionization is related to the amount of energy deposited in the specified material and is given either in units of ergs per gram of material or in units of rads, where 1 rad is equivalent to an energy deposition of 100 ergs per gram of material. The damage induced by atomic displacement is related to the number of atoms that are displaced from their usual sites in crystal lattices (also as a result of energy deposition). Displacement, which is usually significant only in a material whose crystal structure is highly ordered and whose properties are affected by changes in this structure, is given in terms of the amount of damage caused by some standard exposure (e.g., for neutrons, frequently in terms of the damage that would be caused by an equivalent number of 1-MeV neutrons).

When damage to the human body is of concern, the response function is tissue kerma or dose, both of which are ionization responses. When damage to the silicon components of electronics systems is of concern, the response function is silicon ionization or silicon displacement. Values of these various response functions are given in Tables 7 and 8 for energy intervals commonly used in radiation transport calculations.

Table 7. Neutron Response Functions

Energy Group No.	Upper Energy (MeV)	Tissue Dose Responses [rads/(neutron/cm^2)]		Tissue Kerma Response[b] [(ergs/g)/(neutron/cm^2)]	Silicon Ionization [(rads-Si)/(neutron/cm^2)]	Silicon Displacement [(equiv. 1-MeV neutrons/cm^2)/(neutron/cm^2)]
		Henderson Single-Collision Dose	Snyder-Neufeld Multicollision Dose			
1	1.5(+1)[a]	5.46(−9)	7.0(−9)	6.36(−7)	9.28(−10)	2.51
2	1.22(+1)	5.13(−9)	7.0(−9)	5.74(−7)	1.07(−9)	2.40
3	1.0(+1)	4.84(−9)	7.08(−9)	5.17(−7)	1.06(−9)	2.48
4	8.18(0)	4.61(−9)	6.72(−9)	4.87(−7)	7.21(−10)	2.21
5	6.36(0)	4.44(−9)	6.03(−9)	4.5(−7)	2.39(−10)	1.99
6	4.96(0)	4.13(−9)	5.43(−9)	4.21(−7)	7.96(−11)	1.86
7	4.06(0)	4.01(−9)	4.83(−9)	3.98(−7)	5.54(−11)	1.75
8	3.01(0)	3.39(−9)	4.48(−9)	3.43(−7)	5.01(−11)	1.72
9	2.46(0)	3.15(−9)	4.33(−9)	3.15(−7)	4.43(−11)	1.64
10	2.35(0)	3.09(−9)	4.23(−9)	3.05(−7)	3.79(−11)	1.49
11	1.826(0)	2.64(−9)	3.96(−9)	2.63(−7)	2.74(−11)	1.22
12	1.108(0)	1.97(−9)	3.30(−9)	2.05(−7)	2.09(−11)	9.67
13	5.5(−1)	1.12(−9)	1.73(−9)	1.27(−7)	1.25(−11)	5.93
14	1.11(−1)	2.29(−10)	7.0(−10)	4.0(−8)	5.80(−13)	2.22
15	3.35(−3)	[c]	6.07(−10)	1.96(−9)	0	0
16	5.83(−4)		6.72(−10)	3.67(−10)	0	0
17	1.01(−4)		5.35(−10)	1.17(−10)	0	0
18	2.9(−5)		3.88(−10)	1.11(−10)	0	0
19	1.067(−5)		3.42(−10)	1.62(−10)	0	0
20	3.059(−6)		3.27(−10)	2.65(−10)	0	0
21	1.125(−6)		3.22(−10)	4.26(−10)	0	0
22	4.14(−7)		3.2(−10)	9.36(−10)	0	0

[a]Read: 1.5×10^1.

[b]Divide kerma values by 100 to obtain rads. The converted values should be comparable to Henderson's single-collision doses; however, they are based on better cross sections.

[c]These response functions were developed in 1959 for the purpose of correlating calculations and measurements; they were not extended to energies lower than about 0.003 MeV because the instruments cannot detect neutrons with energies that low.

Table 8. Gamma-Ray Response Functions

Energy Group No.	Upper Energy (MeV)	Henderson Tissue Dose $\left[\frac{\text{rads}}{(\text{photon/cm}^2)}\right]$	Silicon Ionization $\left[\frac{(\text{rads-Si})}{(\text{photon/cm}^2)}\right]$
1	10.0	2.42(−9)*	2.83(−9)
2	8.0	2.07(−9)	2.82(−9)
3	6.5	1.76(−()	1.83(−9)
4	5.0	1.59(−9)	1.46(−9)
5	4.0	1.27(−9)	1.17(−9)
6	3.0	1.08(−9)	9.62(−10)
7	2.5	8.75(−10)	8.15(−10)
8	2.0	7.35(−10)	6.90(−10)
9	1.66	6.44(−10)	5.89(−10)
10	1.33	5.30(−10)	4.84(−10)
11	1.0	4.45(−10)	3.93(−10)
12	0.8	3.50(−10)	3.19(−10)
13	0.6	2.56(−10)	2.35(−10)
14	0.4	1.77(−10)	1.68(−10)
15	0.3	1.22(−10)	1.17(−10)
16	0.2	6.60(−11)	7.60(−11)
17	0.1	3.90(−11)	1.02(−10)
18	0.05	8.37(−11)	9.57(−10)

*Read: 2.42×10^{-9}.

It is noted in Table 7 that three different tissue responses are given for neutrons. Actually several concepts of dose and kerma exist, and considerable confusion has arisen with respect to their definitions and interrelationships. No attempt will be made here to distinguish between them, but the reader is referred to a discussion of the various tissue responses presented by Stevens and Claiborne in Chapter 2 of the *Weapons Radiation Shielding Handbook*.[54,m] The responses used most frequently are those for Henderson single-collision doses, which are somewhat lower than the Snyder-Neufeld multicollision doses. The behavior of all the responses are essentially the same, however, so that conclusions based on the Henderson doses will apply to the other responses as well.

Frequently the transport results available for general use will have already been multiplied by response functions. For example, most of the free-field transport results discussed in the following sections are Henderson doses.

9.0 CALCULATIONS OF FREE-FIELD RADIATION ENVIRONMENTS

The free-field initial radiation environments considered in nuclear weapons shielding calculations fall into four categories: (1) prompt gamma-ray environments, (2) neutron environments, (3) secondary gamma-ray environments, and (4) fission-product gamma-ray environments. This section discusses some of the calculations that have been made in each of these categories and points out their possible applications. In most cases the input data and calculational models needed for such applications can be obtained through the Radiation Shielding Information Center,[r] Oak Ridge National Laboratory, P.O. Box X, Oak Ridge, Tennessee, 37830; however, because of the numerous subtleties involved it is recommended that expert assistance be sought before any major calculations are attempted. Government installations that have the capability for performing such calculations include the Air Force Weapons Laboratory, Ballistic Research Laboratory, Naval Weapons Evaluation Facility, Oak Ridge National Laboratory, Lawrence Livermore Laboratory, and Los Alamos Scientific Laboratory. Several private companies also have expertise in this area.

9.1. Prompt Gamma-Ray Environments

The pathways most likely to be followed by prompt gamma rays from the point of detonation to structures located some distance away are depicted in Fig. 2. The only gamma rays emitted from the weapon that can reach a structure are those that travel directly to the structure without undergoing any type of interaction (the uncollided component) plus those that are directed toward the structure after undergoing Compton scatterings (see Section 5.2.3). The scattered gamma rays reaching the structure are most likely to be gamma rays of initially high energy that were emitted in the general direction of the structure and are scattered to it through small angles. High-energy gamma rays that are scattered through large angles lose so much energy that they are no longer important. Thus the possibility that a significant number of prompt gamma rays will

[r] RSIC services in this area are supported by the Defense Nuclear Agency.

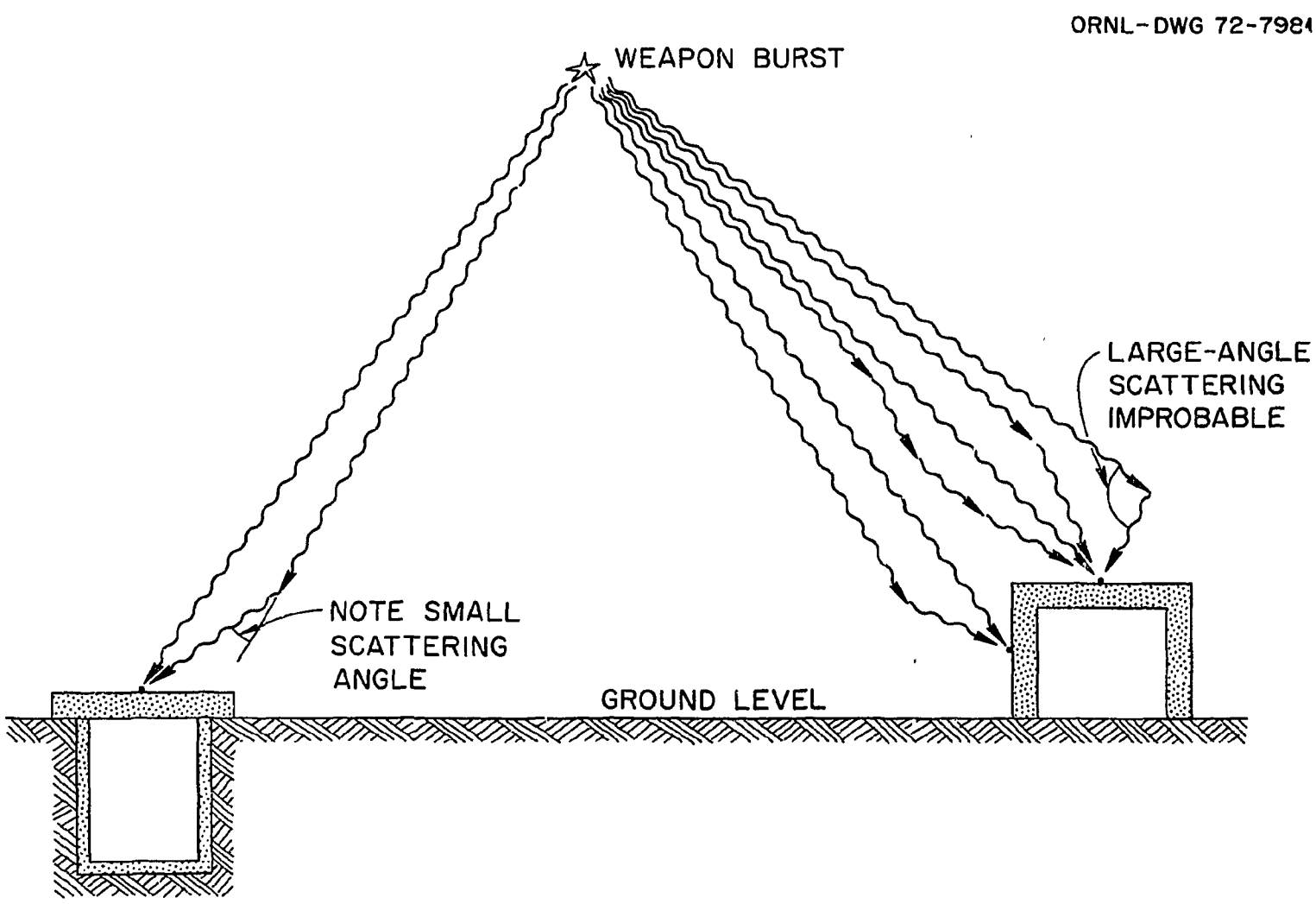

Fig. 2. Typical Pathways Followed by Prompt Gamma Rays from Weapons Burst to Structures. Most scattered gamma rays that reach a structure have scattered through small angles.

enter the back side of a structure is very remote and protection against prompt gamma rays usually can be provided by a barrier between the detonation point and the point of interest. In fact, as has already been pointed out (see Section 2.2.1), it is quite possible that fission gamma rays, together with other prompt gamma rays, can be ignored because they are greatly attenuated in the weapon and in the atmosphere and their relative numbers are very small compared to the gamma rays produced outside the weapon. However, each situation must be assessed, particularly if arrival rates are of concern, since prompt gamma rays can generate a high pulse of radiation for a short duration. Calculations of prompt gamma-ray transport are relatively easy and accurate, with three possible techniques described below.

9.1.1. Application of Dose Buildup Factors

The development of the "buildup factor" technique for estimating prompt gamma-ray doses is based on the penetration of gamma rays from point sources in infinite homogeneous media, which has been well understood for many years. Early in the 1950's the moments method of analysis of gamma-ray transport in infinite media was developed by Spencer and Fano[55,56] and utilized by Goldstein and Wilkins[57] in rigorous calculations of gamma-ray penetration in a number of materials for point isotropic sources having energies of 0.5, 1, 2, 3, 4, 6, 8, and 10 MeV. The results from these calculations are still considered to be good standards whose accuracies are limited only by the detail used in the calculations and by the accuracy of the gamma-ray interaction cross sections, and the latter have not changed drastically during the last 20 years. These early calculations did not include air as one of the media, and neither did they yield results that are doubly differential (in energy and angle). Thus they would appear to be inapplicable to calculations of free-field environments for weapons spectra. However, Goldstein and Wilkins offered a technique for applying their results to materials other than those for which the calculations were performed. Summarizing their data in terms of "dose buildup factors," where a dose buildup factor is defined as a ratio of the total dose to the uncollided dose, they recommended an interpolation (or extrapolation) method

for determining buildup factors for other homogeneous or near-homogeneous mixtures. This technique was used by Contreras et al.[58] to extrapolate the buildup factors for water and aluminum to air, which they and others then applied to the calculation of prompt gamma-ray doses produced by weapons.

The use of the buildup factor involves first calculating the uncollided dose from a point isotropic monoenergetic source for each energy group in the weapons spectrum. This is done by determining the uncollided fluence, which is easily calculated from the expression

$$\Phi_u(R) = S \frac{e^{-\mu(E)R}}{4\pi R^2} \quad ,$$

where $\Phi_u(R)$ is the uncollided fluence at a distance R (number of gamma rays per cm^2 at R); S is the source strength at the burst point (number of gamma rays of energy E given off by the source); $\mu(E)$ = macroscopic total cross section for gamma rays of energy E in the medium (cm^{-1}); $e^{-\mu(E)R}$ = material attenuation factor, which is the probability that a gamma ray of energy E travels a distance R (cm) in the medium without undergoing an interaction; and $1/4\pi R^2$ = geometric attenuation for a point source (cm^{-2}). This expression is used for each energy group, and the corresponding uncollided dose is obtained by applying the appropriate fluence-to-dose conversion factor. The scattered dose is then included by applying the appropriate dose buildup factor to the uncollided dose for each energy group. The total dose is the sum of the doses from all the energy groups. (Note: The terms "uncollided" and "unscattered" are not synonymous, since uncollided refers to photons that have been neither scattered nor absorbed.)

Although the extrapolated buildup factors have given results that are in good agreement with those obtained by other methods (see next section), buildup factors for air obtained directly from moments method calculations are now available. These buildup factors, calculated by Clark,[59] are plotted in Fig. 3 as a function of the relaxation lengths

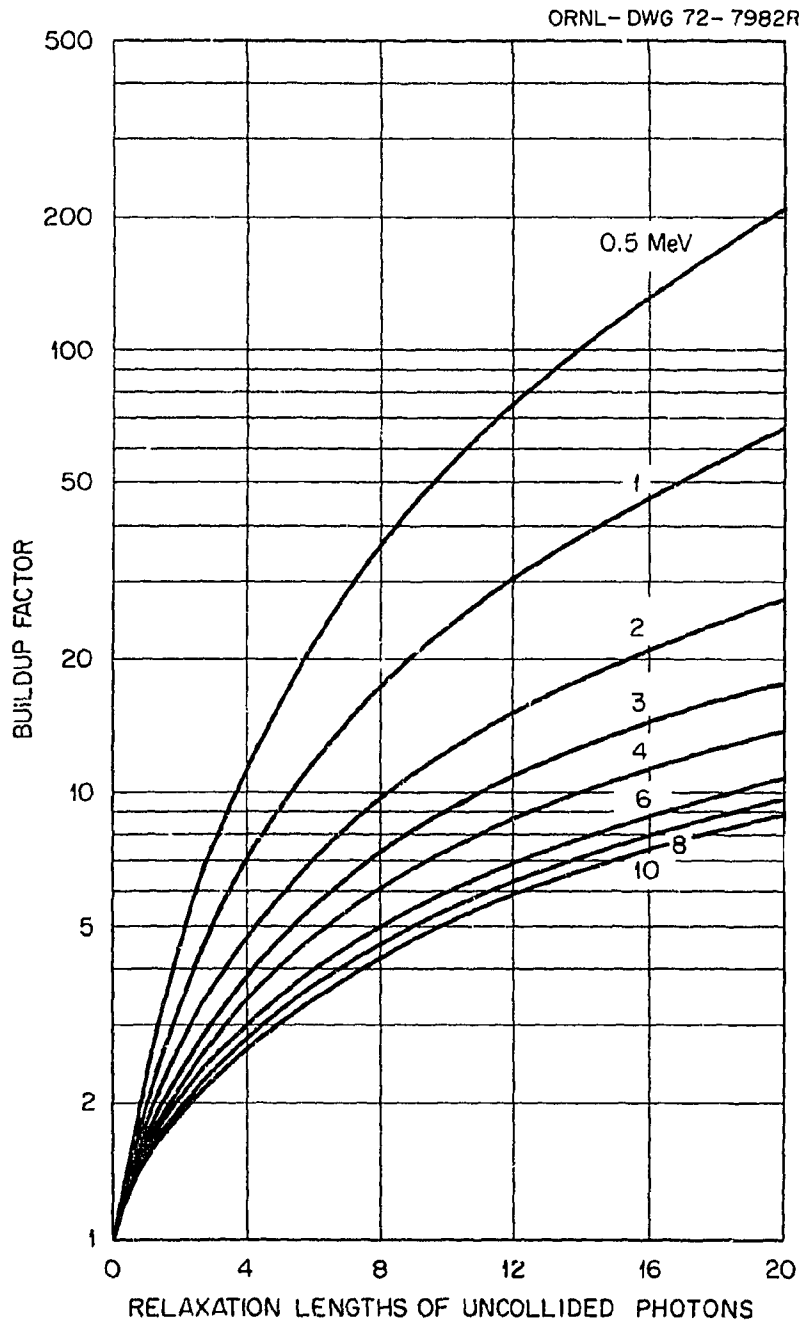

Fig. 3. Gamma-Ray Dose Buildup Factors for Air. (From Clark, ref. 59.)

of the uncollided photons from sources having energies of 0.5, 1, 2, 3, 4, 6, 8, and 10 MeV. A relaxation length, usually denoted by the symbol λ, is the thickness of material required to attenuate radiation by a factor of e. For air, the relaxation length varies from 11.5 g/cm^2 for 0.5-MeV gamma rays to 50 g/cm^2 for 10-MeV gamma rays. (The common use of λ as the reciprocal of the macroscopic cross section is correct only for special cases.)

The advantage of the buildup factor method is that an estimate of the prompt-gamma-ray environment can be obtained with an ordinary desk computer. However, dose buildup factors can be used only to estimate total prompt gamma-ray doses produced by a weapon and they can be used only for infinite media (e.g., infinite air). Differential quantities such as energy and angular distributions must be obtained by other techniques, and corrections for the presence of the ground must be made.

9.1.2. Application of Transport Data Sets

A second technique for estimating prompt gamma-ray environments is the application of sets of transport data, as is mentioned in Sections 7.0 and 8.0. Sets of gamma-ray transport data for a variety of sources in an infinite-air medium in the energy and angular detail required for shielding calculations were made available from the Monte Carlo calculations of Wells.[60] These results, subsequently extended by Marshall and Wells,[61] can be folded and weighted to represent a given weapons gamma-ray emission spectrum; however, they must be corrected for the effect of the ground and for any differences in atmospheric density (see Section 7.0). The general unavailability of gamma-ray transport data sets that consider ground interactions is mostly due to the fact that prompt gamma rays are not expected to be important, especially for a shielded position.

In his original calculations, Wells used source energies of 0.5, 1, 2, 4, 6, and 8 MeV. To see how well doses obtained with the Monte Carlo data compared with those obtained with the extrapolated buildup factors of Contreras et al.,[58] he applied both techniques to a fission source having the spectral characteristics given in Table 9 (from ref. 62).

Table 9. Spectrum of Gamma Rays Emitted from Samples of ^{235}U[a]

Photon Energy (MeV)	Number of Photons[b]	Photon Energy (MeV)	Number of Photons[b]
0.1	17000	4.1	84.0
0.2	12800	4.2	77.0
0.3	10100	4.3	70.0
0.4	8200	4.4	64.5
0.5	6700	4.5	59.0
0.6	5500	4.6	54.0
0.7	4650	4.7	49.0
0.8	3900	4.8	45.0
0.9	3300	4.9	41.0
1.0	2900	5.0	37.5
1.1	2500	5.1	34.5
1.2	2150	5.2	31.5
1.3	1890	5.3	28.5
1.4	1650	5.4	26.0
1.5	1460	5.5	23.8
1.6	1300	5.6	21.7
1.7	1150	5.7	19.6
1.8	1010	5.8	17.9
1.9	900	5.9	16.4
2.0	800	6.0	14.9
2.1	710	6.1	13.4
2.2	630	6.2	12.2
2.3	560	6.3	11.1
2.4	505	6.4	10.1
2.5	450	6.5	9.1
2.6	400	6.6	8.2
2.7	355	6.7	7.4
2.8	315	6.8	6.7
2.9	285	6.9	6.0
3.0	255	7.0	5.4
3.1	230	7.1	5.00
3.2	205	7.2	4.45
3.3	184	7.3	4.00
3.4	165	7.4	3.55
3.5	150	7.5	3.15
3.6	135	7.6	2.80
3.7	123	7.7	2.35
3.8	112	7.8	2.15
3.9	101	7.9	1.85
4.0	92	8.0	1.63

[a]From ref. 62; table represents composite of data from refs. 6 and 7.
[b]Arbitrary units.

The attenuations of the resulting doses were in good agreement, as is shown in Fig. 4. [In Fig. 4 the range (depth) in air is given in terms of grams per square centimeter, and thus the curve can be applied to any air density. The curve shows that within 300 g/cm^2, which for an air density of 1.1 mg/cm^3 would correspond to 2727 m (~1.7 miles), the fission gamma-ray dose emitted from the source is reduced to 1/10,000th its original value. Note, however, that this is material attenuation only; that is, the geometric attenuation is not included.]

The Marshall and Wells[61] calculations extended the low-energy limit of the original results from 0.1 MeV to 0.01 MeV and added a 10-MeV source. It is these data, which were reprinted in Chapter 6 of the *Weapons Radiation Shielding Handbook*,[63,m] that are most frequently used to construct prompt gamma-ray transport results for a weapon when information on the energies and angles of incidence at a distance from the weapon is needed.[64] The data were obtained for an air density of 1.293 g/liter, and the results are given as scattered gamma-ray fluxes at ranges of 164.6, 640.1, 914.4, 1097, and 1372 m (0.1 to 0.8 mile) as functions of the angles of arrival and the energies of arrival. The uncollided fluxes (at source energy) are also given for each range.

The total dose rates (multiplied by $4\pi R^2$) produced by these fluxes are shown in Fig. 5. Dividing these values by $4\pi R^2$ gives the dose rate in rads per hour at a distance R from the source per gamma ray emitted per second at the source. The relative contributions to these dose rates by the scattered and uncollided components can be deduced from Table 10.

More recently angular and energy fluxes of scattered gamma rays from point isotropic sources in an infinite homogeneous air medium obtained from a moments method calculation have been published by O'Dell.[65] His results are given in great detail for distances out to 30 mean free paths and thus could be used in the same manner as the Marshall and Wells data and with considerably more confidence since the moments method does not have the statistical variances inherent in the Monte Carlo method. Also, O'Dell no doubt had the benefit of the very latest gamma-ray cross sec-

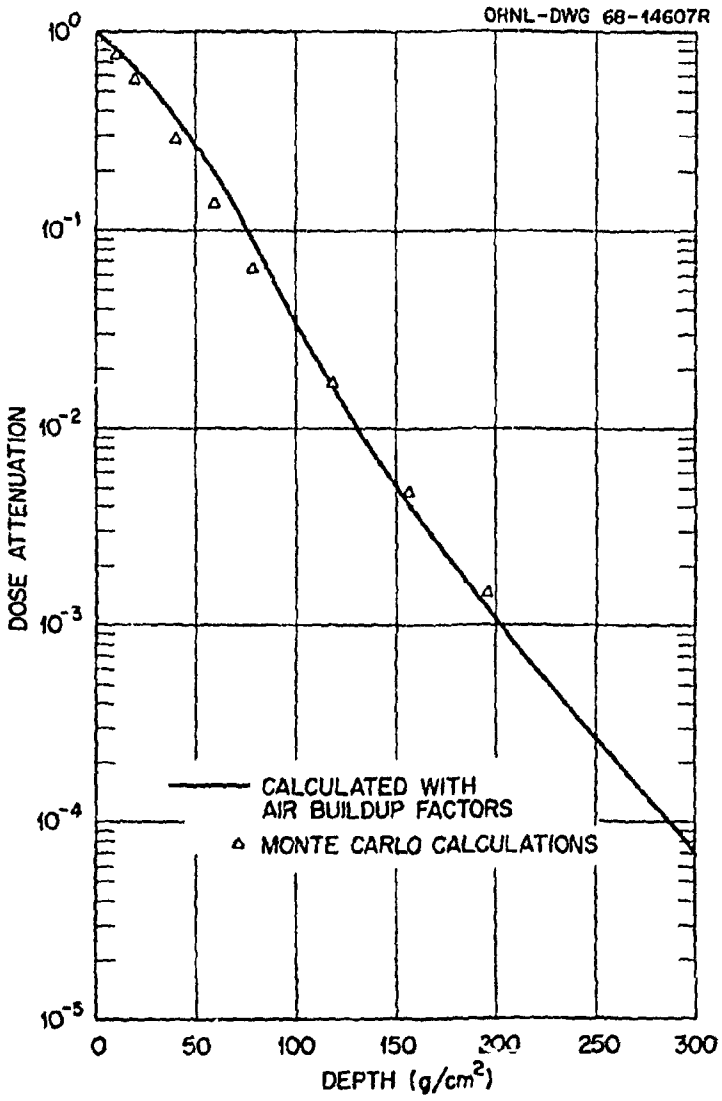

Fig. 4. Attenuation of Fission Gamma Rays in Infinite-Air Medium (No Geometric Effect). Based on ^{235}U fission spectrum of Table 9; buildup factors for air from Contreras et al., ref. 58; Monte Carlo calculations from Wells, ref. 60.

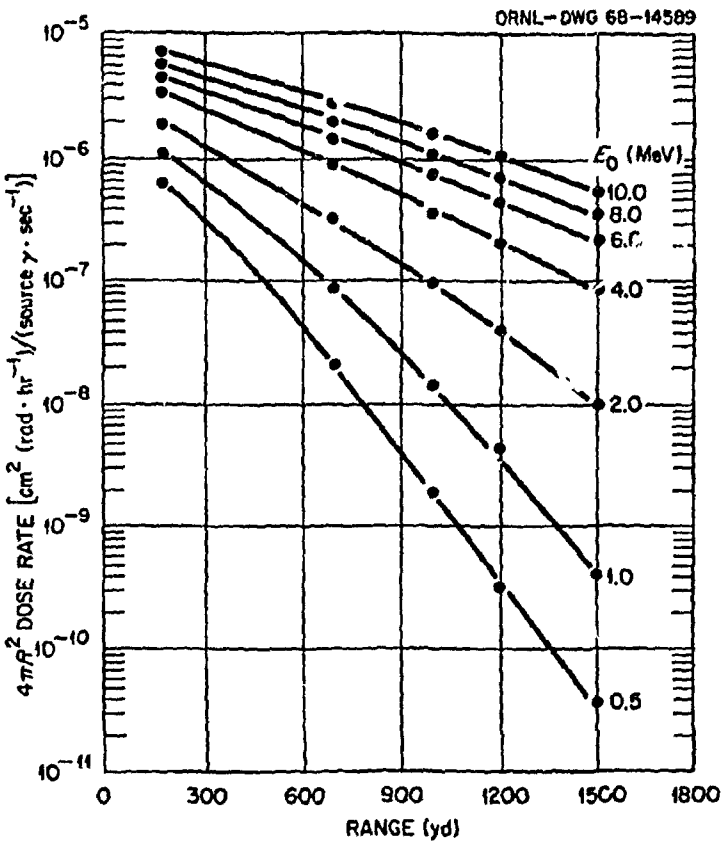

Fig. 5. Gamma-Ray Dose Rate in Infinite Medium of Air as a Function of Range from Point Monoenergetic Sources. (From Marshall and Wells, ref. 61.)

Table 10. Uncollided and Scattered Dose Rates at Various Ranges from Monoenergetic Gamma-Ray Sources in an Infinite Air Medium[a, b]

E_0 (MeV)	R (m)	$4\pi R^2 \cdot$ Dose Rate $\left[\frac{cm^2 \cdot rad \cdot hr^{-1}}{source\ \gamma \cdot sec^{-1}}\right]$		
		Uncollided	Scattered	Total
0.5	164.6	0.1467(−6)[c]	0.4638(−6)	0.6105(−6)
	640.1	0.7140(−9)	0.2172(−7)	0.2243(−7)
	914.4	0.3306(−10)	0.1991(−8)	0.2024(−8)
	1097.0	0.4264(−11)	0.3150(−9)	0.3193(−9)
	1372.0	0.1975(−12)	0.3514(−10)	0.3534(−10)
1.0	164.6	0.4387(−6)	0.6472(−6)	1.086(−6)
	640.1	0.7931(−8)	0.7863(−7)	8.656(−8)
	914.4	0.7831(−9)	0.1416(−7)	1.494(−8)
	1097.0	0.1673(−9)	0.4045(−8)	4.214(−9)
	1372.0	0.1652(−10)	0.3968(−9)	4.133(−10)
2.0	164.6	0.1071(−5)	0.8516(−6)	1.923(−6)
	640.1	0.6958(−7)	0.2646(−6)	3.342(−7)
	914.4	0.1437(−7)	0.8141(−7)	9.578(−8)
	1097.0	0.5021(−8)	0.3504(−7)	4.006(−8)
	1372.0	0.1037(−8)	0.8961(−8)	9.998(−9)
4.0	164.6	0.2492(−5)	0.9188(−6)	3.411(−6)
	640.1	0.3773(−6)	0.5323(−6)	9.096(−7)
	914.4	0.1270(−6)	0.2453(−6)	3.723(−7)
	1097.0	0.6144(−7)	0.1449(−6)	2.063(−7)
	1372.0	0.2068(−7)	0.6221(−7)	8.289(−8)
6.0	164.6	0.3720(−5)	0.8516(−6)	4.572(−6)
	640.1	0.8008(−6)	0.7264(−6)	1.527(−6)
	914.4	0.3301(−6)	0.4389(−6)	7.690(−7)
	1097.0	0.1829(−6)	0.2747(−6)	4.576(−7)
	1372.0	0.7540(−7)	0.1411(−6)	2.165(−7)
8.0	164.6	0.4881(−5)	0.8352(−6)	5.716(−6)
	640.1	0.1265(−5)	0.8089(−6)	2.074(−6)
	914.4	0.5804(−6)	0.5390(−6)	1.119(−6)
	1097.0	0.3453(−6)	0.3768(−6)	7.221(−7)
	1372.0	0.1584(−6)	0.2066(−6)	3.650(−7)
10.0	164.6	0.6352(−5)	0.9096(−6)	7.262(−6)
	640.1	0.1836(−5)	0.9215(−6)	2.758(−6)
	914.4	0.8974(−6)	0.6515(−6)	1.549(−6)
	1097.0	0.5568(−6)	0.4723(−6)	1.029(−6)
	1372.0	0.2721(−6)	0.2732(−6)	5.453(−7)

[a] Air density = 1.293 g/liter.
[b] Table from ref. 63.
[c] Read: 0.1467×10^{-6}.

tions. Unfortunately, however, his data are limited to source energies ranging between 0.1 and 3.0 MeV, which covers only a fraction of the energy spectrum of the gamma rays emitted from a nuclear weapon.

9.1.3. Direct Application of Transport Methods

The best method for predicting the prompt gamma-ray environment produced by a weapon is to perform a complete transport calculation for that weapon under the detonation conditions. For this to be done, the energy spectrum of the gamma rays emitted from the weapon must be known. The transport method should be a two-dimensional discrete ordinates code or a Monte Carlo code, both of which could treat interactions in the ground below the detonation (see Section 6.0), and the most accurate set of cross sections should be employed.

Because it is peak delivery rates of prompt gamma rays that are usually of most concern rather than the total number of gamma rays, time-dependent transport calculations are likely to be required. Such calculations should consider the period of time over which the weapon is emitting gamma rays, as well as the time required for the gamma rays to be transported. As pointed out in Section 7.0, calculations with a time-dependent source have in general not been tackled; however, an investigation by Claiborne and Engle[66] with several simplifying assumptions has shown that peak dose rates produced by gamma rays from fissioning ^{235}U can be bracketed by calculations for an instantaneous source. In their calculations, which were performed in one-dimensional geometry with the discrete ordinates ANISN code, they assumed that the source was located at the center of a sphere of air surrounded by a 120-cm-thick concrete shield, with the front face of the concrete at ranges of 500, 1000, and 5000 m (0.3, 0.6, and 3 miles) from the source. The doses incident on the shield were calculated for each shield range both with and without Compton scattering being treated. The calculation treating scattering yielded total doses (scattered plus uncollided) and the other yielded uncollided doses only. Upper limit dose rates were obtained by dividing

the total doses by the pulse width of the device (1 to 8 shakes), which is equivalent to assuming that the scattered and uncollided gamma rays arrived at the shield surface simultaneously; lower limit dose rates were obtained by dividing the uncollided doses by the pulse width, which is equivalent to assuming that the scattered gamma rays were delayed in their arrival and did not contribute to the peak pulse.

These upper and lower limits were compared with peak total dose rates obtained with the TDA code (Time-Dependent ANISN) for the same source emitting the gamma rays during time intervals that varied from 1 to 8 shakes. Comparisons for the 5000-m range are shown by the three curves in Fig. 6. It is seen that the TDA results are bracketed by the ANISN results. TDA calculations for the 1000-m and 500-m ranges were similarly bracketed by the ANISN calculations.

The same technique can be applied to real weapons spectra in calculations using geometries that more nearly represent those for an actual detonation.

9.2. Neutron Environments

The paths followed by neutrons from a weapons burst to a structure are depicted in Fig. 7. As is the case for prompt gamma rays, the neutrons reaching a structure are those that travel directly from the weapon to the structure without undergoing any type of interaction (the uncollided component) and those that are redirected toward the structure through scatterings against the nuclei of the air or ground. Neutrons can scatter either elastically or inelastically, and, in contrast to gamma rays, those that scatter at large angles do not necessarily lose a large fraction of their energy (see Sections 4.2.1 and 4.2.2). Also, neutrons can undergo a great many successive scatterings before finally being absorbed, which means that they may be incident on all exposed surfaces of a structure with energies ranging from thermal energy to the highest energy in the weapons emission spectrum. These neutrons must always be considered in a shield design, not only because of their direct effects but also

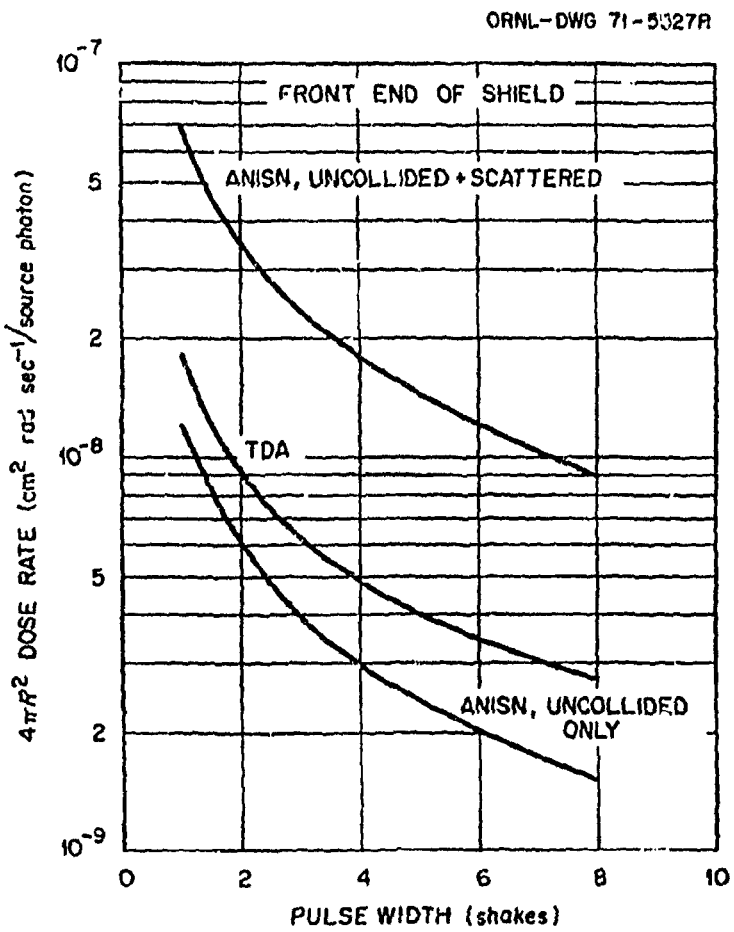

Fig. 6. Peak Gamma-Ray Dose Rate (X $4\pi R^2$) as a Function of Pulse Width for a 5000-m Range from a ^{235}U Fission Source. Air density = 0.92 g/liter. (From Claiborne and Engle, ref. 66.)

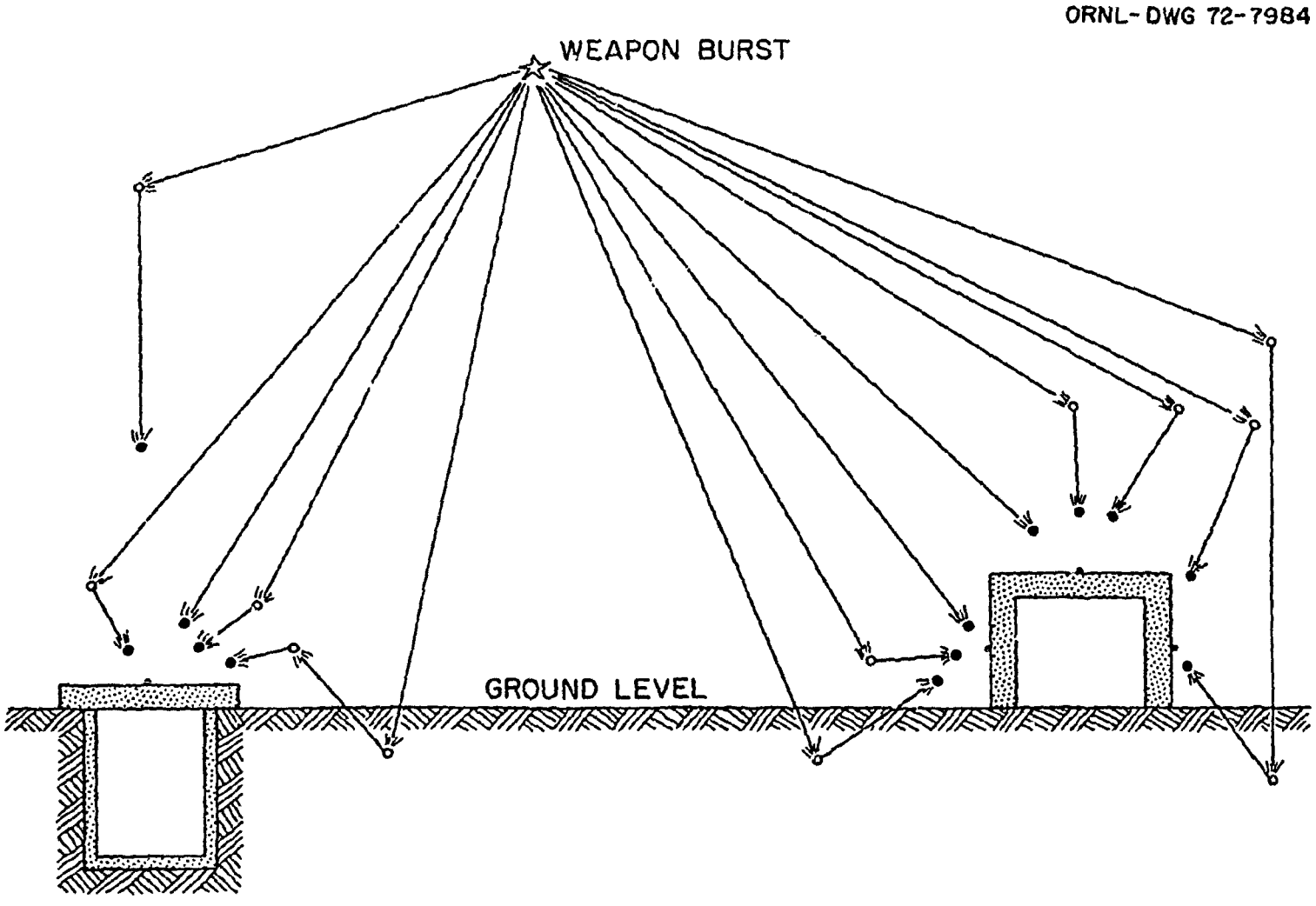

Fig. 7. Typical Pathways Followed by Fission and/or Fusion Neutrons from Weapons Burst to Structures. Open circles show where neutrons change directions by scattering, either elastically or inelastically.

because of their indirect effects (see Section 9.3). Therefore it is extremely important that the neutron free-field environment be described as accurately as possible.

Although serious attempts to predict the neutron fields produced by weapons date back to the mid-1950's, it cannot yet be said that truly accurate neutron-transport calculations can be performed. On the other hand, the situation has improved tremendously since 1965 when apparently similar calculations for the simplest problem gave such different results that the validity of the transport methods themselves was questioned. Later calculations exonerated the transport methods[67] and showed that the discrepancies were largely due to differences in the cross-section data used and to the manner in which the cross sections were input into the calculations (see Section 6.2). Subsequent comparisons of calculated integral quantities (doses) with the limited amount of experimental data available indicated which cross-section sets were the best and led to the conclusion in 1970 (ref. 68) that integral quantities could be calculated to within an uncertainty of 20-100% for ranges of approximately a mile and to within a factor of 3 for ranges of 2 to 3 miles. But this degree of success in calculating integral quantities was no doubt partially due to compensating errors in the cross sections, and when the same cross sections are used to calculate differential quantities, such as energy spectra and angular distributions, the associated errors are larger. As a result, intensive efforts have been underway during the last few years to improve the accuracy of the cross-section sets for nitrogen and oxygen, particularly those for nitrogen since that element comprises approximately 80% of the atmosphere (see Section 11.0). In the meantime, calculations of the transport of neutrons through the atmosphere have continued with the best cross sections available and several techniques have evolved for predicting free-field neutron environments produced by weapons detonations.

9.2.1. Application of Transport Data Sets

As for prompt gamma rays, one technique for calculating weapon-induced neutron environments is through the application of the transport data sets mentioned in Sections 7.0 and 8.0. The most comprehensive set of neutron air-transport data available is from a series of Monte Carlo and discrete ordinates calculations performed in 1968 by Straker[69] for an air-ground medium and in 1969 by Straker and Gritzner[70] for an infinite-air medium. In all cases the source was assumed to be a point isotropic source emitting neutrons instantaneously within an atmosphere having a density of 1.11 mg/cm^3. The calculations were performed for a number of "monoenergetic" sources (actually sources covering very small energy intervals) plus a source having a fission energy spectrum and a source having a leakage spectrum typical of that for an intermediate-yield thermonuclear weapon. Some of the results were time dependent in the sense that the times of arrival at the points of interest were determined.[s] The calculations for the air-ground medium were performed primarily for a source height of 15 m, which for most weapons is equivalent to a surface burst, but a few additional calculations were done for a source height of 343 m. A summary of the cases calculated is given in Table 11, and the energy spectra of the fission

[s]As contrasted to a time-dependent source (see Section 7.0).

Table 11. Summary of Cases Included in Neutron Air-Transport Calculations by Straker and Gritzner*

Source Energy (MeV)	Spatial Range of Calculations (m)				
	Time-Independent Cases			Time-Dependent Cases	
	Infinite Air	15-m Source Height	343-m Source Height	Infinite Air	15-m Source Height
12.2–15 (~14)	4800	1500	1500	1500	1375
10.0–12.2	1800	1500			1375
8.18–10.0	1800	1500			1375
6.36–8.18	1800	1500			1375
4.06–6.36	1800	1500			1375
2.35–4.06	1800	1500			1375
1.1–2.35	1800	1500			1375
0.11–1.11	1800	1500			1375
0.0033–0.11	1800	1500			
Fission	4800	1500	1500	1500	1375
Typical thermonuclear	1800		1500		1375

*Reported in refs. 69 and 70.

and thermonuclear sources are given in Table 12 in the energy group format used for the calculations. This thermonuclear spectrum was supplied by B. D. Diven of Los Alamos Scientific Laboratory.

Table 12. Thermonuclear and Fission Neutron Energy Source Spectra

Energy Group No.	Upper Energy (MeV)	Number of Neutrons per Group[a]	
		Thermonuclear[b]	Fission
1	1.5(+1)[c]	7.06(−2)	1.556(−4)
2	1.22(+1)	2.56(−2)	8.934(−4)
3	1.0(+1)	1.41(−2)	3.479(−3)
4	8.18(0)	1.47(−2)	1.390(−2)
5	6.36(0)	1.80(−2)	3.456(−2)
6	4.96(0)	1.70(−2)	3.505(−2)
7	4.06(0)	2.50(−2)	1.072(−1)
8	3.01(0)	1.90(−2)	8.896(−2)
9	2.46(0)	5.00(−3)	2.319(−2)
10	2.35(0)	2.80(−2)	1.203(−1)
11	1.826(0)	6.20(−2)	2.180(−1)
12	1.108(0)	8.50(−2)	1.984(−1)
13	5.5(−1)	1.02(−1)	1.404(−1)
14	1.11(−1)	3.65(−1)	1.549(−2)
15	3.35(−3)	1.22(−1)	0
16	5.83(−4)	2.4(−2)	0
17	1.01(−4)	2.00(−3)	0
18	2.9(−5)	0	0
19	1.067(−5)	0	0
20	3.059(−6)	0	0
21	1.125(−6)	0	0
22	4.14(−7)	0	0

[a]The individual energy groups here were used for the infinite-air medium; they were grouped as indicated by the braces for the air-ground medium.
[b]Spectrum supplied by B. D. Diven, Los Alamos Scientific Laboratory.
[c]Read: 1.5×10^{1}.

The transport results from these calculations were obtained in great detail. For the time-*in*dependent (or time-integrated) cases, neutron fluences and neutron doses were determined as functions of the distance from the source, of the energy of the incident neutrons, and of the angles of arrival. For the time-*de*pendent cases, fluxes and dose rates were obtained for a smaller number of the same variables. With results in this

detail available for eight different monoenergetic sources ranging in energy from 0.0033 to 15 MeV, it is possible to predict differential quantities of the radiation fields produced by almost any weapon under the same conditions by folding and weighting the data to correspond to the weapons emission spectra.[64] If it is known that the energy spectrum of neutrons leaking from a weapon is predominantly a fission spectrum, the transport data for the fission source can be used directly; that is, the data need only be multiplied by the number of neutrons leaking from the weapon.[t] Similarly, if the typical thermonuclear leakage spectrum is assumed, the transport data for that source can be used directly.

The massive amount of data produced by these calculations precludes their publication in any single document; however, the results are available on magnetic tape from the Radiation Shielding Information Center, which can also supply the editing and folding codes required to apply them to specific weapons. Because the neutrons produced within a weapon will be either fission neutrons or the approximately 14-MeV neutrons produced by the fusion reaction (the fusion neutrons are covered in these calculations by the 12.2- to 15-MeV source energy band), Straker[71] examined the results for these two sources to determine their relative importance and also to investigate the effects of the ground on the differential quantities required for shielding calculations. Some of his conclusions are as follows:

(1) In infinite air the total neutron dose produced per source neutron is higher for the 14-MeV source than for the fission source at all ranges. This is illustrated by the solid curves in Fig. 8, which shows the attenuation of the neutron doses from the two sources. At a range of 1400 m, the neutron dose from a fission source is only 35% of that from a 14-MeV source.

---

[t] The likelihood that the neutrons *leaking from* a weapon will have a fission energy spectrum is remote, since the fission neutrons produced within the weapon will interact with the weapon materials and the energy spectrum will change.

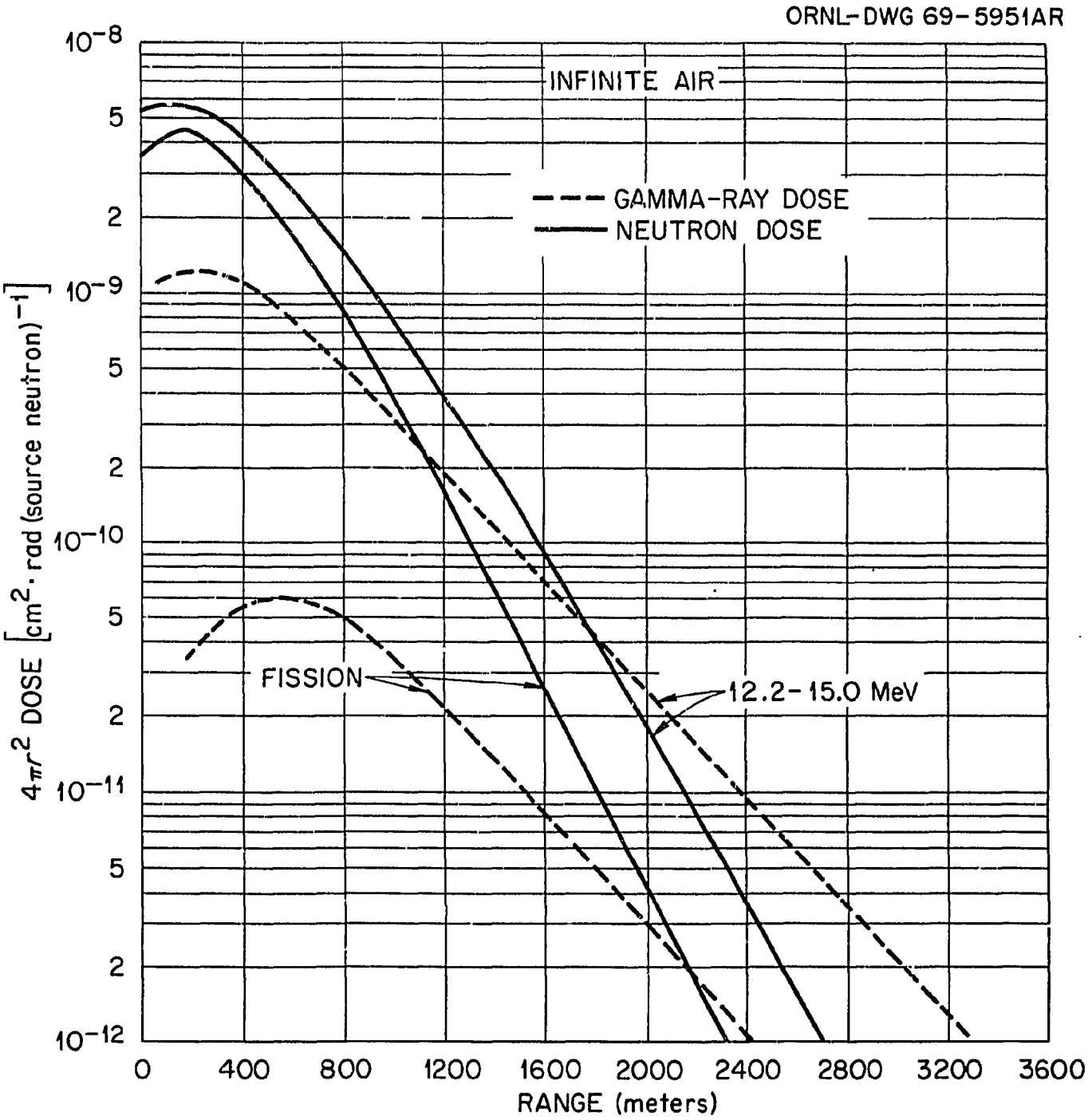

Fig. 8. Neutron and Secondary Gamma-Ray Doses Due to Fission and 12.2- to 15-MeV Neutron Sources in Infinite Air. (From Straker, ref. 71.)

(2) The effect of the ground is to increase the total neutron dose within some minimum range and to decrease it at all other ranges. The effect is approximately the same for both sources for a given source height and a given slant range. For example, for an air-ground medium with a 15-m source height, the dose from either source is about 50% of the dose in an infinite-air medium at a slant range of 400 m and about 20% at a slant range of 1400 m. For a 343-m source height, these percentages change to 89% for a slant range of 600 m and 50% for a slant range of 1400 m.

(3) At large ranges, the energy spectrum of the neutrons as a function of range from either source is approximately the same in an air-ground medium as it is in an infinite-air medium, but the magnitudes of the fluences in each energy group of the spectrum are reduced in the air-ground medium by about the same factor that the total dose is reduced at the same range.

(4) The neutron component most affected by the ground is the thermal-neutron component. At ranges close to the source (~100 m) the number of thermal neutrons on the air-ground interface can be as much as a factor of 100 greater than the number of thermal neutrons at the same range in infinite air. Also, at these ranges the thermal-neutron fluences produced on the interface by the fission source are a factor of 3 higher than those produced by the 14-MeV source. At large ranges the effect of the ground on the thermal-neutron component diminishes greatly. [The magnitude of the thermal-neutron fluence is particularly significant with respect to the production of secondary gamma rays (see Section 9.3).]

(5) The angular variation of the neutron dose from either source is approximately the same in the air-ground medium as in an infinite-air medium.

(6) At large ranges (~900 m), the neutron dose *rates* from either source are lower in an air-ground medium than in an infinite-air medium.

(7) The peak neutron dose rates due to 14-MeV neutrons are higher by factors of 5 to 8 than those due to fission neutrons in both air-ground and infinite-air media.[u]

(8) At a range of 900 m (∿0.6 mi), the peak neutron dose rate from a 14-MeV source is delivered between 1.8×10^{-5} sec and 2.0×10^{-5} sec, at which time the dose rate in an air-ground medium (source height of 15 m) is 65% of that in an infinite-air medium.

(9) At a range of 900 m, the peak neutron dose rate from a fission source is delivered between 2.7×10^{-5} sec and 5.4×10^{-5} sec in an air-ground medium (source height of 15 m), but it is delivered between 5.4×10^{-5} sec and 9×10^{-5} sec in an infinite-air medium. The peak rate in the air-ground medium is lower than that in infinite air by about a factor of 2.

Prior to the Straker calculations, Mooney and Wells,[72] as part of the DNA Handbook effort,[m] had applied a 1962 set of neutron air-transport data calculated by Ritchie and Anderson[73] to several classes of weapons and had arrived at another significant conclusion: the energies and angular distributions of the neutrons have only a weak dependence on the slant range for ranges greater than 300 m. The significance of this conclusion is that for the ranges of interest to shielding, beyond some minimum range, a single energy spectrum and single angular distribution of the incident neutrons is a reasonable approximation of the radiation field description to be used in shielding calculations performed for a particular weapon detonated at a given height regardless of the structure location and regardless of the air density. Later, upon examining the results from an unpublished Straker calculation for the thermonuclear source at a height of 100 m, Mooney reaffirmed this conclusion. As a result, Mooney and Wells used representative energy and angular distributions to describe the radiation fields incident on various structures for all ranges beyond the minimum range (see Section 10.0).

---

[u] See also Fig. 10 discussed under Section 9.3.

From conclusions 3 and 5 listed above it would appear that the required energy and angular distributions could be obtained from infinite-air calculations and that only their magnitudes need be corrected for the presence of the ground. Not enough evidence is available to support this statement unequivocally; however, even before most of the above conclusions were published, it had been assumed by some investigators that Straker's and Gritzner's transport data sets for "monoenergetic" sources in infinite air could be used to predict the neutron fields produced by any weapon at any height above the ground. In particular, Harris, Lonergan, and Huszar[74] had used the data sets as a basis for developing parametric models that describe neutron transport in the atmosphere. These models are in turn used as a basis in the ATR code (for Air Transport of Radiation) for constructing neutron environments for given weapons by folding operations that use considerably less computer time that would be required if the transport results were folded directly. Corrections are introduced to transform the parameterized homogeneous air results to other constant densities or to nonuniform air densities. Corrections for an air-ground interface are also included. The code is structured to allow the user a maximum degree of flexibility in calculating different problems, with a minimum number of restrictions on the input data. This system, which has only recently become available from the Radiation Shielding Information Center, should present the simplest and cheapest method for predicting detailed weapons neutron environments for a range of conditions.

The Straker transport data sets have also been applied to the calculation of neutron environments produced by specific weapons. Using the data sets for the 15-m burst height, Mooney and French,[75] again as part of the DNA Handbook effort,[m] calculated the neutron doses produced by eight representative weapons for which the number of neutrons released per weapon kiloton was known. Although Straker's transport data sets are limited to slant ranges of 1500 m, the neutron doses for the eight weapons were obtained for ranges out to 5000 m by an extrapolation procedure. The results are presented as plots of R^2 rads per weapon kiloton as a function of slant range, and a simple expression is provided that uses the plots to predict the total neutron dose produced at a given slant range by any

one of the eight weapons of any yield.[v] Variables in the expression allow corrections to be made for atmospheric density and burst height, the latter based on a variation of a "first-last collision" model originally developed by French to correct infinite-air results for air-ground interface effects.[76] The authors state that the neutron dose predicted by their method will be accurate to within 25%. Since the variation in weapon type among the eight weapons used for these calculations is rather large, the possibility that the results for at least one of the weapons is applicable to a given problem should be investigated before any large transport calculation is requested for a particular weapon. An unclassified discussion of the technique is given in a journal article.[77]

The Straker neutron transport data sets have also been used by a special working group convened by an ad hoc Subcommittee on Radiation Shielding appointed by the National Academy of Sciences' Advisory Committee on Civil Defense. This working group was charged with recommending nuclear weapons free-field environments for use in initial radiation shielding calculations for civil defense structures. Their study[78] was limited to weapons not exceeding 1 megaton and to ranges at which the maximum overpressure would be 100 psi. While these limits are lower than those with which the military is often concerned, several of their conclusions are of general interest. They determined, for example, that the thermonuclear source described in Table 12 produces a neutron-*induced* dose (this would include the secondary gamma-ray dose) at 1 mile that is equivalent to the dose produced by a weapon whose leakage neutrons are 30% 14-MeV neutrons and 70% fission neutrons. They concluded that the thermonuclear spectrum was an appropriate standard for their study. They then used Straker's transport data sets for the thermonuclear source at a 100-m height to calculate the tissue doses at slant ranges corresponding to specific overpressures produced by 40-kiloton, 300-kiloton, and 1-megaton weapons. In each case the height was adjusted by the Mooney-French tech-

---

[v] Mooney and French used their dose results for structure penetration calculations in which they assumed that the energy and angular distributions calculated by Straker for a distance of 900 m from the thermonuclear source at the 100-m height were applicable for ranges beyond 300 m for all eight weapons in any air density (see Section 10.1.1).

nique to the "triple-point" burst height, which is the height required for the mach stem to originate at the slant range corresponding to the specified overpressure. The resulting neutron doses, along with doses from other initial radiation components that will be discussed later, are given in Table 13. For reasons already discussed, the committee recommends that when their results are applied to specific structures a single energy spectrum and angular distribution be used. They specifically recommend the distributions produced by the thermonuclear source in infinite air at a range of 1200 m.

Table 13. Initial Radiation Doses at Various Slant Ranges from a Thermonuclear Weapon[a] Detonated at Triple Point Burst Heights[b]

Weapon Yield	Overpressure (psi)	Triple-Point Burst Height (m)	Slant Range (m)	Tissue Dose (rads)			
				Neutrons	Secondary Gamma Rays	Fission-Product Gamma Rays	Total[c]
40 kiloton	5	1210	2358	~1	4	<1	5
	10	900	1470	200	320	45	565
	15	785	1204	1,300	1,300	200	2,800
	20	720	1053	3,700	3,000	560	7,260
	30	625	879	12,000	8,000	1,600	21,600
	70	440	587	85,000	40,000	10,000	135,000
	100	410	528	350,000	55,000	15,000	420,000
300 kiloton	5	2350	4624				
	10	1760	2884	1	5	2.5	8
	15	1530	2362	11	40	25	76
	20	1400	2064	60	150	100	310
	30	1220	1715	430	670	560	1,660
	70	860	1150	12,000	7,800	8,400	28,200
	100	800	1037	24,000	13,000	14,000	51,000
1 megaton	5	3510	6901				
	10	2620	4304				
	15	2290	3525	<1	1	2	3
	20	2090	3080	<1	6	16	22
	30	1820	2560	10	58	160	228
	70	1280	1716	1,400	2,200	6,000	9,600
	100	1190	1547	3,800	4,800	13,000	21,600

[a]See Table 12 for weapon neutron emission spectrum.
[b]Table from ref. 78.
[c]Note that prompt fission gamma rays are not included.

In spite of the widespread use of both the infinite-air and the air-ground transport data sets, it has recently been demonstrated by Straker[79] and also by Engle and Mynatt[80] that the neutron interaction cross sections used to obtain the data sets are not now the best available. When Straker performed his original calculations he used nitrogen and oxygen cross sections identified in the Evaluated Nuclear Data File[81] as MAT 1012 and 1013 cross-section sets respectively. The continuing evaluation of nitrogen and oxygen cross sections as more information becomes available has largely been the work of P. G. Young and D. G. Foster of Los Alamos Scientific Laboratory, and in 1970 they released preliminary sets of nitrogen and oxygen cross sections identified as ENDF MAT 506 and MAT 501 respectively. Straker studied the effects of the differences in the old and new cross sections by using both sets to calculate neutron quantities comparable to those measured in several experiments. The resulting comparisons, particularly those of differential quantities, revealed deficiencies in both cross-section sets, but overall the preliminary Young and Foster cross sections gave the best integral results. Straker states that on the basis of the comparisons, calculations with the newer cross sections would give results that are good to within 20 to 30% for ranges less than 1500 m.

Somewhat later Young and Foster released cross-section evaluations[82] for nitrogen and oxygen that are included in the ENDF/B-III files. The evaluation for nitrogen, identified as ENDF 1133, is essentially the same as the preliminary MAT 506 set, but the evaluation for oxygen, identified as ENDF 1134, represents a substantial revision of the preliminary MAT 501 set. These newer cross sections were used by Engle and Mynatt[80] to calculate several types of responses, both time-dependent and time-integrated, at ranges extending out to 3000 m in infinite air, and they compared their results with those obtained from similar calculations using the cross sections originally used by Straker and Gritzner.[69,70] A comparison at a range of 2600 m shows that for a 14-MeV source the newer cross sections give an integrated Henderson single-collision dose that is approximately 30% higher, a Snyder-Neufeld multiple-collision dose that is approximately 30% higher, and a neutron ionization that is about 50% higher. For the thermonuclear source, the doses obtained with the two sets of cross sections at 2600 m

are approximately the same, but the ionization obtained with the newer cross sections is about 25% higher. One would infer from these comparisons that the integral quantities based on the Straker-Gritzner data should be adjusted upward at large ranges if the source has a hard emission spectrum. (The same inference cannot be made for sources with soft emission spectra.)

9.2.2. Direct Application of Transport Methods

While the advantages of applying transport data sets are obvious, the continuing development of cross-section sets and transport methods, plus the interest generated in specific problems, tends to encourage the direct application of a transport method to calculate the neutron environment produced by a particular weapon detonated under given conditions. The transport method most frequently applied is either a two-dimensional discrete ordinates method or a Monte Carlo method and the problem is usually tailored to yield the differential quantities required for subsequent shielding calculations. For example, if a region of weakness in the structure is obvious, the radiation incident on that region is usually calculated in greater detail. An example of this procedure is referred to in Section 10.1.4.

9.3. Secondary Gamma-Ray Environments

Unlike the prompt gamma rays and the fission and fusion neutrons, secondary gamma rays are not produced within the confines of the weapon.[w] Rather they are produced by interactions of the ubiquitous neutrons with the nuclei of the air and ground within the vicinity of the burst. Secondary gamma rays are also produced in structural materials, but the consideration of such materials is usually restricted to those in the structure of concern and the gamma-ray production is handled as part of the calculation of the penetration through the structure rather than as part of the calculation of the free-field environment.

---

[w] Except for those secondary gamma rays that are considered to be part of the prompt radiation (see Table 6).

The pathways whereby secondary gamma rays reach a structure are depicted in Fig. 9. In each case the gamma ray directed toward the structure is produced when a neutron interacts with a nitrogen or oxygen nucleus in the air or with one of the nuclei comprising the ground. If the interaction producing the gamma ray is a capture process or a charged-particle reaction (see Sections 4.2.3 and 4.2.4), the neutron itself disappears, but if the interaction is an inelastic scattering (see Section 4.2.2), the neutron continues its travel in a changed direction with reduced energy. Any of these photon-producing interactions can be preceded by a succession of neutron scatterings that alter the course of travel of a neutron and reduce its energy.

It has been recognized for many years that insofar as integral quantities are concerned the secondary gamma-ray environment is more important than the prompt gamma-ray environment, but calculations of secondary gamma-ray production and transport have been impeded by the lack of both an adequate calculational method and the required gamma-ray production cross sections. Until recent years the secondary gamma-ray environment was usually assumed to be due to capture gamma rays produced in the nitrogen of the atmosphere with all other interactions disregarded. In general, calculations of these gamma rays were based on empirical equations resulting from an analysis of gamma-ray data obtained during weapons tests. This was the procedure used in Chapter 7 of the *Weapons Radiation Shielding Handbook*.[83,m] Now more exact calculations are being attempted with various gamma-ray sources treated. It is to be pointed out, however, that the production cross sections used in the calculations are still under investigation (see Section 11.0).

9.3.1. Application of Transport Data Sets

Even with the uncertainty regarding the production cross sections, the availability of transport data sets for secondary gamma rays has outmoded the earlier empirical techniques for calculating secondary gamma-ray environments. These transport data sets are used in the same manner as those for neutrons.[64] In fact, the most comprehensive

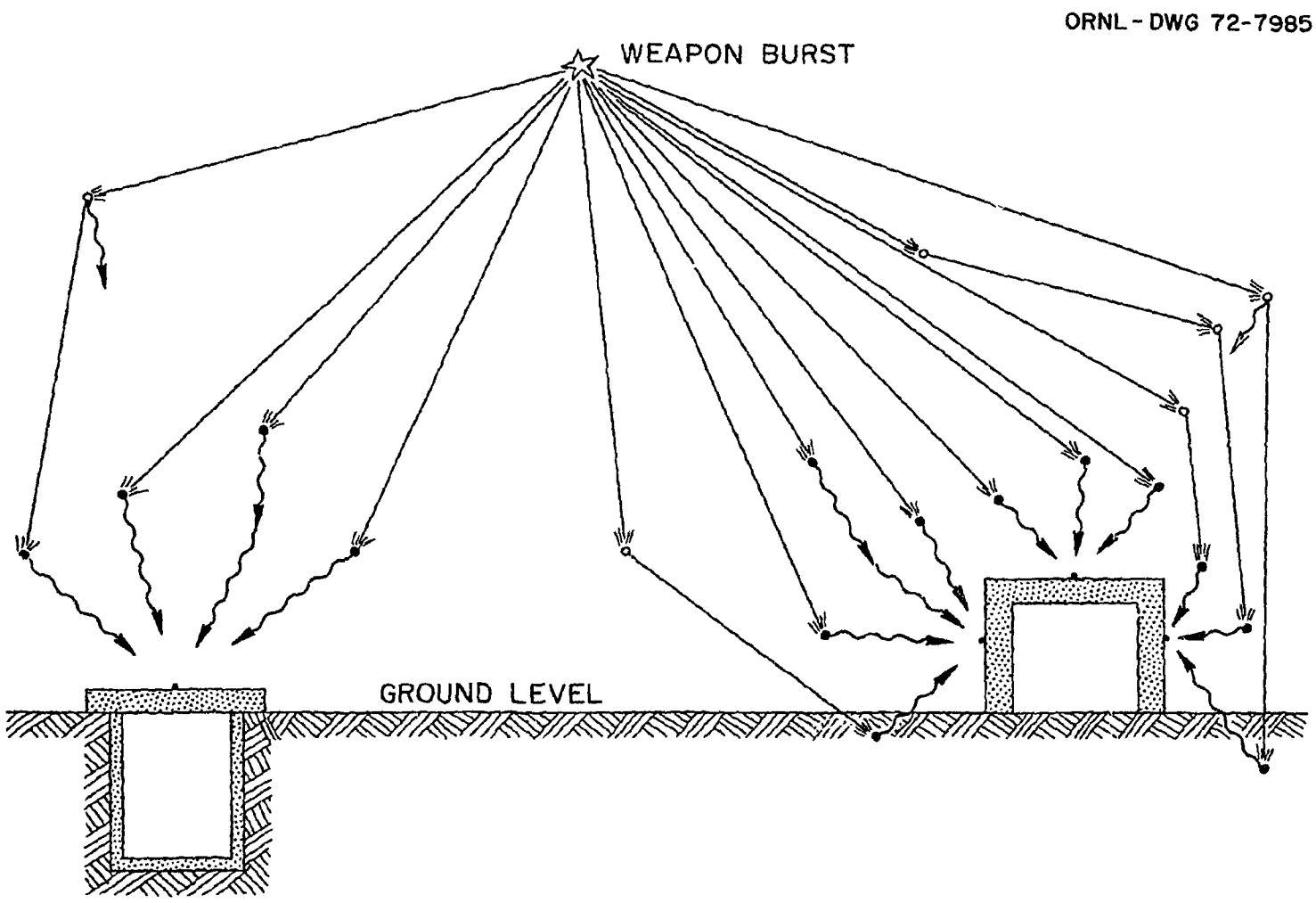

Fig. 9. Typical Pathways Followed by Secondary Gamma Rays Produced by Neutron Interactions in the Air and in the Ground. Solid circles show where neutrons are absorbed and gamma rays are born; open circles show where neutrons are scattered, with those scatterings that are inelastic producing inelastic-scattering gamma rays.

transport data sets for secondary gamma rays were obtained simultaneously with the most comprehensive sets for neutrons: in 1968 by Straker[69] for an air-ground medium and in 1969 by Straker and Gritzner[70] for an infinite-air medium (see Section 9.2.1). The calculations were coupled so that the interactions treated in the neutron transport calculations were the same interactions that produced the gamma rays, which then were treated in a gamma-ray transport calculation. Thus secondary gamma-ray transport data sets are available for all the cases listed in Table 11, and the same folding and editing codes can be used to apply the data sets to particular weapons neutron spectra.

In the summary paper of his transport calculations, Straker[71] compared the secondary gamma-ray results obtained for the 14-MeV and fission sources to determine their relative importance and the effects of the ground on the differential quantities needed for shielding calculations. His conclusions are as follows:

(1) In infinite air the total secondary gamma-ray dose produced per source neutron is higher for the 14-MeV source than for the fission source at all ranges. This is illustrated by the dashed curves in Fig. 8, which shows the attenuation of the secondary gamma-ray doses from the two sources. Over the entire range the dose from the 14-MeV source is approximately a factor of 10 higher than the dose from the fission source, which means that if the two sources were mixed (in infinite air) the 14-MeV source would contribute at least 50% of the dose if it comprised as much as 10% of the source.

(2) The effect of the ground is to increase the secondary gamma-ray dose within some minimum range and to decrease it at all other ranges. For the 14-MeV source the minimum range appears to be about 600 m, while for the fission source it is about 800 m. The increase over a larger range for the fission source is largely due to the capture of thermalized neutrons in the air and ground.

(3) At large ranges (greater than ∿600 m), the energy spectrum of the secondary gamma rays produced by the 14-MeV neutron source is approximately the same in an air-ground medium as it is in an infinite-air medium, but the magnitudes of the fluences in each energy group of the spectrum are reduced in the air-ground medium by about the same factor that the total dose is reduced at the same range.

(4) At large ranges (greater than ∿600 m), the energy spectrum of the secondary gamma rays produced by the fission source in an air-ground medium differs from that in the infinite-air medium. This, too, is apparently caused by an increase in thermal-neutron capture gamma rays and an accompanying decrease in inelastic-scattering gamma rays.

(5) At large ranges (on the order of 900 m) the angular variation of the secondary gamma-ray dose from either source is more peaked in the forward direction for the air-ground case than it is for the infinite-medium case.

(6) At short ranges (on the order of 300 m) the secondary gamma-ray dose *rates* produced by the 14-MeV source within short times (less than 10^{-5} sec) are a factor of 100 higher than those produced by the fission source in both an air-ground medium and an infinite-air medium.

(7) In the time interval between about 5×10^{-5} sec and 1×10^{-2} sec, the secondary gamma-ray dose rates produced at the 300-m range in an air-ground geometry exceed those produced in an infinite-air medium for both sources. For the 14-MeV source the difference becomes as great as a factor of 100 and for the fission source as great as a factor of 500. At greater times the secondary gamma-ray dose rates from the two sources are comparable, both for the infinite-air medium and for the air-ground medium. Thus the higher total doses produced by the 14-MeV source are almost entirely due to the higher dose rates from fast-neutron interactions in the early time intervals.

The dose rates due to secondary gamma rays that arrive at the detector within the same time interval in which the neutrons arrive are referred to as short-time dose rates [x] It was observed during these calculations that for a given source and geometry, the time distributions of the short-time secondary gamma-ray dose rates are similar to those of the neutron dose rates and that this similarity holds at all ranges. This is apparent from Fig. 10, in which the time distributions of the dose rates at various ranges from a 14-MeV source and a fission source, both at an altitude of 15 m, are normalized on the time scale by the minimum time required for radiation to reach the detector and on the dose scale by the total dose. Results for slant ranges of 150, 300, 600, 900, and 1200 m are given. The difficulty in distinguishing between the curves clearly illustrates that the time distributions of both the neutron dose rates and the secondary gamma-ray dose rates may be obtained to a first approximation (plus or minus a factor of 3) from a single curve fit to these results. The difference in shape between the distributions for the two sources shows that the source energy spectrum is an important factor in determining the time-dependent dose rate.

Straker's and Gritzner's secondary gamma-ray transport data sets for an infinite medium have been used by Harris, Lonergan, and Huszar[74] to develop parametric models that describe secondary gamma-ray transport in the atmosphere. These models, along with those for neutron transport (see Section 9.2.1), are included in the ATR code, which should present the simplest and cheapest method for predicting secondary gamma-ray weapons environments for a range of conditions.

As part of the DNA Handbook effort,[m] Mooney and French[75,77] used Straker's data sets for the 15-m source height to calculate the secondary gamma-ray environments for the same eight weapons for which they calculated the neutron environments (see Section 9.2.1). Again they extrapolated the Straker data, which was limited to ranges of 1500 m, out to

---

[x] Note, however, that the dose rates due to prompt gamma rays will arrive even earlier.

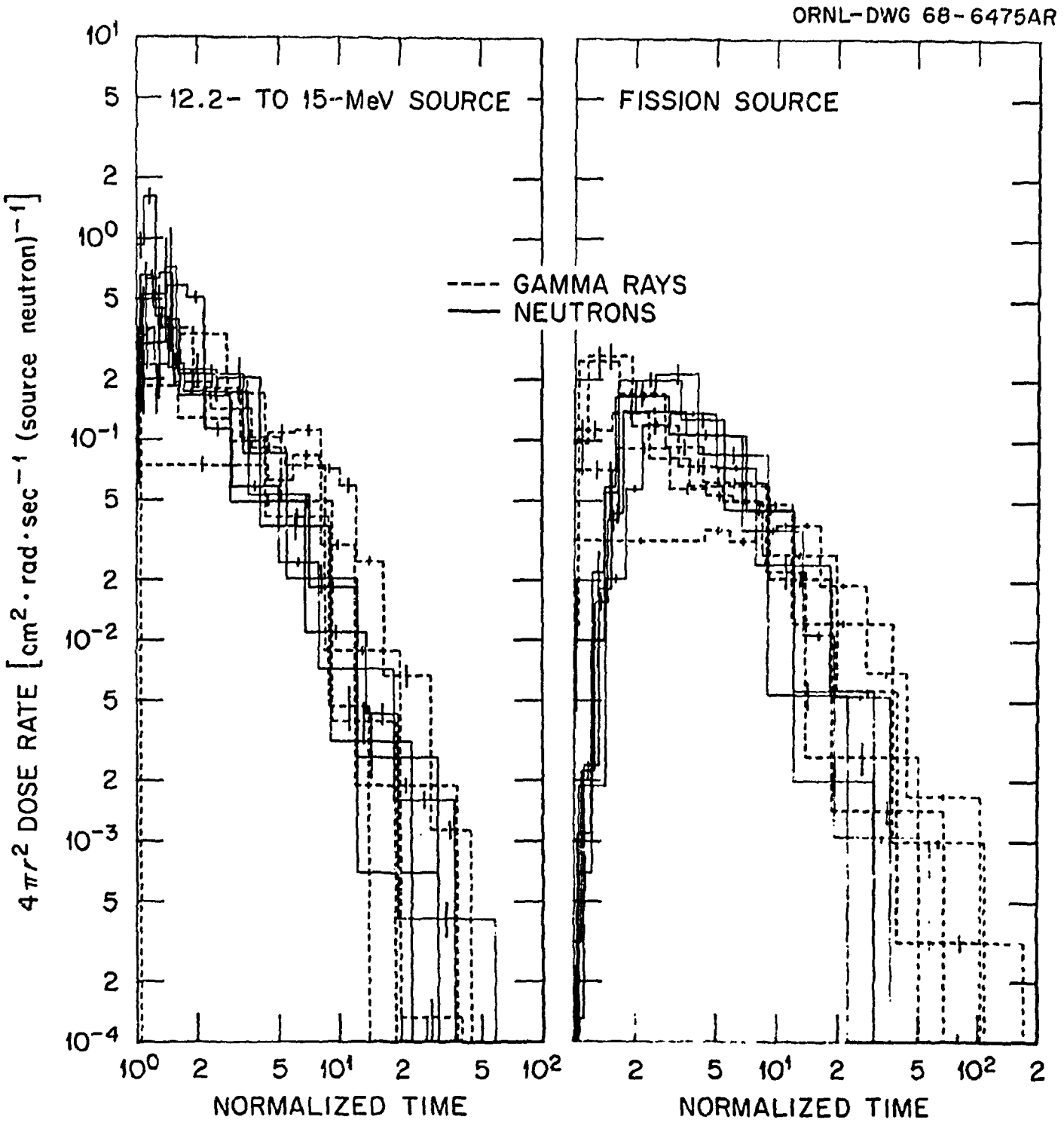

Fig. 10. Comparison of Neutron and "Short-Time" Secondary Gamma-Ray Dose-Rate Time Distributions Produced at Various Ranges from a 12.2- to 15-MeV Neutron Source and a Fission Neutron Source. Distributions for all ranges are normalized to the minimum travel time. (From Straker, ref. 71.)

ranges of 5000 m. While they believed their extrapolations of the neutron data were reasonably accurate, they do not express the same confidence in the gamma-ray data; however, they do offer their gamma-ray dose data as conservative estimates, which like the neutron data can be corrected for differences in the source heights and atmospheric densities. Therefore if an approximation of the secondary gamma-ray environment for a particular weapon is needed, the possible similarity of the weapon to one of the eight calculated by Mooney and French should be investigated.[y]

The special working group that was convened for civil defense studies[78] (see Section 9.2.1) also calculated secondary gamma-ray doses based on Straker's transport data sets. The results they obtained for 40-kiloton, 300-kiloton, and 1-megaton thermonuclear weapons detonated at triple point burst heights are included in Table 13.[z]

As he did for the neutron calculations (see Section 9.2.1), Straker used the best cross sections available for the production of secondary gamma rays in the atmosphere and air, collecting them from several sources. However, in subsequent calculations[79] he has shown that his original cross-section sets do not yield the same transport results as those obtained with the ENDF MAT 506 nitrogen set and the MAT 501 oxygen set released by Young and Foster in 1970. The differences are most noticeable for gamma rays produced by the interactions of neutrons with energies greater than

---

[y]Mooney and French used their dose results for structure penetration calculations (see Section 10.2), for which they assumed that the energy and angular distributions calculated by Straker for a distance of 1200 m from the thermonuclear source at a height of 100 m were applicable for ranges beyond 300 m for all eight weapons in any air density. They point out, however, that the secondary gamma-ray fluences calculated by Straker had shown no tendency toward reaching equilibrium even at the 1500-m range and the distributions at 1200 m were selected for lack of a better technique.

[z]This group also recommends that the energy and angular distributions calculated for a distance of 1200 m from the thermonuclear source be used for shield penetration calculations, but they suggest the infinite-air distributions rather than those for a 100-m source height.

8 MeV. But Straker also found that the secondary gamma-ray results obtained with both sets of cross sections compared favorably with the data from at least one experiment. He concluded that a choice between the two sets was not obvious.

The matter was investigated further in the Engle and Mynatt[80] calculations of several types of responses at ranges out to 3000 m in infinite air (see Section 9.2.1). They found that the later Young and Foster secondary gamma-ray production cross sections (identified as ENDF/B-III 1133 and 1134)[82] give gamma-ray dose and ionization responses that are lower than those obtained with the original cross sections used by Straker and Gritzner.[69,70] The largest difference is between the ionization responses, which at 2600 m is a factor of about 1.8 lower for the 14-MeV source and a factor of 1.6 lower for the thermonuclear source. The Henderson doses obtained for both sources are also lower when the new cross sections are used, but not so much so.

In further investigation, Engle and Mynatt found that when they employed a hybrid cross-section set consisting of the Young and Foster neutron-interaction cross sections and the Straker gamma-ray production cross sections, the results were 20 to 30% higher than those obtained with the original Straker set. The difference is consistent with the higher neutron fluences obtained by Engle and Mynatt with the Young and Foster neutron cross sections (see Section 9.2.1).

The implication from all these comparisons is that the Straker and Gritzner secondary gamma-transport data are probably conservative for hard neutron source emission spectra; however, adjusting them upward by about 30% would ensure conservatism. (Again, adjustments for sources with relatively soft emission spectra, such as a fission source, are not necessarily indicated.)

9.3.2. Direct Application of Transport Methods

As is the case for other radiation environments, the most accurate way to predict the secondary gamma-ray environment produced by a particular weapon is to perform a complete transport calculation for that weapon under the detonation conditions. The weapons neutron emission spectrum will be required, and the latest gamma-ray production cross sections should be used. The calculation will probably be performed either with a two-dimensional discrete ordinates method or a Monte Carlo method, either of which can treat interactions in the ground (see Sections 6.3 and 6.4).

9.4. Fission-Product Gamma-Ray Environments

The pathways whereby fission-product gamma rays reach a structure are depicted in Fig. 11.[aa] As pointed out in Section 2.2.5, fission-product gamma rays are emitted from the debris cloud created by the weapon burst while the shape of the cloud is constantly changing and its height above the ground is increasing. During the initial stages of the cloud formation, the gamma rays reaching the point of interest are emitted directly from the debris, and it is this fraction of the fission-product gamma rays that is important insofar as *initial* radiation is concerned. If the burst is a surface or near-surface burst, materials from the ground are entrained in the cloud, after which the cloud assumes a toroidal shape as it begins its ascent. As it ascends, the hot gases in the cloud begin to cool and condense. Very soon solid particles are formed which consist of a mixture of activated and nonactivated materials from the weapon and ground, the fission products being included in the activated materials. The heavier particles immediately begin their descent toward the ground, all the time emitting gamma rays. The onset of fallout depends on the weapon yield and burst height. Typical times for a near-surface burst are 7 sec for a 100-kiloton weapon and 70 sec for a 10-megaton weapon.[84] Although the

---

[aa] For completeness, Fig. 11 also depicts pathways for activation gamma rays produced by neutron interactions in the ground; however, these gamma rays are neglected in calculations of initial radiation environments.

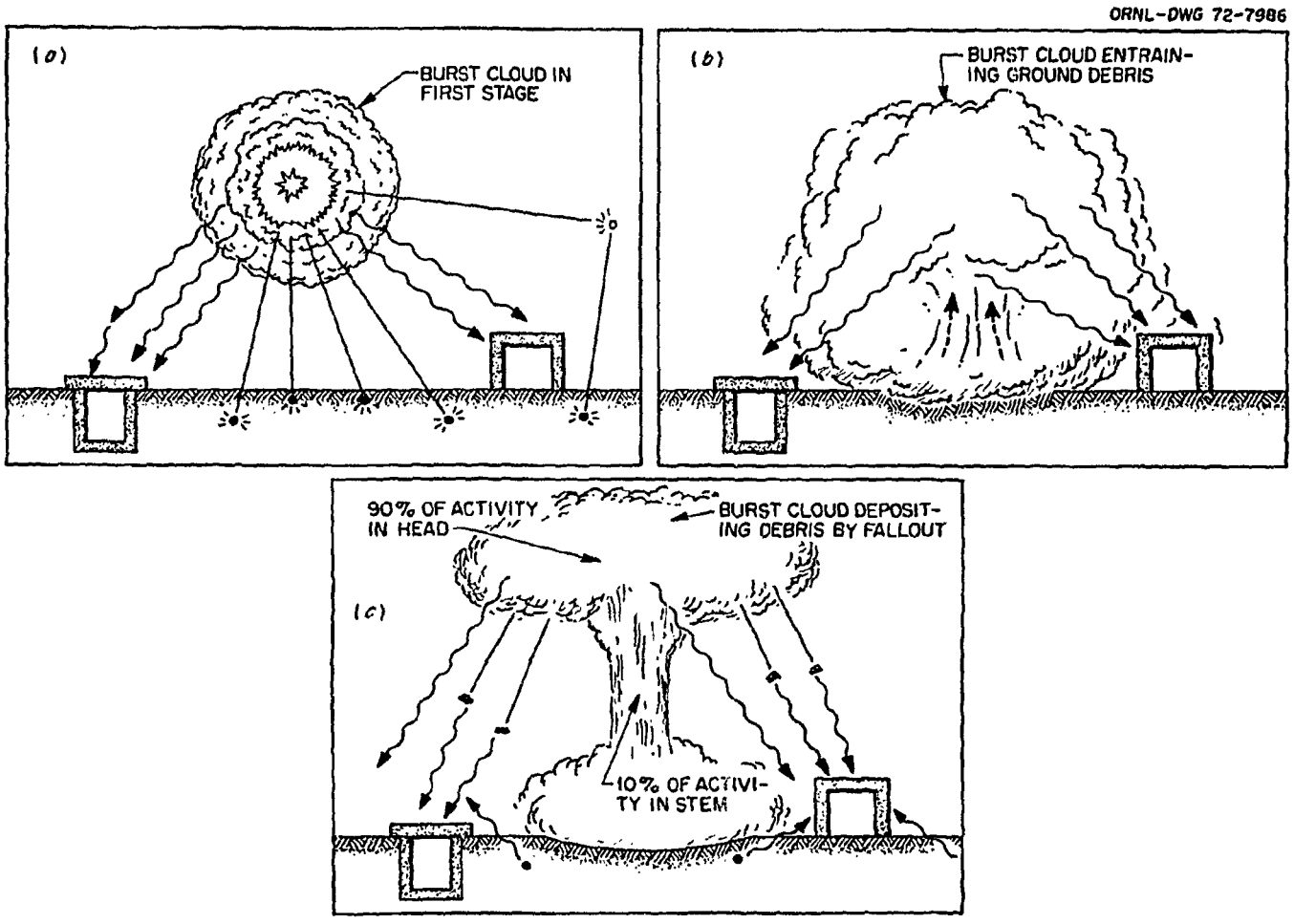

Fig. 11. Typical Pathways Followed by Fission-Product Gamma Rays and Activation Gamma Rays During First Minute of Cloud Formation (Near-Surface Burst). (*a*) Fission-product gamma rays are emitted directly from cloud and neutrons emitted in burst are captured in ground; (*b*) fission-product gamma rays continue to be emitted from cloud and activated residue is picked up in cloud; and (*c*) fission-product gamma rays and activation gamma rays are emitted both from cloud and from fallout particles, and activation gamma rays are emitted from ground.

7 sec is well within the 1-min period assigned to initial radiations, the gamma rays from the fallout particles make a negligible contribution to the initial dose compared with those emitted directly from the cloud. Thus they are not included in calculations of the free-field measurements.

The many parameters influencing the distribution of fission-product gamma rays within a volume surrounding a weapon burst make estimates of the radiation environment they produce extremely difficult. These parameters include the height of burst, the air density and pressure, the expansion and rise time of the debris cloud, the total weapon yield, the fission fraction of the weapon, the distribution of the fission products within the cloud, the decay rates of the fission products, and the enhancement of the fission-product gamma rays at some locations by the shock wave. This enhancement results from the creation of a near-vacuum within the fireball as the shock wave moves outward and a concomitant decrease in the mass of air that a gamma ray would encounter during its travel to the position of interest. If the position happens to be inside the vacuum, then there will be essentially no material attenuation of the gamma rays.

Several techniques have been used for calculating fission-product gamma-ray environments. A relatively simple model was developed by Wells,[60] who used a point source in an undisturbed atmosphere. The source's gamma-ray emission spectrum was assumed to be that measured for fission products 10.7 sec after fission.[22] To this spectrum Wells applied his original gamma-ray transport data sets for infinite air (see Section 9.1.2). Only the source intensity was allowed to vary with time. While the results from such calculations can be differential in energy and angle, as is required for shield penetration calculations, they obviously suffer from the neglect of several of the important factors.

In contrast with Wells' "simple" method, York et al.[85] developed a computer program which considers essentially all of the factors influencing the distribution of fission-product gamma rays. In principle, this program could calculate fission-product gamma-ray distributions precisely;

however, a calculation with the program is very large and uncertainties associated with the input compromise the reliability of the results.

A third approach has been to calculate fission-product gamma-ray doses (but not energy and angular distributions) from empirical relations that fit available weapons test data. This was the technique used in Chapter 7 of the *Weapons Radiation Shielding Handbook*,[83,m] the equations used being those of Loewe et al.[86] The assumption in this technique is that the test data consist entirely of secondary gamma rays and fission-product gamma rays (no prompt gamma rays) and that the two can be distinguished by their times of arrival. When this technique is used the energy and angular distributions required for shield penetration calculations are obtained from point-source calculations such as those performed by Wells (see above).

Recently the DNA Handbook effort[m] has yielded a method that approaches the simplicity of the Wells' method but accounts for most of the factors that influence the distribution of the fission-product gamma rays. In developing the method, Mooney and French[75,87] assumed a point isotropic source whose intensity and decay rate were taken to be the same as those obtained from absolute-magnitude laboratory measurements by Engle and Fisher[19] fitted to an expression by Loewe et al.[86] A gamma-ray attenuation function was obtained by folding the decay spectrum for ^{235}U at 0.2 to 0.5 sec after fission, also measured by Engle and Fisher, with the Monte Carlo infinite-air transport data for monoenergetic gamma rays calculated by Marshall and Wells.[61] The air-ground interface was assumed to have a constant effect of 20% (based on an examination of BREN data).[88] The rate of cloud rise was computed by an equation given by Loewe et al.[86] and the effect was computed as an increase in the geometrical distance from cloud center to the detector over the time period from 0 to 60 sec. Only the hydrodynamic enhancement of the dose is treated with empirical expressions, which are based on models given by Loewe et al.[86] and Richards.[89] The Mooney-French method ignores an expanded volume source, and also the attenuation in the cloud debris, but an investigation of the expanded source maintained at ground level (that is, no cloud rise allowed)

indicated that neglect of this parameter would not influence the results greatly. The final equation includes a term for the fission fraction of the weapon and a term for the weapon yield. The equation has been coded for numerical solution by computer.

The impetus for developing a model that relies more on basic physical data and less on empirical data stemmed from the availability of Straker's sets of air-transport data for the production and transport of secondary gamma rays in an air-ground geometry (see Section 9.3.1). With these data, Mooney and French determined the fraction of the dose measured during weapons tests that was due to air and ground secondary gamma rays and assumed that the remainder could be attributed to fission-product gamma rays. Thus a technique became available for testing a model for calculating fission-product gamma-ray doses. The technique was used to test the method for several low-yield devices in the range from 1 to 40 kilotons and several high-yield devices in the range from 200 kilotons to 5 megatons. Typical comparisons for the low-yield and high-yield devices are shown in Figs. 12 and 13 respectively. For the low-yield comparisons, 80% of the measured points are within 25% of the calculated totals and for the high-yield comparisons 80% of the measured points are within 50% of the calculated totals. In contrast to those for the low-yield devices, the calculated totals for the high-yield devices tend to be higher than the measurements, which indicates the high-yield predictions are more conservative.

The special working group that was convened for civil defense studies (see Section 9.2.1) used the Mooney-French method for calculating fission-product doses for 40-kiloton, 300-kiloton, and 1-megaton thermonuclear weapons with fission fractions. Their results are included in Table 13.

In the present state of the art, the Mooney-French method is the most practical method for calculating fission-product gamma-ray doses.

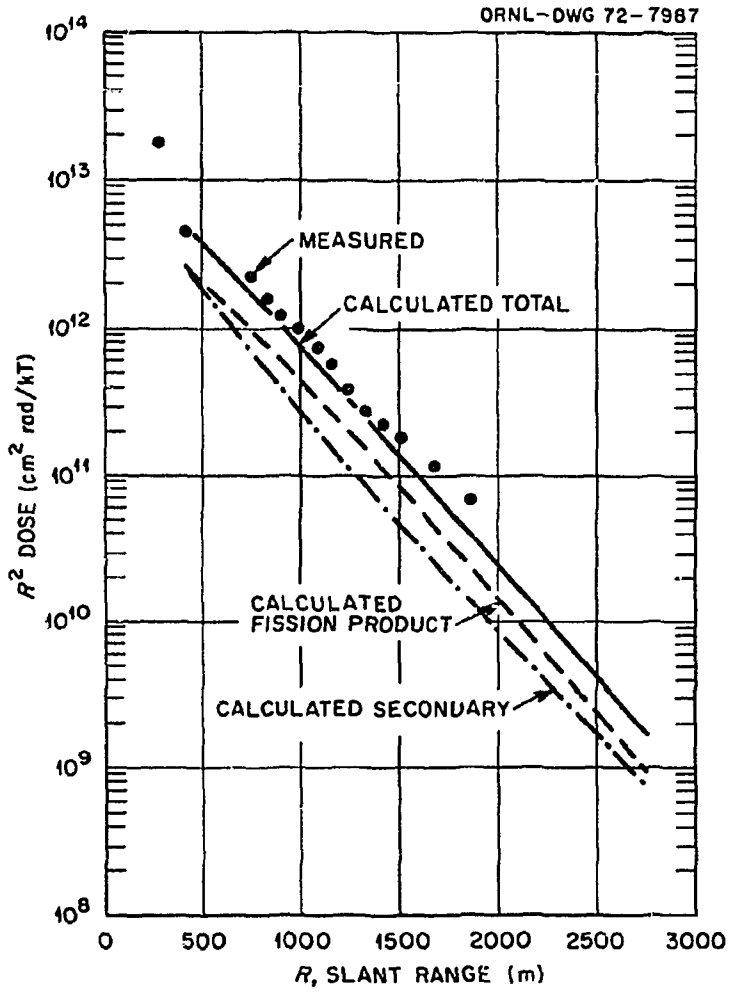

Fig. 12. Calculated and Measured Gamma-Ray Tissue Doses Produced by a Low-Yield Weapon. (From Mooney and French, ref. 87.)

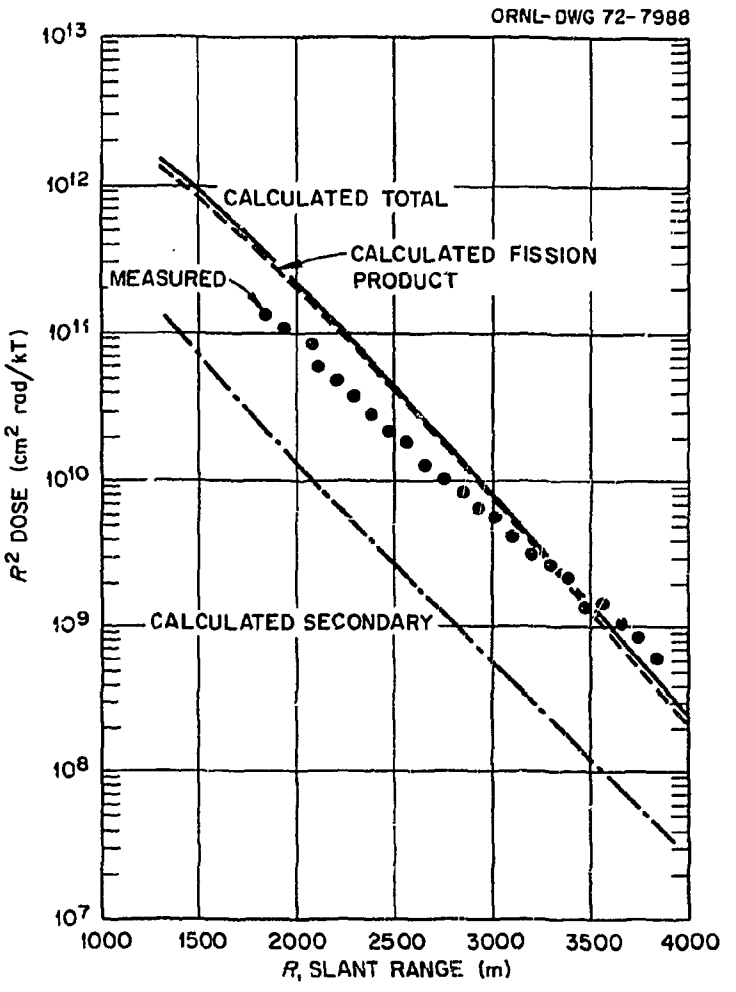

Fig. 13. Calculated and Measured Gamma-Ray Tissue Doses Produced by a High-Yield Weapon. (From Mooney and French, ref. 87.)

10.0 CALCULATIONS OF RADIATION PENETRATING INTO STRUCTURES

Section 9 has shown that the weapons radiations incident on a structure consist of neutrons produced by the fission and fusion reactions and gamma rays produced by several sources. For underground structures it has always been assumed that the earth around the structure protects it from radiations entering the sides and only those radiations incident on the top need be considered. For aboveground structures it is assumed that radiations may enter through all walls except the floor. In either type of structure, radiations may find less-resistant pathways through low-density regions, particularly through entranceways or through gaps between abutting components.

The incident radiations can interact with the structure itself in several ways. For example, as is depicted by the wavy lines shown in Fig. 14, gamma rays incident on a structure can pass directly through a wall, they can be scattered in the wall either toward or away from the structure cavity, or they can be absorbed in the wall. If the absorption results in pair production (see Section 5.2.2), then two 0.511-MeV gamma rays will be emitted in opposite directions from approximately the same point at which the original gamma ray is absorbed. If this point is near the inner surface of the structure, then one of the gamma rays will probably enter the structure cavity, along with those that pass directly into or are scattered into the cavity.

Neutrons similarly can pass directly through a wall or be scattered or absorbed (see straight lines in Fig. 14). In both the scatterings and the absorptions, the probability is high that the interaction will produce at least one secondary gamma ray, frequently of high energy, which in turn can pass directly into the cavity or be scattered or absorbed in the wall. Again, if the gamma-ray absorption causes pair production close to the inner surface of the structure, one of the two newly produced gamma rays may continue into the cavity.

In a highly shielded underground structure, the gamma rays produced by the neutron interactions in the structure cover and walls constitute

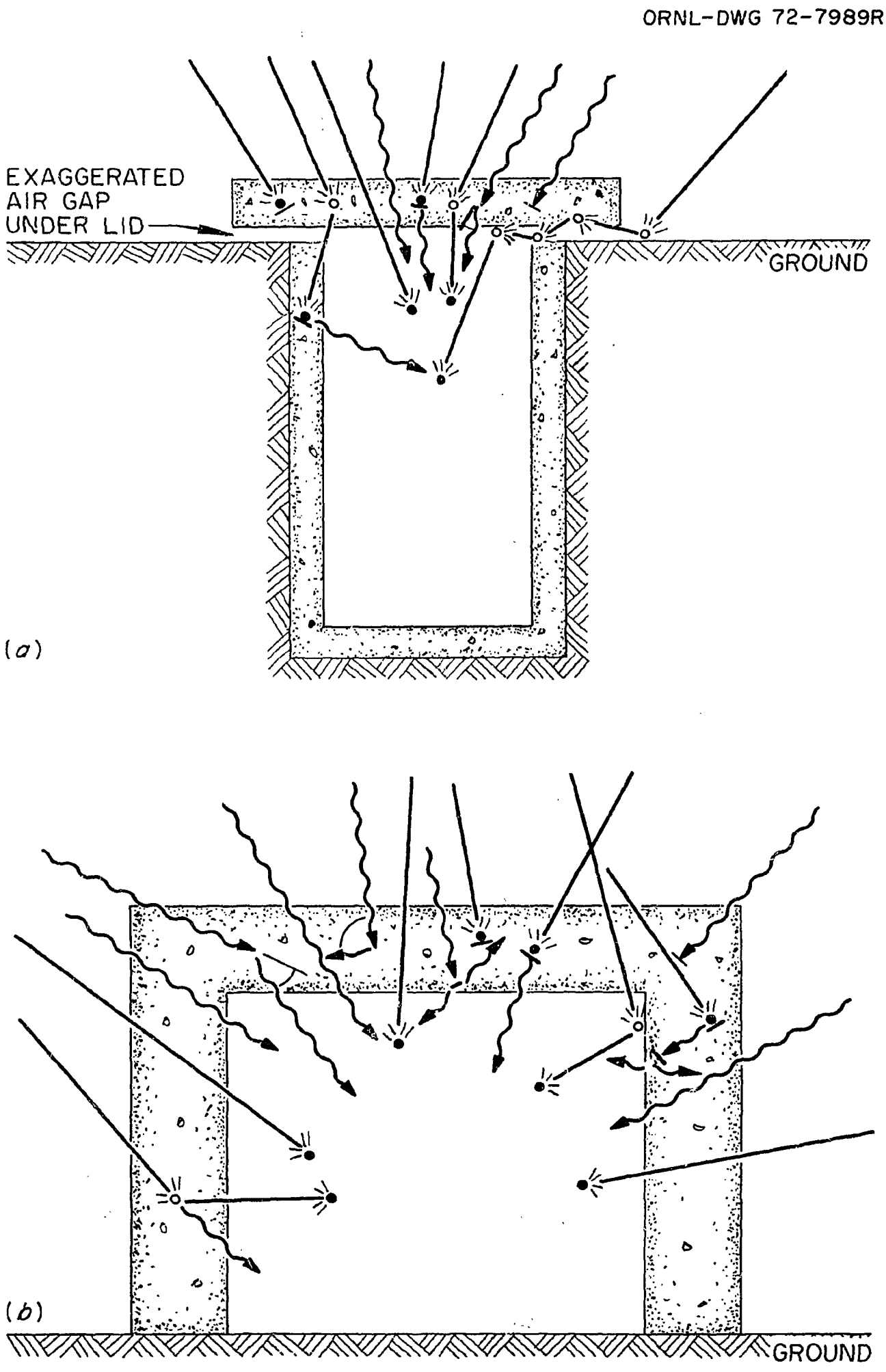

Fig. 14. Typical Interactions of Weapons Radiations in the Walls of (*a*) Underground Structures and (*b*) Aboveground Structures. The wavy lines represent gamma-ray paths; the straight lines represent neutron paths; the open circles show neutron-scattering locations; and a single dash indicates that a neutron or gamma ray has been absorbed.

the single most important radiation component entering the cavity. In fact, if only the total amount of radiation (fluence) arriving at a particular location in the structure is of concern, it can be assumed that the radiation will be comprised of a very large fraction of secondary gamma rays produced in the walls and a small (sometimes negligible) fraction of neutrons penetrating from the outside. As the shielding thickness is reduced, the relative contributions by the wall secondary gamma rays and the neutrons decrease and increase respectively and gamma rays incident on the outside of the structure assume an increasing importance. However, in almost any reasonably shielded underground structure, the gamma rays incident on the outside surface should be of no concern inside the cavity *unless* the rates at which the radiations arrive (fluxes) are important. In that case, both the secondary gamma rays produced in the environmental materials outside the structure and the prompt gamma rays emitted directly from the weapon may contribute significantly.

The situation is somewhat different for aboveground structures. Not only is a greater surface exposed to the incident radiation (four walls and a roof as opposed to the roof only in an underground structure), but the surfaces are oriented so that the gamma rays can enter with high energies: that is, many of the gamma rays incident on an aboveground structure will have traveled directly from their birth sites, whereas most of the gamma rays incident on an underground structure will have first undergone scatterings that have reduced their energies and concomitantly their ability to penetrate the walls of the structure (see Section 5.2.3). An exception for an underground structure would be a detonation directly overhead, from which gamma rays could enter the structure unscattered.

For both underground and aboveground structures, however, decisions as to which radiation components should be considered in a given shielding problem must be made on the basis of the type of response being calculated and on the degree of accuracy required. In some cases, order-of-magnitude estimates of a response inside a structure can be obtained by

using structure-penetration data already available. In other cases it will be clear that a complete transport calculation utilizing the methods described in earlier sections will be necessary.

The amount of structure-penetration data on initial weapons radiation is limited.[bb] Parametric calculations for several structures of simple geometry have been made for given burst conditions by Radiation Research Associates for inclusion in the *Weapons Radiation Shielding Handbook*,[m] along with techniques for applying the results to similar structures exposed under similar circumstances. These techniques are described in this section. Other calculations have been performed at Oak Ridge National Laboratory for individual structures of specific interest. The dual purpose of the ORNL calculations is to provide immediate answers for structures under design and to develop more efficient transport calculational techniques for general application. In this paper they are used to illustrate how a problem should be approached if the best possible answer is demanded, which is frequently the case.

It should be mentioned that in addition to the calculations for specific structures, an increasing body of penetration data are being generated for neutron and gamma rays incident on infinite slabs[cc] of various materials, primarily concrete and soil. In the absence of appropriate structure data, it may be possible to use these results to estimate the penetration of radiation through one wall of a structure. Infinite-slab data are available both for monoenergetic sources incident at given angles and for a few sources having a spectrum of energies and a given angular distribution. Theoretically, the monoenergetic source results can be folded and weighted to represent the incident energy and angular distributions that would be produced by a nuclear weapon, similar to the manner

---

[bb] This is in contrast to fallout radiation, for which a large amount of penetration data are available.

[cc] In this context the term "infinite slab" is used to mean both a one-dimensional slab bounded by a vacuum and a one-dimensional slab embedded in an infinite medium of the same material (see Section 6.6.1). The latter would be the geometry used in moments method calculations.

in which the air-transport data described in Section 9.0 can be folded and weighted to represent a given weapons spectrum. However, for this technique to be useful, the process would have to be automated, which, as yet, it has not. No attempt will be made in this chapter to cover slab-penetration calculations except as they are used for specific structures. However, the reader is referred to ref. 25 and to the Radiation Shielding Information Center for descriptions of such calculations and their possible uses.

10.1. Underground Structures

10.1.1. Concrete-Covered Rectangular and Cylindrical Structures

The parametric studies of the penetration of radiation into various types of simple structures included the concrete-covered rectangular and cylindrical underground structures shown in sketches *a* and *b* of Fig. 15. Descriptions of the calculations are presented in refs. 72 and 90 and in Chapter 7 of the *Weapons Radiation Shielding Handbook*.[83,m] The calculations were limited to single-compartment structures, to surface or near-surface detonations of weapons having large fission fractions, and to distances for which the overpressure is between 5 and 100 psi, but no closer than 500 m. In each case the penetration into the structure was assumed to be due to a free-field environment composed entirely of neutrons, fission-product gamma rays, and nitrogen-capture gamma rays.

Neutron-Induced Doses. The calculations of the penetration of the free-field neutrons into the concrete-covered structures were performed by Mooney and Wells,[72] who used as their incident field the neutron energy and angular distributions they calculated for a slant range of 700 m from a high-yield weapon detonated at an altitude of 100 yd. At the time these free-field calculations were performed, the Straker air-transport data sets[69] described in Section 6.9 were not yet available; therefore the incident distributions were obtained by applying to the weapons spectrum an earlier set of neutron transport data which Ritchie and

ORNL-DWG 69-9694R

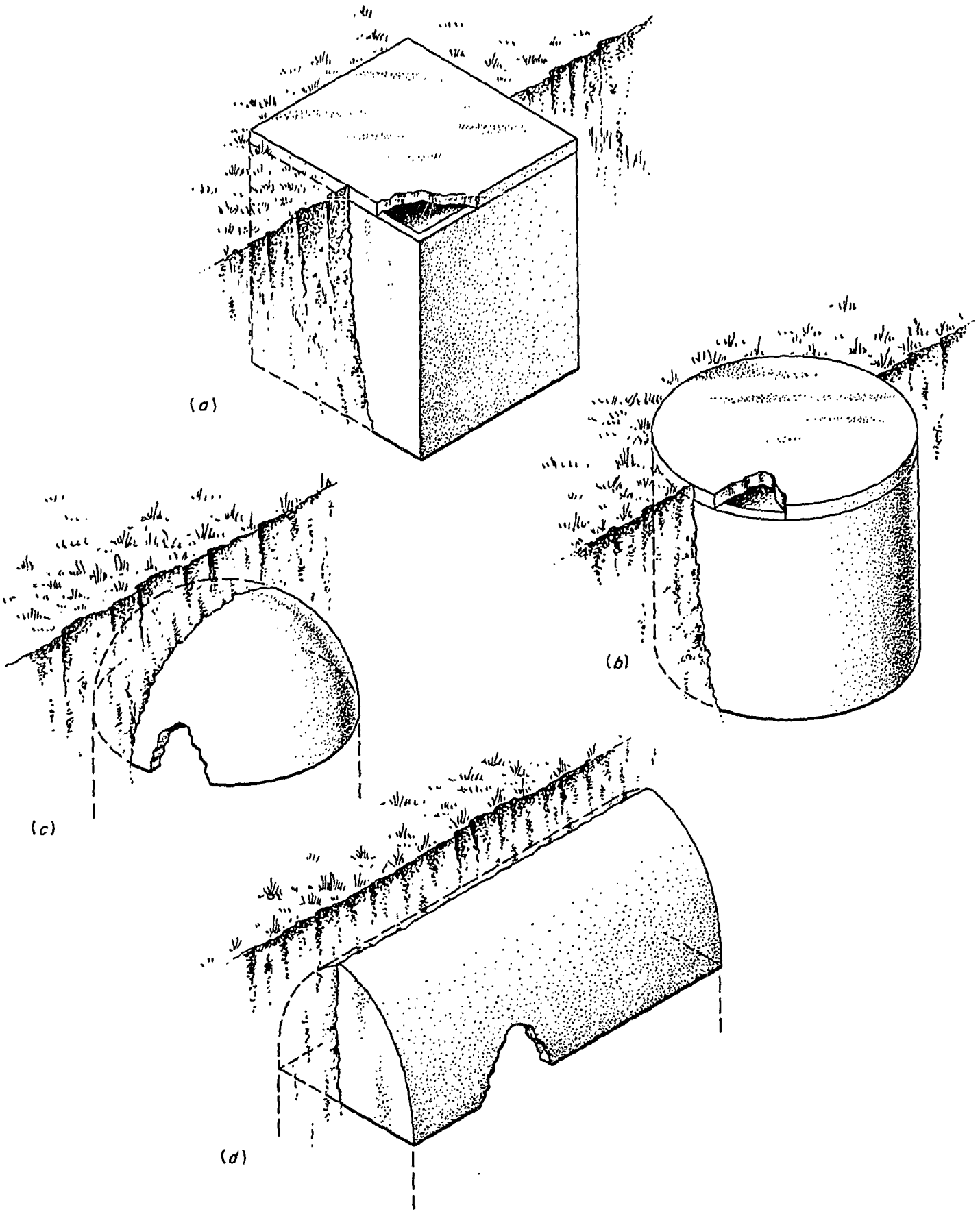

Fig. 15. Four Types of Underground Structures. (*a*) Concrete-covered rectangular structures; (*b*) concrete-covered cylindrical structures; (*c*) soil-covered dome structures; and (*d*) soil-covered arch structures.

and Anderson[73] had calculated by the Monte Carlo method.[dd] (Ritchie and Anderson performed their calculations for monoenergetic sources ranging in energy from 0.01 to 14 MeV maintained at an altitude of 100 yd, which set the detonation height assumed for these structure-penetration calculations.)

These incident distributions were normalized to a unit neutron fluence and regrouped into an energy and angular structure acceptable as input in the ANISN discrete ordinates code.[43] The ANISN code was then used to calculate the penetration of both the neutrons and the capture gamma rays they produced through infinite slabs of concrete with thicknesses of 4, 12, 20, 36, 48, and 60 in. (Inelastic-scattering gamma rays produced in the concrete were neglected in these calculations.) The next step was to use the energy and angular distributions of the neutrons and secondary gamma rays emerging from the slabs as input in a computer code which could accommodate the source described by the under-surface of the structure cover and calculate the fraction of the penetrating dose that would be transported directly to points within the structure, both on and off the structure centerline. To these were added doses contributed by neutrons that reached the same points by scattering from the structure walls and floors, as well as doses due to gamma rays produced by the capture of neutrons in the walls and floors. These wall contributions were calculated by Maerker[91] with a Monte Carlo code he had developed to predict neutron and secondary gamma-ray doses due to neutrons incident on the entrances of rectangular tunnels (see Section 10.3).

The ratios of the total neutron-*induced* doses calculated for given locations in the structure to the normalized neutron dose incident on the outside of the structure are called structure protection coefficients

---

[dd] This was one of the several calculations that showed that the neutron energy- and angle-dependent fluences have a weak dependence on range (see Section 9.2.1). Of the different weapons investigated, the incident distributions from the high-yield weapon were considered to be the most conservative and thus were selected for the structure-penetration calculations.

(SPC's). Each SPC is limited to a particular location in a structure that has specified dimensions and a specified concrete cover thickness and is exposed under specified burst conditions. The SPC's obtained in these calculations are tabulated in refs. 72 and 83 for structures having the dimensions and concrete composition given in Tables 14 and 15 respectively. The references also give an expression for calculating SPC's for other cover thicknesses.

Table 14. Dimensions of Concrete-Covered Underground Rectangular and Cylindrical Structures

Structure Depth (ft)	Cross Section of Rectangular Structure (ft)	Diameter of Cylindrical Structure (ft)
7	2.66 × 2.66	3.0
10	5.0 × 5.0	5.64
	10.0 × 10.0	11.28
	15.0 × 15.0	16.93
	20.0 × 20.0	22.57
20	5.0 × 5.0	5.64
50	10.0 × 10.0	11.28
	15.0 × 15.0	16.93
75	20.0 × 20.0	22.57
	5.0 × 5.0	5.64

Table 15. Elemental Composition of Concrete Covers on Rectangular and Cylindircal Underground Structures

Element	Atoms/cm^3
H	8.50×10^{21}
C	2.02×10^{22}
O	3.55×10^{22}
Ca	1.11×10^{22}
Si	1.70×10^{21}
Mg	1.86×10^{21}
Fe	1.93×10^{20}
Al	5.56×10^{20}
K + Na	5.66×10^{19}

The development of these SPC's provides a method for obtaining first estimates of the effectiveness of concrete covers as neutron shields on underground rectangular or cylindrical single-compartment structures that have concrete covers flush with the ground and are in the vicinity of a surface or near-surface burst, providing they meet other specified criteria. The SPC's are simple to apply if the incident neutron dose is known[ee] and

[ee] In the DNA Handbook[83] these SPC's were applied to incident neutron doses obtained by applying the Ritchie-Anderson transport data sets to the emission spectra of several weapons.

if the energy spectrum and angular distribution of the incident neutrons contributing to that dose are approximately the same as those used in the concrete-penetration calculations. It is not yet clear how large a variation can be allowed in the incident energy and angular distributions, but in an extension to this study Mooney and Wells[92] showed that for these same burst conditions and subsurface structures the total neutron-induced doses inside the structures are approximately the same for a fission-neutron source as they are for a source consisting of 75% fission neutrons and 25% 14-MeV neutrons. The agreement is attributed to the fact that the higher neutron dose from the harder source is offset by the larger capture gamma-ray dose resulting from the more abundant low-energy neutrons from the fission source.

Nitrogen-Capture and Fission-Product Gamma-Ray Doses. Values of SPC's for the nitrogen-capture and fission-product gamma-ray doses incident on the underground concrete-covered structures were similarly determined. These calculations were performed by Marshall and Wells,[90] who considered only those gamma rays that traveled directly from the underside of the cover to the point of interest (that is, gamma rays scattered from the walls to the point were neglected, but their effect would be negligible). They used incident gamma-ray energy and angular distributions obtained by applying the gamma-ray air-transport data sets described in Section 9.1.2 to point isotropic sources maintained at an altitude of 100 yd. The distributions at a slant range of 1200 yd were selected. In the case of the nitrogen-capture gamma rays, the source was assumed to have a fission neutron energy spectrum, and the spatial and energy distributions of the neutrons in the atmosphere (the capture sources) were taken from an early (unpublished) Straker calculation for a fission neutron source in infinite air. In the case of the fission-product gamma rays, the source was assumed to have the energy spectrum measured for fission products by Engle and Fisher.[19] Again the incident distributions were normalized to a unit fluence and the penetration through various concrete slab thicknesses was calculated with the ANISN code[43] for a one-dimensional slab geometry. The resulting SPC's are given in refs. 83 and 90 as expressions that include terms to account for the fraction of the

concrete-attenuated doses that reach specific locations within the structures. These SPC's for incident gamma rays can be applied to incident doses in the same manner as those described above for incident neutrons, and thus they provide a method for the design (or evaluation) of concrete covers as gamma-ray shields on the same underground rectangular or cylindrical structures and for the same burst conditions that were assumed for the SPC's for the neutron-induced dose. Since these SPC's were not based on an emission spectrum from an actual weapon they should be equally applicable to all weapons, except, of course, that the weapon should be predominantly a fission weapon.[ff]

Total Doses. The total dose at a point inside any given structure is the sum of the neutron-induced dose, the nitrogen-capture gamma-ray dose, and the fission-product gamma-ray dose obtained with the appropriate SPC's. (The prompt gamma-ray dose is ignored.) Examples of how these SPC's can be applied to obtain total doses in cylindrical and rectangular underground structures are given in ref. 83.

It will be noted in ref. 83 that the tabulated SPC's have no error estimates attached to them. In 1966, when the calculations were performed, it was not known how accurate the calculational technique was or how well the cross-section sets that were used actually described the neutron interactions and secondary gamma-ray production in the concrete. Subsequently the ANISN transport code has been shown to give results that agree with two other methods for a similar calculation (see discussion of missile silo calculations below), which tends to confirm the reliability of the calculational technique. However, the reliability of the cross sections is still not established. It is known that the old cross sections for thermal-neutron capture-gamma-ray production in concrete underpredicted the high-energy gamma-ray production to the extent that the capture gamma-ray dose may have been as much as 50% lower than would be predicted with present-day cross sections. The neglect of secondary gamma-ray production

---

[ff] In the DNA Handbook[83] these SPC's were applied to nitrogen-capture and fission-product gamma-ray doses obtained with the empirical equations of Loewe et al.[86]

by the inelastic scattering of high-energy neutrons in the concrete also would have underpredicted the secondary dose. The general concensus among those performing similar calculations (see missile silo calculations described in Sections 10.1.3 and 10.1.4) is that the neutron-induced doses now being calculated (1972) are accurate to within a factor of 5 to 10; however, this quotation includes uncertainties associated with the calculation of the incident neutron field. It has been stated in the introduction to Section 9.2 that the incident neutron dose can now be calculated to within a factor of 2 to 3, which means that the uncertainty associated with current calculations of the penetration into the silo is on the order of a factor of 3 to 4. Thus it does not seem unreasonable to assume that the SPC's for neutron-induced doses quoted in refs. 72 and 83 are accurate to within factors of 6 to 8, with the probability the resulting doses would be low rather than high.

The calculations on which the SPC's for the nitrogen-capture gamma-ray doses are based are considered to be fairly accurate since the gamma-ray interaction cross sections are better known. However, it is not known whether the incident gamma-ray spectra are realistic. The secondary gamma rays produced in the environment were limited to nitrogen-capture gamma rays and these in turn depended on a neutron distribution in the atmosphere based on an early neutron transport calculation. Limiting the source to nitrogen-capture gamma rays probably produced a conservative incident spectrum, since other gamma rays produced in the atmosphere (e.g., inelastic-scattering gamma rays) tend to have lower energies than nitrogen-capture gamma rays (see Table 2). Therefore, if it is assumed that the incident gamma-ray dose has been correctly calculated, a factor of 3 to 4 attached to these SPC's is probably reasonable.

The errors associated with the SPC's available for the fission-product gamma-ray doses similarly depend on the reliability of the incident spectrum, which again is difficult to assess. The spectrum used is probably conservative since it was a spectrum that had been measured during an early time period (0.2 to 0.5 sec after fission). So again if it is assumed that the incident gamma-ray dose has been correctly calculated, then SPC's

should give fission-product gamma-ray doses that are correct to within a factor of 3 to 4.

One other fact must be reiterated. These SPC's are applicable only to structures that are uniformly shielded across the top. That is, no allowances are made for irregularities in the shield such as air gaps between components, low-density regions, and accessways. Radiation entering through such irregularities must be determined separately and added to that penetrating the walls of the structure (see Section 10.3).

10.1.2. Soil-Covered Dome and Arch Structures

The concept of the SPC's described in the preceding paragraphs was extended[83] to the soil-covered dome and arch structures depicted in sketches *c* and *d* in Fig. 15. Again the free-field environment was assumed to be composed entirely of neutrons, nitrogen-capture gamma rays, and fission-product gamma rays. The structure dimensions and soil cover thicknesses are given in Table 16.

Table 16. Dimensions and Soil Cover Thicknesses for Dome and Arch Structures

Structure Type	Radius R (ft)	Length (ft)	Soil Cover Thicknesses (ft)
Dome	7.5		1.875, 5, 9
	20		5.0, 7.5, 9
	30		7.5, 9, 11
Arch	7.5	60	1.875, 5, 9
	20	160	5.0, 7.5, 9
	30	240	7.5, 9, 11

Neutron-Induced Doses. The SPC's for the neutron-induced doses in these structures were based on the soil-penetration calculations of Karcher and Wilson,[93] who assumed that the incident neutron source was isotropic and could be characterized by only four energy groups with an upper limit of 10 MeV. They calculated the attenuation of the neutrons and the concomitant production and attenuation of capture and inelastic-scattering gamma rays in the soil by a combination of removal theory, removal-diffusion theory, and point-kernel techniques[94] applied to an infinite-slab geometry.

An examination of the Karcher and Wilson data showed that the behavior of radiation in the various soils could be typified by only four soil groups and further that the attenuation depends much more on the water content of the soil than on its composition. In fact, even between the four soil groups the differences in attenuation disappear with free water contents greater than 10%. Therefore the SPC's were generated for a single soil composition, for densities of 1.0, 1.5, and 2.0 g/cm^3, and for free water contents of 10, 30, and 50 percent. Because the Karcher and Wilson data provided no information on the angular distributions of the neutrons and gamma rays emerging from the undersides of the soil slabs, it was assumed that angular distributions for neutrons emerging from equivalent mass thicknesses of concrete were applicable. The doses at given points in the structures were obtained by integrating over the curved interior surfaces of the domes and arches, with variations in the soil cover thickness as a function of position on the structure accounted for. As is the case for the cylindrical and rectangular underground structures, these SPC's are given as the ratio of the neutron-induced dose at a particular location in a particular structure to the normalized neutron dose incident on the soil cover. The resulting SPC's for neutrons incident on slab-covered dome and arch structrues are included in ref. 83.

Since these SPC's were not generated for a specific weapons neutron leakage spectrum, they are equally applicable to any weapon that produces incident neutrons with energies within the range of those used for the calculations. Also, they are equally applicable for any burst location

since the assumption that the neutrons are isotropically incident precludes their arrival from any preferred directions. In reality, isotropic incidence is not a good assumption, but a description of the incident angular distributions may be unnecessary anyway. These studies have shown that for the large soil thicknesses used most of the penetrating dose is due to gamma rays produced by the capture of neutrons that have scattered so many times they have "forgotten" their original directions.

Nitrogen-Capture and Fission-Product Gamma-Ray Doses. SPC's for doses in the soil-covered dome and arch structures due to incident gamma rays could not be based on soil-penetration calculations because none had been performed for gamma rays. Therefore, it was assumed that the gamma-ray penetration calculations performed for the concrete covers discussed in Section 10.1.1 were applicable for soil covers with equivalent mass thicknesses. As a result, the energy and angular distributions assumed for the incident nitrogen-capture gamma rays were those calculated for a slant range of 1200 yd from a point isotropic fission neutron source maintained at a height of 100 yd above an air-ground interface. Similarly, the energy and angular distributions assumed for the incident fission-product gamma rays were those calculated for a point isotropic source emitting gamma rays with the energy spectrum measured by Engle and Fisher,[19] again for a slant range of 1200 yd and a source height of 100 yd. Since the soil thicknesses were much larger than the concrete thicknesses, the attenuation curves used for soil thicknesses greater than 25 in. were simple exponential functions whose magnitudes and slopes were determined by fits to the concrete-penetration curves. The angular distributions of the gamma rays emerging from the soil were also assumed to be the same as those emerging from concrete. The resulting SPC's, tabulated in ref. 83, are given for the same locations in dome and arch structures as those for the neutron-induced doses.

Total Doses. The total dose at a given location inside a soil-covered dome or arch structure is the sum of the neutron-induced dose, the nitrogen-capture gamma-ray dose, and the fission-product gamma-ray dose

obtained with the appropriate SPC's. The prompt gamma rays are ignored, but in structures of this type they would not make a noticeable contribution. Sample problems in which the doses in structures of this type are determined are included in ref. 83.

So many uncertainties are associated with the SPC's for the dome- and arch-type structures that a very large error -- on the order of a factor of 25 -- must be attached to them. For example, the SPC's for the neutron-induced dose were based on calculations performed with transport methods that were too simplified. Also, limiting the upper energy of the neutron spectrum to 10 MeV may cause the dose to be underestimated, although if the weapon utilizes the fission process alone, it is not likely that a large fraction of the incident spectrum would consist of high-energy neutrons. The effect of neglecting wall interactions by neutrons that have passed through the structure cavity at least once was not determined, and if the effect were nonnegligible, both the neutron dose and the secondary gamma-ray dose would be underestimated. Finally, it is not known whether it is realistic to assume that infinite-slab penetration data are applicable to a geometry in which one side of the slab is curved. On the other hand, the SPC's were based on the most conservative soil-penetration data available, which would tend to overestimate the neutron-induced dose.

Since the SPC's for the incident nitrogen-capture and fission-product gamma rays were based on the same incident spectra as those for the cylindrical and rectangular structures, they have the same inherent uncertainties, plus the fact that they were based on concrete-penetration data rather than soil-penetration data. The latter point should not be too serious, however, in view of the predictable behavior of gamma rays as a function of the atomic number of the material.

Why SPC's with such large errors are included will be questioned by the reader. The answer is that these data are the only parametric attenuation data available for structures of these types. At the time the

calculations to obtain these SPC's were performed they constituted a large calculational effort. Nowadays the calculations for domes could be repeated with one of the available two-dimensional codes with much more accuracy and much less, although not insignificant, labor.

10.1.3. Missile Silo -- Idealized Geometry

As mentioned previously, structure penetration calculations have been performed at ORNL both to provide needed information for specific designs and to investigate how different transport methods can be applied for the most efficient solution of a given problem. One relatively recent series of calculations was performed in response to a request to the Defense Nuclear Agency. The quantities requested were time-integrated and time-dependent ionization and displacement profiles produced by weapons radiation penetrating into the idealized silo shown in Fig. 16. The calculations were performed for two different weapons neutron energy spectra and three thicknesses of the concrete cover (40, 50, and 60 in.).[95] The covers were assumed to fit tightly enough to disallow radiation streaming through the crevices.

When a calculation of this type is done, it is to provide the most accurate answers possible within the limitations of the state of the art. This implies that the latest cross sections will be used and that the geometry will be mocked up as realistically as possible. Thus the free-field environment will be calculated as an integral part of the problem, rather than being constructed from the transport data sets described in Section 9.0, although the simplifying assumptions regarding the source will still be required; that is, a point isotropic source with an instantaneous emission of its radiations will be used (see Section 7.0). In its entirety, the problem will consist of the point source in the atmosphere at some height above the ground and at some slant range from the silo, and the radiation will be followed from the source through the air, through the silo cover, and into the silo.

To solve this problem in a single pass on a computer would require three-dimensional geometry, which dictates th of a Monte Carlo code.

ORNL-DWG 71-1638R

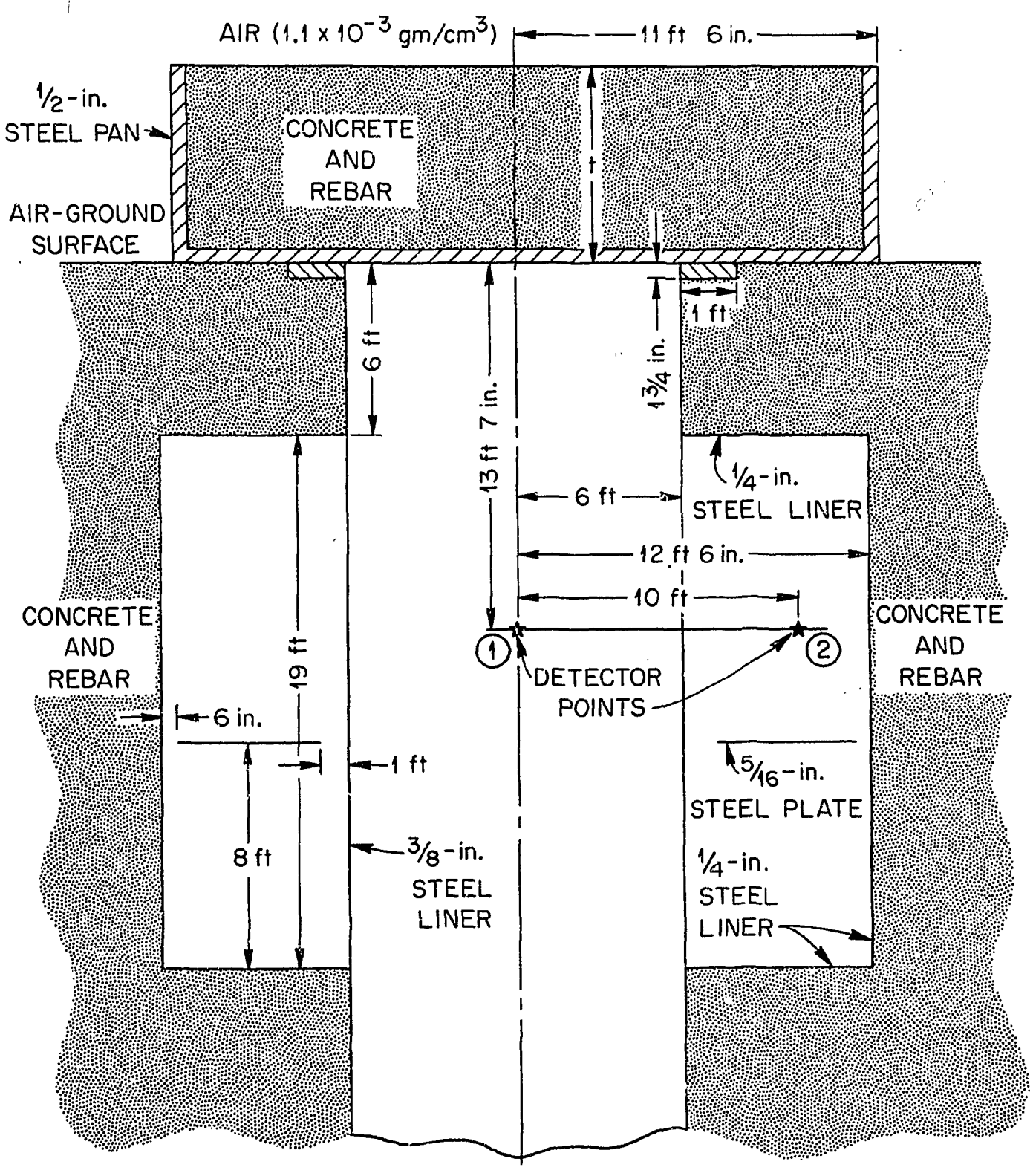

Fig. 16. Idealized Silo Configuration.

But this approach would be highly impractical, since excessively long computer running times would be necessary to reduce the errors to acceptable levels. The alternative is to divide the problem into parts that can be represented by simpler geometries and to use the output of one calculation as input for the next. This was the technique used for the idealized silo problem. (As was pointed out in Section 6.5, this procedure was not possible until a Monte Carlo code had been developed which could use the same multigroup cross-section structure that the discrete ordinates code uses.[gg])

Time-Dependent Calculations. The division of the problem to obtain time-*dependent* results is illustrated in Fig. 17*a*. The free-field environment, given as time-, angle-, and energy-dependent neutron and secondary gamma-ray fluxes[hh] arriving at the silo position, was calculated in slab geometry with the Monte Carlo code MORSE.[49] The time interval from 0 to 3×10^{-4} sec was covered in 29 time bins, and the angular distribution was described in eight polar angles in the downward direction. The energy groups were the 22 neutron groups and 18 gamma-ray groups shown in Tables 7 and 8 respectively.

In the second step of the time-dependent calculations, the 29 time bins from the MORSE calculations were used as input to the discrete ordinates TDA code[45] to calculate, in one-dimensional (infinite-slab) geometry, the radiation penetration through the cover. These results were given as energy- and angle-dependent fluxes at the bottom surface of the cover in 42 time bins extending out to 1×10^{-2} sec. The longer time period was used to determine whether a significant number of gamma rays were produced in the concrete at the later times.

[gg] Conversely, in the last few months a discrete ordinates code (ANISN) has been modified to use point cross sections,[96] so that other combinations of Monte Carlo and discrete ordinates codes are now possible.

[hh] Prompt gamma rays were neglected.

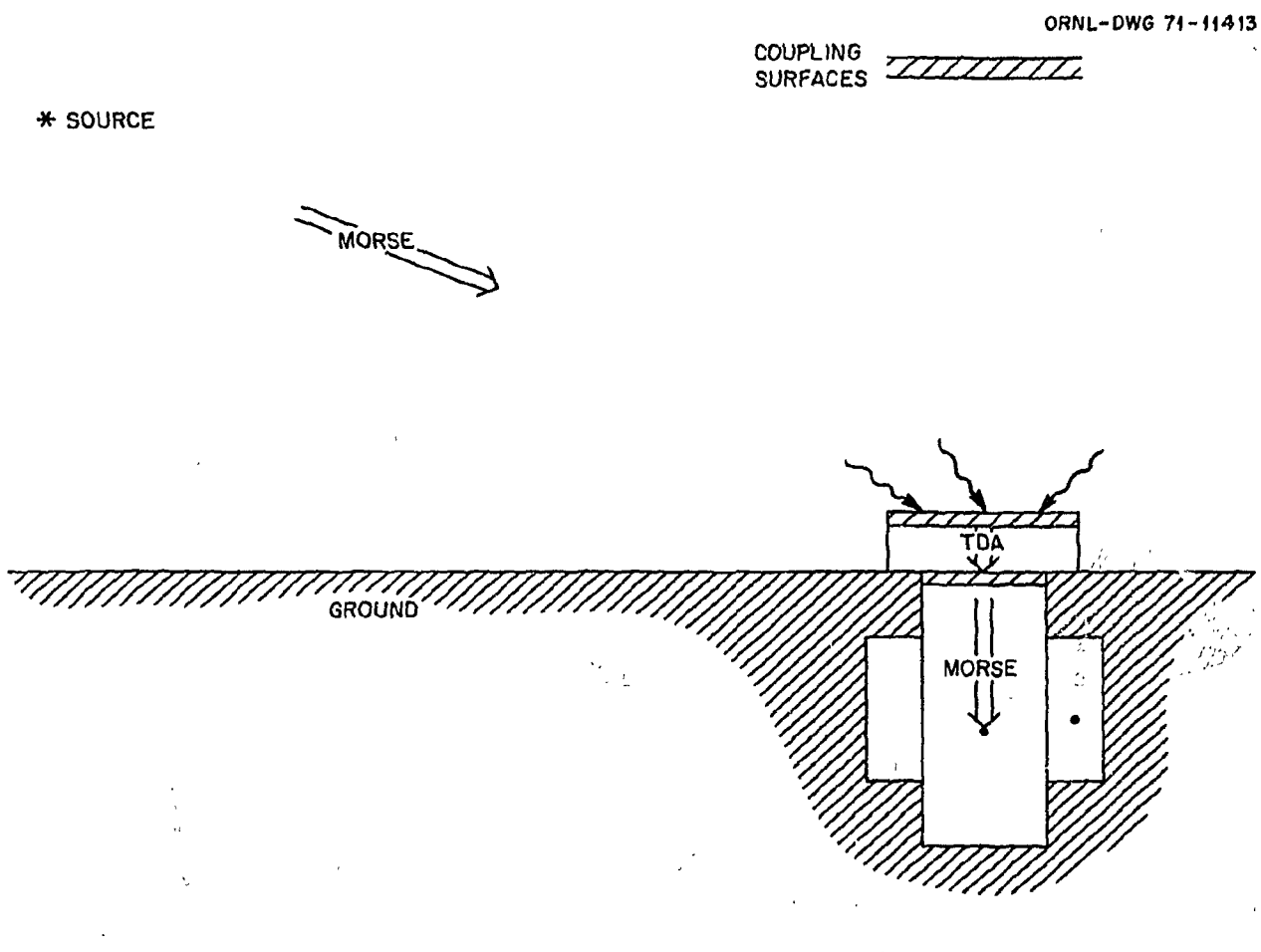

Fig. 17. Schematics Showing Applications of Different Calculational Techniques to Various Parts of Idealized Silo Problem. (*a*) Time-Dependent Calculations; (*b*) Time-Integrated Calculations.

In the final step of the time-dependent series, the TDA results were used as input for a second MORSE calculation, this time in two-dimensional cylindrical geometry, to determine the neutron and secondary gamma-ray fluxes within the silo. One detector point was taken to be on the silo axis at a depth of 13 ft 7 in. and the other at the same depth 10 ft off the axis. In this calculation the bottom of the silo was assumed to be located 2 ft below the offset region.

Time-Independent Calculations. The division of the idealized silo problem to obtain time-*independent* results is illustrated in Fig. 17*b*. The free-field environment was first calculated with the discrete ordinates code DOT[44] in cylindrical geometry. The dimensions of the cylinder were such that the boundaries extended well beyond the silo position and well above the weapon burst point. The lower portion of the cylinder consisted of 50 cm of ground so that interactions in the ground could be accounted for. In spite of the fact that the cylinder included a large volume, corrections were introduced to account for the effects of the assumption in the calculation that a vacuum surrounded the cylinder.

In this series of calculations, the penetration through the silo cover was treated by two different techniques. In the first, the cover was assumed to be a one-dimensional slab and a calculation with the discrete ordinates code ANISN[43] was performed, using as input the fluences calculated in the preceding DOT calculation. The fluences emerging from the slab were then converted to silicon ionization and displacement units and compared with the silicon responses obtained in the TDA calculation after the latter had been integrated over time.

In the second technique, the penetration through the cover and on into the silo itself was treated in a single two-dimensional DOT calculation in cylindrical geometry. Vacuum boundaries were assumed to exist in the radial direction 30 cm beyond the silo wall and in the axial direction 60 cm below the bottom of the offset room.

From these DOT calculations were extracted the fluences immediately below the silo cover and at the two designated detector points within the silo. In addition, plots (profiles) were made which showed the positions within the silo at which the levels of radiation were approximately the same (i.e., isoplots were obtained). All these data were converted to silicon ionization and displacement units and compared with the time-integrated results from the MORSE and TDA calculations at common points.

Results. At all points compared, the results from the various calculations were in good agreement. Thus these calculations proved that at least for an idealized silo geometry the discrete ordinates and Monte Carlo transport methods can be coupled to perform separate steps of a radiation transport problem, and the fact that they gave the same results tends to validate both methods. It does not validate the results, however, since the cross sections used in both methods were the same and they may be in error. In fact, the primary investigators in these calculations, E. A. Straker and F. R. Mynatt, have stated that the answers obtained are reliable only to within a factor of 5 to 10. (Translated into shield thickness, this could mean the addition or subtraction of 8 to 12 in. of concrete.)

An analysis of these silo results reveals several trends which tend to support statements made in several earlier sections of this chapter about the relative importance of the different radiation components. These trends can be summarized as follows:

(1) The attenuation of a given type of response (neutron ionization, neutron displacement, or gamma-ray ionization) produced by both weapons spectra is the same in concrete covers of equal thickness. This indicates that the same type of response produced by other weapons will be similarly attenuated, providing the neutron spectra of the weapons do not differ greatly from those used in this study.

(2) For a 50-in. cover the total gamma-ray ionization inside the silo is due almost entirely to secondary gamma rays produced in the concrete cover, *but*

(3) The peak gamma-ray ionization rate is produced approximately equally by the secondary gamma rays incident on the cover and the secondary gamma rays produced in the cover.

(4) The peak gamma-ray ionization rate coincides with the arrival of the neutron front at the silo position, and thus coincides with the peak neutron ionization rate, *but*

(5) The peak gamma-ray ionization rate is always at least a factor of 20 higher than the peak neutron ionization rate.

(6) The total ionization produced by gamma rays in the silo exceeds that produced by neutrons by factors of 350 to 600.

The reader is cautioned not to regard the preceding statements as being applicable to all situations. On the other hand, it is encouraging to note that insofar as total doses or ionizations are concerned, an increasing body of evidence is accumulating which indicates that the number of variables that must be considered in structure shielding calculations may eventually be reduced to the extent that parameterized data of general applicability can be made available.

10.1.4. Missile Silo -- Complicated Geometry

Calculations for a second missile silo structure that more nearly represents the real situation were performed by F. R. Mynatt et al.,[97] also at ORNL. The source was assumed to be the typical thermonuclear source described in Table 12 detonated at various heights and ground ranges. The structure geometry is shown in Fig. 18. In this case an obvious slit exists under one side of the concrete cover, and the so-called T-box assembly and cable holes introduce low-density regions that extend from

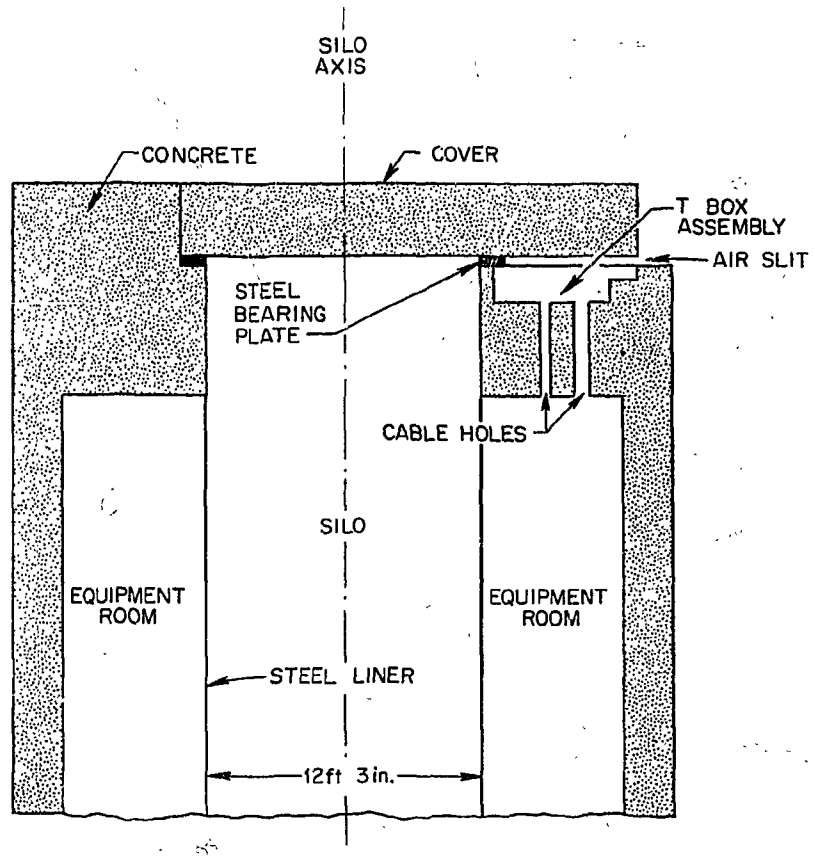

Fig. 18. Complicated Silo Configuration.

the outside of the structure to its interior. The question is: for a given silo cover thickness and given burst conditions, how much does radiation streaming through the low-density regions enhance the doses and dose rates (or comparable quantities) penetrating into the silo?

In the first calculations performed in this study, the time-independent free-field environment was calculated with the discrete ordinates DOT code in two-dimensional geometry for a burst height of 1000 ft and ground ranges of 1000 and 1500 ft. The resulting energy and angular distributions of the neutrons and secondary gamma rays incident at the silo position (no prompt gamma rays were considered) were used in subsequent DOT and MORSE calculations of the ionization and displacement responses within the silo due to radiation arriving through the low-density regions and through the cover. Comparing the various responses determined the relative importance of streaming through each of the low-density regions. Plots of the results from the cover-penetration calculations are shown in Figs. 19*a* and 19*b* and in Figs. 20*a* and 20*b*. The compositions of the air, ground, and concrete assumed for these calculations are given in Table 17, and the detailed results are included in ref. 97.

In addition to the time-integrated calculations, a few time-dependent calculations were performed with the MORSE code to determine the relative importance of peak pulses of radiation that would be delivered by the neutrons and secondary gamma rays arriving through the low-density region. Also an integral part of these and continuing calculations is a series of studies to determine the variation of the calculated results to the number of angles used to describe the incident radiations. A calculation with a low-order angular quadrature requires less computing time than one with a high-order quadrature, but the latter may be required to properly describe the entrance of neutrons into the low-density regions of the structure. Also, the possibility of using a free-field environment calculated with the one-dimensional ANISN code rather than the two-dimensional DOT code is being investigated, the assumption being that for silo covers that are level with the ground, only the neutrons in the downward angles are important and that the neutrons in these angles will not

be affected very much by the ground. If this is found to be true, then a great savings in computer time would be effected.

Other studies will investigate the effect of the source height for near-surface bursts and attempt to locate the positions within the silo at which the highest responses could be expected. Finally a series of "sensitivity" studies will be performed to determine the effect that individual changes in the cross-section input have on the calculated results.

10.2. Aboveground Structures (Concrete Blockhouses)

As part of the DNA Handbook effort,[m] the concept of the SPC's described in Sections 10.1.1 and 10.1.2 has been extended by Mooney and Wells to the case of simple aboveground concrete blockhouses.[98,99] Each structure was assumed to have only one compartment and to be constructed entirely of concrete of the composition shown in Table 18. The structure lengths and widths both extended from 10 to 50 ft and the inside height was fixed at 10 ft. Altogether, a total of 19 structures were considered (see Table 19), with wall thicknesses from 6 to 60 in. Figure 21 shows the basic geometry for the structures. In all cases, the wall closest to the point of detonation was considered to be the front wall, and the free-field environment was assumed to consist of neutrons, secondary gamma rays produced in the air and ground, and fission-product gamma rays. (Prompt gamma rays were not considered.)

Neutron Doses. For the calculations of the penetration of the free-field neutrons into the concrete blockhouses it was assumed that the incident field could be described by the energy and angular distributions calculated by Straker (unpublished) for a slant range of 900 m from an intermediate-yield thermonuclear source at an altitude of 100 m (see Table 12 for weapon neutron emission spectrum). The distributions at the 900-m slant range were selected after an analysis of the data had shown that the energy and angular distributions changed only slightly beyond distances greater than 300 m. From this it was deduced, as pointed out in Section 9.2.1, that the energy and angular distributions at mid-range (900 m) from the Straker calculations were representative of all

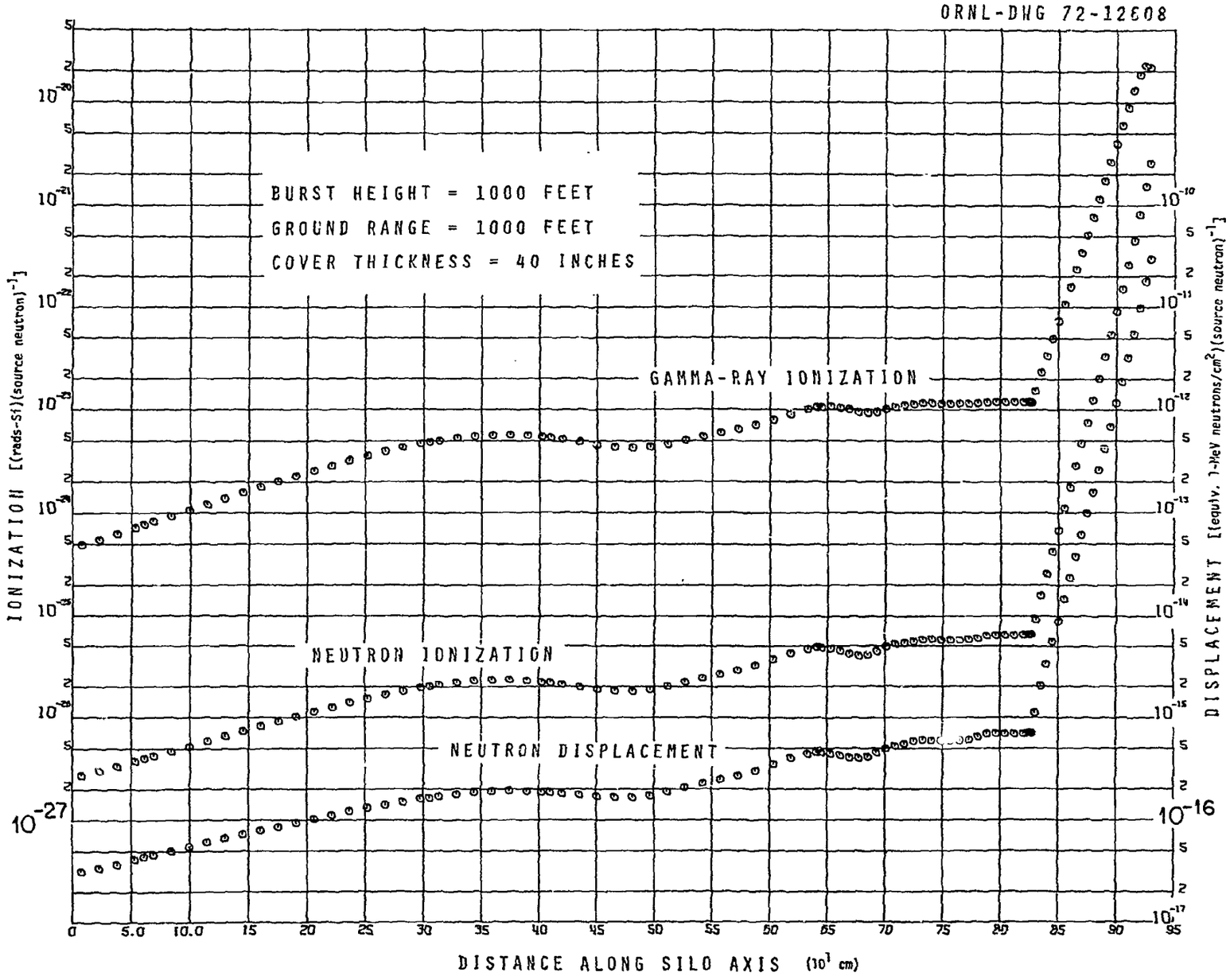

Fig. 19a. Silicon Ionization and Displacement Responses in Missile Silo Due to Radiation Penetrating Through Cover. Radiation consists of neutrons and secondary gamma rays produced by weapon with typical thermonuclear neutron emission spectrum. Ground range is 1000 ft; cover thickness is 40 in.; zero point on silo axis is 827 cm below silo cover. (Note in press: Subsequent review of these calculations has revealed that the gamma-ray ionization values are too low by approximately 40%.)

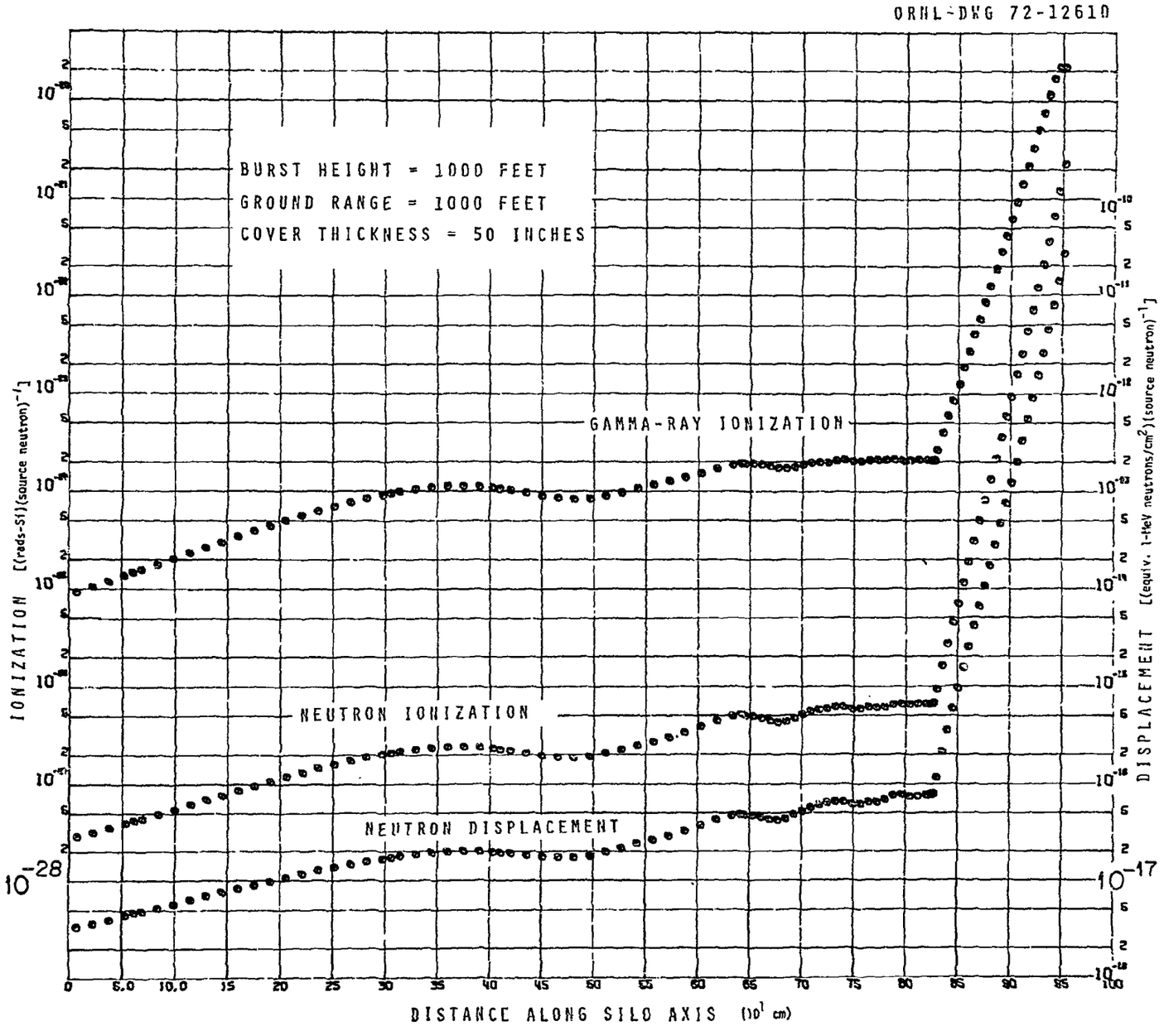

Fig. 19b. Silicon Ionization and Displacement Responses in Missile Silo Due to Radiation Penetrating Through Cover. Radiation consists of neutrons and secondary gamma rays produced by weapon with typical thermonuclear neutron emission spectrum. Ground range is 1000 ft; cover thickness is 50 in.; zero point on silo axis is 827 cm below silo cover. (Note in press: Subsequent review of these calculations has revealed that the gamma-ray ionization values are too low by approximately 40%.)

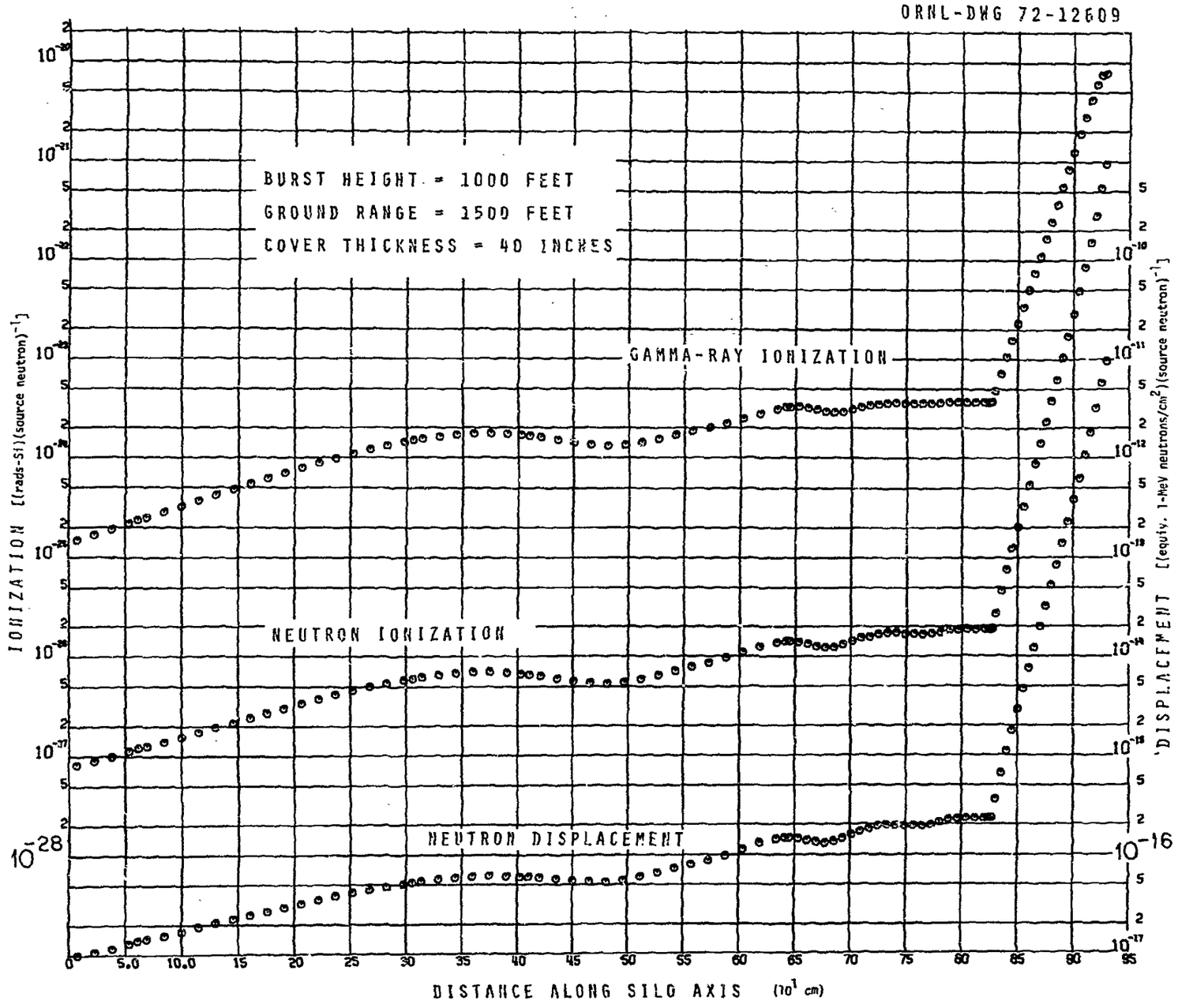

Fig. 20a. Silicon Ionization and Displacement Responses in Missile Silo Due to Radiation Penetrating Through Cover. Radiation consists of neutrons and secondary gamma rays produced by weapon with typical thermonuclear neutron emission spectrum. Ground range is 1500 ft; cover thickness is 40 in.; zero point on silo axis is 827 cm below silo cover. (Note in press: Subsequent review of these calculations has revealed that the gamma-ray ionization values are too low by approximately 40%.)

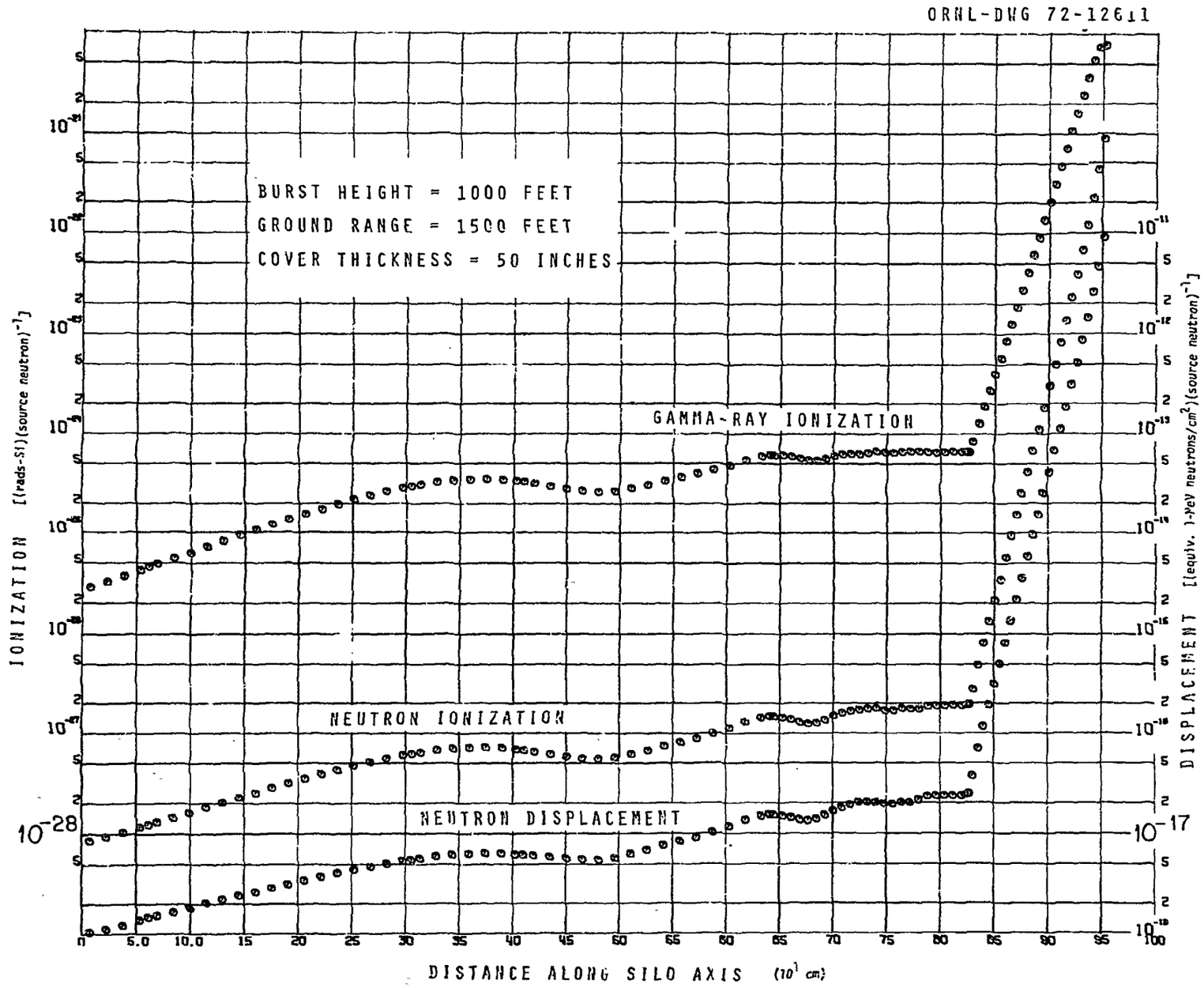

Fig. 20b. Silicon Ionization and Displacement Responses in Missile Silo Due to Radiation Penetrating Through Cover. Radiation consists of neutrons and secondary gamma rays produced by weapon with typical thermonuclear neutron emission spectrum. Ground range is 1500 ft; cover thickness is 10 in.; zero point on silo axis is 827 cm below silo cover. (*Note in press: Subsequent review of these calculations has revealed that the gamma-ray ionization values are too low by approximately 40%.*)

Table 17. Typical Compositions of Materials Considered in Weapons Radiation Transport Calculations[a]

Element	Composition [atoms/(barn·cm)][b]			
	Air (ρ = 1.11 mg/cc)	Ground (ρ = 1.7 g/cc)	Concrete[c] (ρ = 2.62 g/cc)	Steel[c] (ρ = 7.86 g/cc)
H		9.77(−3)	1.065(−2)	
C			1.310(−4)	2.168(−3)
N	3.635(−5)			
O	9.620(−6)	3.48(−2)	4.084(−2)	
Na			1.071(−3)	
Mg			1.620(−4)	
Al		4.88(−2)	2.738(−3)	
Si		1.16(−2)	1.332(−2)	5.508(−4)
P			5.000(−6)	7.644(−5)
S			8.400(−5)	7.384(−5)
K			8.280(−4)	
Ca			2.426(−3)	
Ti			2.600(−5)	
Cr			1.200(−5)	1.820(−4)
Mn			7.500(−5)	8.622(−4)
Fe			5.269(−3)	8.197(−2)
Ni			1.300(−5)	2.016(−4)
Cu			1.500(−5)	2.608(−4)
Mo			1.800(−5)	2.961(−4)

[a]From ref. 95.
[b]That is, atoms/10^{-24} cm^3.
[c]To simplify the calculations some of these elements are usually combined.

Table 18. Composition of Concrete Assumed for Concrete Blockhouses[a]

Element	g/cm^3	Atoms/cm^3
H	0.015	8.96(+21)[b]
O	1.057	3.98(+22)
Na	0.041	1.07(+21)
Mg	0.085	2.11(+21)
Al	0.137	3.06(+21)
Si	0.487	1.04(+22)
P	0.002	3.98(+19)
S	0.002	3.76(+19)
K	0.015	2.31(+20)
Ca	0.295	4.43(+21)
Ti	0.011	1.39(+20)
Mn	0.003	3.29(+19)
Fe	0.178	1.92(+21)
Total	2.329	7.22(+22)

[a]Type O-HW1, natural cured.
[b]Read: 8.96 × 10^{21}.

Table 19. Inside Dimensions of Aboveground Structures

L/W	Length (ft)	Width (ft)
=1	10	10
	20	20
	30	30
	40	40
	50	50
>1	20	10
	30	10
	40	10
	50	10
	30	20
	40	20
	50	20
<1	10	20
	10	30
	10	40
	10	50
	20	30
	20	40
	20	50

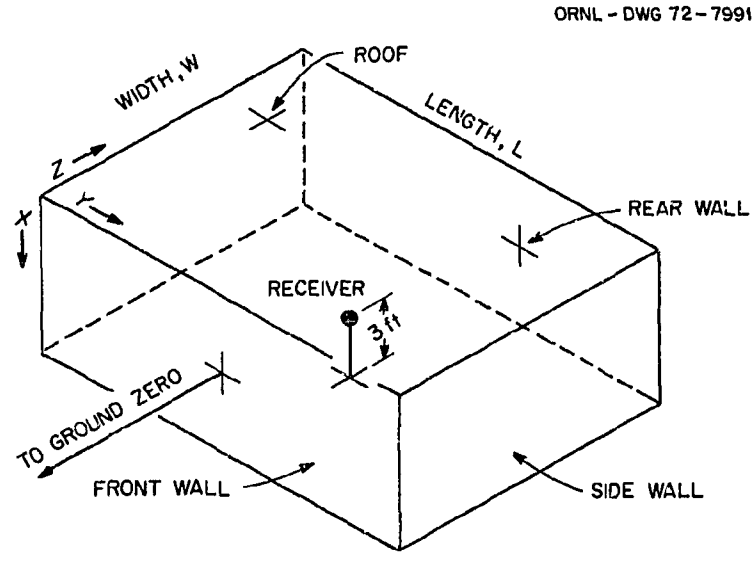

Fig. 21. Aboveground Structure Geometry. (From refs. 98 and 99.)

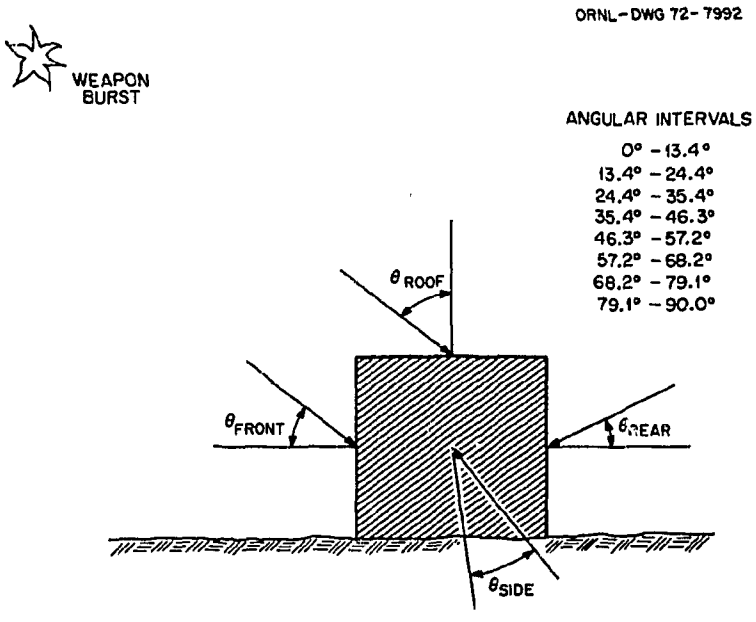

Fig. 22. Coordinate Systems Used to Describe Angular Distributions of Radiation Incident on Walls of Aboveground Structures.

ranges. Before the distributions could be used for the aboveground structures, however, it was necessary to rotate them into fixed coordinate systems relative to the normals to the various outside surfaces of the aboveground building (see Fig. 22) and to use each set of distributions as the incident field in calculations of the penetration of the neutrons through various wall thicknesses (up to 60 in.). For these penetration calculations the walls were represented as infinite slabs of concrete and the calculations were performed with the ANISN code.[43] The neutron fluence emerging from the slab surface was converted to dose and summed over energy to obtain polar angle distributions of the dose relative to the slab normal as a function of slab thickness. The dose at the point of interest inside the structure was then determined by dividing each wall into equal subareas and calculating the contributions to the neutron dose at that point by all the subareas and summing them. (Neutrons backscattered from the walls were neglected.) The resulting total dose is the neutron dose inside the structure due to a unit free-field dose incident on the structure, and thus can be interpreted as an SPC which when applied to an incident neutron dose will give the corresponding dose in the structure.[ii]

The SPC's for the neutron dose 3 ft above the center of the floor in each of the 19 structures are listed in Table 20. Presumably these SPC's can be applied to the neutron doses produced by any weapon whose detonation height and emission spectrum do not deviate too much from those of the thermonuclear weapon assumed for these calculations.[jj] [Note: Because the free-field neutron environment has traditionally been described in terms of Henderson single-collision tissue doses (see Section 8.0) and the results for neutrons that have penetrated through shields are usually given in terms of Snyder-Neufeld multicollision tissue doses,

---

[ii] In this case these SPC's give only the neutron dose and do not include the secondary gamma-ray dose produced by interactions of the neutrons in the structure as those for the underground structures did.

[jj] In the DNA Handbook,[98] these SPC's, plus those for other locations in the structures, were applied to the free-field doses produced by the eight representative weapons mentioned in Section 9.2.1.

Table 20. Structure Protection Coefficients[a] for Calculating Neutron Doses in Aboveground Concrete Blockhouses[b] (Structure Height = 10 ft)[c]

Structure Wall Thickness (in.)	Structure Length[c] (ft)	SPC_n for Structure Width[c] of				
		10 ft	20 ft	30 ft	40 ft	50 ft
6	10	4.657(−1)[d]	4.055(−1)	3.639(−1)	3.398(−1)	3.243(−1)
	20	4.536(−1)	4.204(−1)	3.846(−1)	3.577(−1)	3.381(−1)
	30	4.376(−1)	4.105(−1)	3.807(−1)		
	40	4.225(−1)	3.965(−1)		3.490(−1)	
	50	4.138(−1)	4.006(−1)			3.214(−1)
12	10	1.188(−1)	9.915(−2)	8.710(−2)	8.041(−2)	7.623(−2)
	20	1.180(−1)	1.054(−1)	9.416(−2)	8.623(−2)	8.079(−2)
	30	1.142(−1)	1.037(−1)	9.407(−2)		
	40	1.107(−1)	1.005(−1)		8.534(−2)	
	50	1.085(−1)	1.023(−1)			7.774(−2)
18	10	3.117(−2)	2.515(−2)	2.168(−2)	1.980(−2)	1.865(−2)
	20	3.154(−2)	2.736(−2)	2.395(−2)	2.165(−2)	2.012(−2)
	30	3.064(−2)	2.715(−2)	2.421(−2)		
	40	2.982(−2)	2.642(−2)		2.177(−2)	
	50	2.928(−2)	2.700(−2)			1.970(−2)
24	10	8.527(−3)	6.697(−3)	5.682(−3)	5.140(−3)	4.812(−3)
	20	8.724(−3)	7.404(−3)	6.387(−3)	5.715(−3)	5.270(−3)
	30	8.515(−3)	7.398(−3)	6.505(−3)		
	40	8.306(−3)	7.219(−3)		5.819(−3)	
	50	8.164(−3)	7.402(−3)			5.240(−3)
36	10	6.664(−4)	5.003(−4)	4.122(−4)	3.661(−4)	3.386(−4)
	20	6.953(−4)	5.679(−4)	4.770(−4)	4.188(−4)	3.807(−4)
	30	6.819(−4)	5.737(−4)	4.927(−4)		
	40	6.692(−4)	5.631(−4)		4.364(−4)	
	50	6.590(−4)	5.795(−4)			3.899(−4)
48	10	5.537(−4)	4.046(−5)	3.272(−5)	2.870(−4)	2.635(−5)
	20	5.840(−5)	4.669(−5)	3.860(−5)	3.346(−5)	3.014(−5)
	30	5.751(−5)	4.748(−5)	4.018(−5)		
	40	5.656(−5)	4.673(−5)		3.536(−5)	
	50	5.576(−5)	4.812(−5)			3.149(−5)
60	10	4.720(−6)	3.377(−6)	2.693(−6)	2.341(−6)	2.134(−6)
	20	5.013(−6)	3.943(−6)	3.219(−6)	2.765(−6)	2.473(−6)
	30	4.951(−6)	4.028(−6)	3.375(−6)		
	40	4.875(−6)	3.975(−6)		2.955(−6)	
	50	4.809(−6)	4.092(−6)			2.624(−6)

[a]Ratio of multicollision neutron dose inside structure to single-collision neutron dose incident on structure.
[b]From Mooney, ref. 99, and Mooney and Wells, ref. 98.
[c]Inside dimensions.
[d]Read: 4.657×10^{-1}.

each SPC given in Table 20 is the ratio of the multicollision dose inside the structure to the single-collision dose incident on the structure.]

Concrete-Capture Gamma-Ray Doses. In addition to neutron fluences, the ANISN calculations for infinite slabs of concrete described in the preceding paragraphs yielded emerging gamma-ray fluences due to the capture of thermal, epithermal, and fast neutrons in concrete. (Gamma rays produced by the inelastic scattering of high-energy neutrons in the concrete were neglected because of inadequate input data.) These results were handled in the same manner as those for neutrons, and the corresponding SPC's, given in Table 21, should be applicable to the same free-field neutron doses for which the SPC's given in Table 20 are applicable.[jj] Note that in this case the SPC is the ratio of the gamma-ray dose inside the structure to the single-collision neutron dose incident on the structure. Also note that only the gamma rays produced by neutrons making their first pass through a structure wall are considered; that is, gamma rays produced by neutrons entering a wall after having passed through the structure cavity are neglected.

Air and Ground Secondary Gamma-Ray Doses. For the calculations of the penetration of the air and ground secondary gamma rays into the concrete blockhouses it was assumed that the incident field could be described by the secondary gamma-ray energy and angular distributions calculated for a slant range of 1200 m from the intermediate-yield thermonuclear weapon at the 100-m altitude. These distributions were obtained by Straker concomitantly with the neutron distributions (see above) and thus are for the same burst conditions. However, as was pointed out in Section 9.3.1, the gamma-ray distributions failed to reach equilibrium even at the largest range covered (1500 m); therefore the distributions at 1200 m were arbitrarily selected for the concrete-penetration calculations. The distributions were rotated into the same coordinate systems used for the neutron distributions (see Fig. 22), and an ANISN infinite-slab calculation was performed for each set. The gamma rays emerging from the slabs were treated in the same manner as described above to

Table 21. Structure Protection Coefficients[a] for Calculating Doses in Aboveground Concrete Blockhouses Due to Gamma Rays Produced by Neutron Captures in Structure[b] (Structure Height = 10 ft)[c]

Structure Wall Thickness (in.)	Structure Length[c] (ft)	SPC_{cc} for Structure Width[c] of				
		10 ft	20 ft	30 ft	40 ft	50 ft
6	10	5.590(−2)[d]	5.259(−2)	5.201(−2)	5.189(−2)	5.175(−2)
	20	5.344(−2)	4.741(−2)	4.619(−2)	4.582(−2)	4.564(−2)
	30	5.309(−2)	4.652(−2)	4.457(−2)		
	40	5.310(−2)	4.620(−2)		4.312(−2)	
	50	5.301(−2)	4.685(−2)			4.183(−2)
12	10	6.671(−2)	6.115(−2)	5.861(−2)	5.744(−2)	5.673(−2)
	20	6.345(−2)	5.824(−2)	5.550(−2)	5.390(−2)	5.287(−2)
	30	6.159(−2)	5.651(−2)	5.361(−2)		
	40	6.074(−2)	5.517(−2)		5.046(−2)	
	50	6.015(−2)	5.582(−2)			4.762(−2)
18	10	3.302(−2)	2.951(−2)	2.762(−2)	2.675(−2)	2.626(−2)
	20	3.125(−2)	2.891(−2)	2.700(−2)	2.579(−2)	2.503(−2)
	30	2.993(−2)	2.779(−2)	2.604(−2)		
	40	2.928(−2)	2.682(−2)		2.395(−2)	
	50	2.887(−2)	2.726(−2)			2.210(−2)
24	10	1.394(−2)	1.223(−2)	1.125(−2)	1.078(−2)	1.051(−2)
	20	1.314(−2)	1.220(−2)	1.121(−2)	1.058(−2)	1.016(−2)
	30	1.245(−2)	1.164(−2)	1.079(−2)		
	40	1.213(−2)	1.111(−2)		9.746(−3)	
	50	1.192(−2)	1.141(−2)			8.813(−3)
36	10	2.161(−3)	1.845(−3)	1.651(−3)	1.553(−3)	1.501(−3)
	20	2.029(−3)	1.881(−3)	1.690(−3)	1.561(−3)	1.479(−3)
	30	1.901(−3)	1.779(−3)	1.625(−3)		
	40	1.832(−3)	1.675(−3)		1.421(−3)	
	50	1.795(−3)	1.765(−3)			1.235(−3)
48	10	3.107(−4)	2.638(−4)	2.321(−4)	2.163(−4)	2.073(−4)
	20	2.912(−4)	2.697(−4)	2.407(−4)	2.201(−4)	2.066(−4)
	30	2.701(−4)	2.545(−4)	2.313(−4)		
	40	2.598(−4)	2.364(−4)		1.964(−4)	
	50	2.534(−4)	2.572(−4)			1.653(−4)
60	10	4.576(−5)	3.908(−5)	3.394(−5)	3.163(−5)	3.1013(−5)
	20	4.287(−5)	3.983(−5)	3.553(−5)	3.241(−5)	3.028(−5)
	30	3.939(−5)	3.752(−5)	3.412(−5)		
	40	3.796(−5)	3.435(−5)		2.816(−5)	
	50	3.690(−5)	3.872(−5)			2.319(−5)

[a]Ratio of gamma-ray dose inside structure to single-collision neutron dose incident on structure.
[b]From Mooney, ref. 99, and Mooney and Wells, ref. 98.
[c]Inside dimensions.
[d]Read: 5.590×10^{-2}.

obtain the SPC's for the structures. These SPC's, given in Table 22, should be applicable to the same weapons for which the SPC's listed in Tables 20 and 21 are applicable.[jj]

Fission-Product Gamma-Ray Doses. The incident energy and angular distributions of the fission-product gamma rays were obtained from a separate calculation in which it was assumed that the energy spectrum of the fission-product gamma rays emitted from the weapon and its debris cloud during the first minute following the detonation was the same as that measured by Engle and Fisher for the 0.2- to 0.5-sec period.[19] This spectrum was folded with the gamma-ray transport data set of Marshall and Wells[61] to obtain the energy and angular distributions at various ranges. The results indicated that these distributions did not vary beyond about 600 m, so the data at 1200 m were selected as being representative of all ranges.

Unlike the distributions for neutrons and secondary gamma rays, the representative distributions for fission-product gamma rays could not be prepared for use in concrete penetration calculations merely by rotating them into the fixed coordinate systems depicted in Fig. 22. This is because the representative distributions are described with respect to a line passing from the center of the debris cloud to the structure, and the locations of the corresponding angles at the structure change as the cloud rises during the first minute after the burst. Thus it was necessary to alter the representative distributions to account for the changing directions of the incident gamma rays. The first step was to use the empirical expressions of Loewe et al.[86] to calculate source height versus time curves for weapons of various yields detonated at a 100-m altitude. With the Engle and Fisher spectrum used as the source, this calculation was extended to obtain a time plot of the cumulative dose from each weapon at a 100-psi overpressure range. Each dose curve was then divided into a number of time intervals containing equal fractions of the dose, and a source height for each interval was selected on the basis of the time in each interval at which one-half the dose for that interval arrived at the structure. With these source heights defining the angle of elevation

Table 22. Structure Protection Coefficients[a] for Calculating Doses in Aboveground Concrete Blockhouses Due to Gamma Rays Produced by Neutron Interactions in the Air and Ground[b] (Structure Height = 10 ft)[c]

Structure Wall Thickness (in.)	Structure Length[c] (ft)	SPC_{ag} for Structure Width[c] of				
		10 ft	20 ft	30 ft	40 ft	50 ft
6	10	3.247(−1)[d]	2.632(−1)	2.133(−1)	1.789(−1)	1.532(−1)
	20	3.275(−1)	2.810(−1)	2.400(−1)	2.070(−1)	1.810(−1)
	30	3.269(−1)	2.835(−1)	2.460(−1)		
	40	3.263(−1)	2.837(−1)		2.191(−1)	
	50	3.261(−1)	2.837(−1)			1.968(−1)
12	10	1.190(−1)	9.336(−2)	7.281(−2)	5.892(−2)	4.883(−2)
	20	1.207(−1)	1.020(−1)	8.509(−2)	7.146(−2)	6.090(−2)
	30	1.203(−1)	1.027(−1)	8.736(−2)		
	40	1.200(−1)	1.026(−1)		7.635(−2)	
	50	1.199(−1)	1.025(−1)			6.741(−2)
18	10	4.506(−2)	3.498(−2)	2.691(−2)	2.144(−2)	1.746(−2)
	20	4.578(−2)	3.851(−2)	3.185(−2)	2.650(−2)	2.236(−2)
	30	4.565(−2)	3.379(−2)	3.276(−2)		
	40	4.553(−2)	3.871(−2)		2.851(−2)	
	50	4.548(−2)	3.869(−2)			2.503(−2)
24	10	1.725(−2)	1.332(−2)	1.016(−2)	8.022(−3)	6.456(−3)
	20	1.756(−2)	1.472(−2)	1.213(−2)	1.003(−2)	8.414(−3)
	30	1.752(−2)	1.485(−2)	1.250(−2)		
	40	1.747(−2)	1.481(−2)		1.085(−2)	
	50	1.746(−2)	1.481(−2)			9.496(−3)
36	10	2.571(−3)	2.000(−3)	1.523(−3)	1.190(−3)	9.457(−4)
	20	2.624(−3)	2.203(−3)	1.818(−3)	1.503(−3)	1.254(−3)
	30	2.619(−3)	2.223(−3)	1.874(−3)		
	40	2.612(−3)	2.221(−3)		1.624(−3)	
	50	2.610(−3)	2.221(−3)			1.420(−3)
48	10	3.976(−4)	3.105(−4)	2.369(−4)	1.846(−4)	1.458(−4)
	20	4.065(−4)	3.416(−4)	2.827(−4)	2.337(−4)	1.949(−4)
	30	4.062(−4)	3.451(−4)	2.911(−4)		
	40	4.055(−4)	3.451(−4)		2.528(−4)	
	50	4.053(−4)	3.454(−4)			2.210(−4)
60	10	6.217(−5)	4.877(−5)	3.728(−5)	2.900(−5)	2.280(−5)
	20	6.364(−5)	5.355(−5)	4.439(−5)	3.674(−5)	3.063(−5)
	30	6.367(−5)	5.416(−5)	4.573(−5)		
	40	6.355(−5)	5.420(−5)		3.974(−5)	
	50	6.352(−5)	5.425(−5)			3.747(−5)

[a]Ratio of gamma-ray dose inside structure to gamma-ray dose incident on structure that is due to neutron capture and inelastic-scattering gamma rays produced in the air and ground.

[b]From Mooney, ref. 99, and Mooney and Wells, ref. 98.

[c]Inside dimensions.

[d]Read: 3.247×10^{-1}.

of the source at the detector, the energy and angle distributions of the fluence about the source-structure axis for each time interval were rotated into a fixed coordinate system. Next the sum of the energy and angle distributions of the fluence over all time intervals in the fixed coordinate system was divided into the fluence in each of the energy and angle intervals to give an energy and angle distribution normalized to a unit fluence incident on the structure. The resulting distributions for each weapon yield were then rotated into the four coordinate systems relative to the normals to the various outside surfaces of the aboveground building (see Fig. 22). A comparison of the distributions for the different weapons revealed little dependence on weapon yield, which Mooney and Wells attribute to the fact that the rate at which the horizontal range increases with weapon yield for the 100-psi overpressure range is approximately the same as the rate at which the fission-product cloud altitude increases with time. Thus the elevation angle defined by the source-detector axis for each of the time intervals does not vary significantly with weapon yield. It was therefore concluded that the energy and angle distributions of the fission-product gamma-ray fluence at the 100-psi overpressure range for a 1-megaton weapon would be representative for all yields.

These energy and angle distributions for the four fixed coordinate systems were then used in ANISN calculations to determine their penetration through infinite slabs of concrete. The gamma rays emerging from the slabs were treated in the same manner as those from the other ANISN calculations to obtain the SPC's for the structures. These SPC's, listed in Table 23, should be applicable to any weapon containing a fission fraction.[kk]

Total Doses. The structure protection coefficients listed in Tables 20-23 may be used to estimate the total initial radiation dose,

[kk] In the DNA Handbook they were applied to the doses calculated for a range of weapons by the Mooney-French method described in Section 9.4.

Table 23. Structure Protection Coefficients[a] for Calculating Fission-Product Gamma-Ray Doses in Aboveground Concrete Blockhouses[b] (Structure Height = 10 ft)[c]

Structure Wall Thickness (in.)	Structure Length[c] (ft)	SPC_{fp} for Structure Width[c] of				
		10 ft	20 ft	30 ft	40 ft	50 ft
6	10	1.659(−1)[d]	1.190(−1)	9.010(−2)	7.440(−2)	6.569(−2)
	20	1.789(−1)	1.500(−1)	1.230(−1)	1.039(−1)	9.100(−2)
	30	1.810(−1)	1.559(−1)	1.339(−1)		
	40	1.819(−1)	1.580(−1)		1.200(−1)	
	50	1.819(−1)	1.580(−1)			1.100(−1)
12	10	4.130(−2)	2.809(−2)	1.939(−2)	1.479(−2)	1.220(−2)
	20	4.480(−2)	3.579(−2)	2.800(−2)	2.230(−2)	1.849(−2)
	30	4.530(−2)	3.720(−2)	3.039(−2)		
	40	4.550(−2)	3.759(−2)		2.629(−2)	
	50	4.579(−2)	3.769(−2)			2.329(−2)
18	10	1.159(−2)	7.739(−3)	5.129(−3)	3.699(−3)	2.909(−3)
	20	1.250(−2)	9.799(−3)	7.469(−3)	5.779(3)	4.630(−3)
	30	1.259(−2)	1.009(−2)	8.110(−3)		
	40	1.269(−2)	1.020(−2)		6.879(−3)	
	50	1.279(−2)	1.029(−2)			6.010(−3)
24	10	3.489(−3)	2.309(−3)	1.500(−3)	1.049(−3)	7.959(−4)
	20	3.739(−3)	2.889(−3)	2.179(−3)	1.659(−3)	1.299(−3)
	30	3.789(−3)	3.000(−3)	2.630(−3)		
	40	3.820(−3)	3.030(−3)		1.979(−3)	
	50	3.859(−3)	3.039(−3)			1.709(−3)
36	10	3.389(−4)	2.269(−4)	1.459(−4)	9.930(−5)	7.190(−5)
	20	3.599(−4)	2.769(−4)	2.079(−4)	1.569(−4)	1.200(−4)
	30	3.639(−4)	2.849(−4)	2.240(−4)		
	40	3.669(−4)	2.880(−4)		1.849(−4)	
	50	3.710(−4)	2.900(−4)			1.569(−4)
48	10	3.649(−5)	2.480(−5)	1.600(−5)	1.070(−5)	7.659(−6)
	20	3.839(−5)	2.960(−5)	2.240(−5)	1.689(−5)	1.279(−5)
	30	3.890(−5)	3.050(−5)	2.389(−5)		
	40	3.929(−5)	3.079(−5)		1.969(−5)	
	50	3.960(−5)	3.089(−5)			1.670(−5)
60	10	4.159(−6)	2.869(−6)	1.869(−6)	1.250(−6)	8.880(−7)
	20	4.369(−6)	3.379(−6)	2.579(−6)	1.949(−6)	1.479(−6)
	30	4.410(−6)	3.479(−6)	2.739(−6)		
	40	4.449(−6)	3.509(−6)		2.259(−6)	
	50	4.480(−6)	3.519(−6)			1.899(−6)

[a]Ratio of fission-product gamma-ray dose inside structure to fission-product gamma-ray dose incident on structure.
[b]From Mooney, ref. 99, and Mooney and Wells, ref. 98.
[c]Inside dimensions.
[d]Read: 1.659×10^{-1}.

excluding that due to prompt gamma rays, reaching a point 3 ft above the center of the floor in each of the 19 structures as follows:

$$D_T = [D_n \times (\mathrm{SPC}_n + \mathrm{SPC}_{cc})] + [D_{ag} \times \mathrm{SPC}_{ag}] + [D_{fp} \times \mathrm{SPC}_{fp}] \quad ,$$

where D_n, D_{ag}, and D_{fp} are the incident neutron, air-ground secondary gamma-ray, and fission-product gamma-ray doses respectively. Mooney[99] states that the SPC's for structures not specifically listed may be obtained by interpolation and/or extrapolation; however, the inside heights of the structures should not be too different from 10 ft. (Note: The dose calculated in this manner is for a structure which is uniformly protected over the exposed surfaces. When an entranceway is added to the structure, then the doses due to neutrons and gamma rays arriving through the entranceway must be added to the total dose.)

As a matter of interest, a comparison of the SPC's for the various dose components as a function of the wall thickness on a 10-ft cubical structure is shown in Fig. 23. Keep in mind that the lower the SPC the greater that particular radiation component will be attenuated in the structure wall. For wall thicknesses greater than 20 in. the fission-product gamma rays and neutrons undergo a greater attenuation than do the air-ground or concrete-capture secondary gamma rays. Thus it would appear that the secondary gamma rays would comprise the major fraction of the radiation that penetrates into the structure cavity. This is illustrated by the following sample problems:

Prob. A

Consider a 30-ft long and 10-ft wide aboveground structure (10 ft height) with a 48-in. wall thickness exposed to the doses given in Table 13 for a range of 879 m from a 40-kiloton weapon (corresponds to a 30-psi overpressure). These doses are:

$$D_n = 12{,}000 \text{ rads}$$
$$D_{ag} = 8{,}000 \text{ rads}$$
$$D_{fp} = 1{,}600 \text{ rads}$$

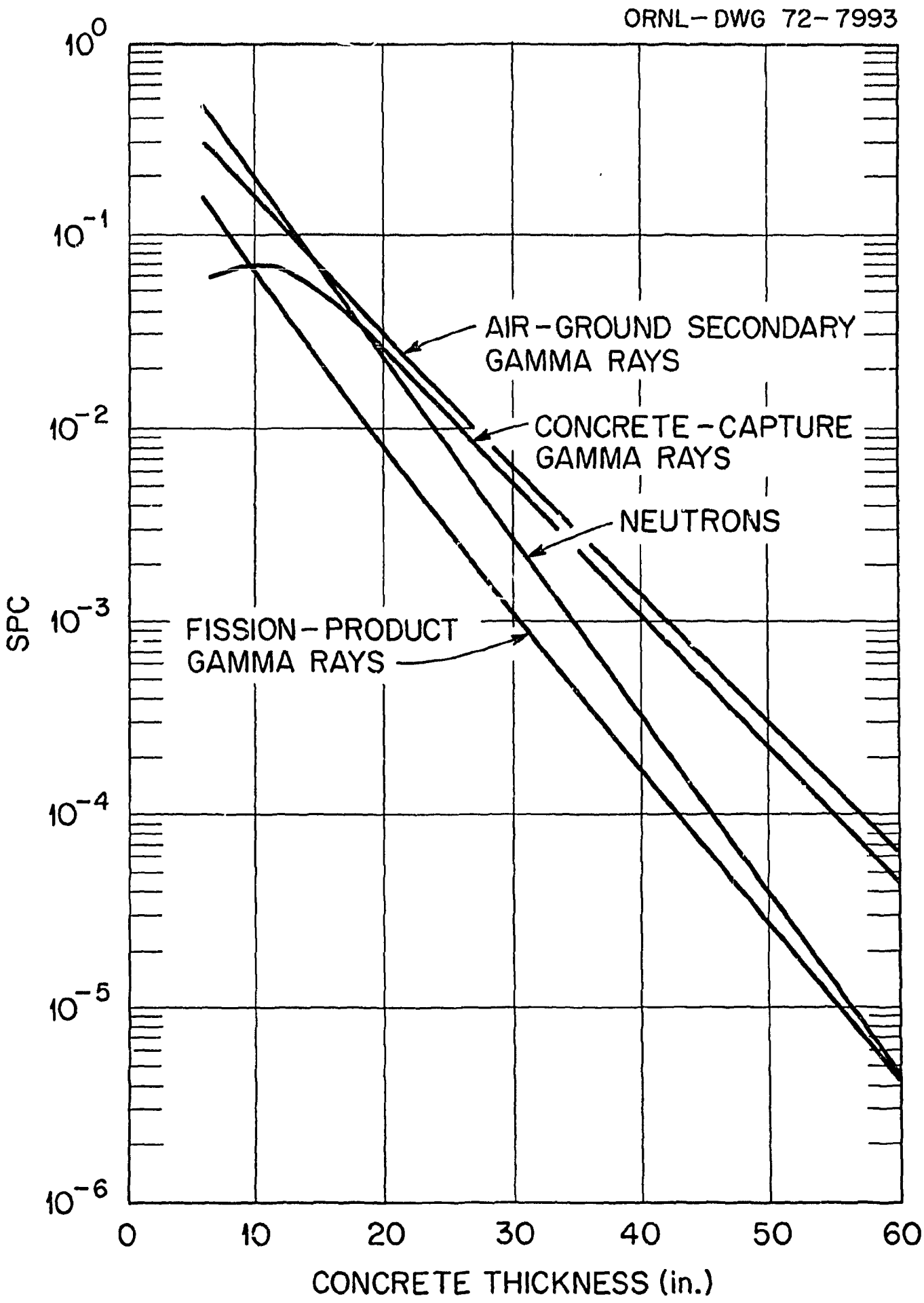

Fig. 23. Structure Protection Coefficients for a 10-ft Cubical Structure as a Function of Concrete Wall Thickness. (From Mooney, ref. 99.)

The SPC values for the structure as obtained from Tables 20-23 are:

$$SPC_n = 5.751 \times 10^{-5}$$
$$SPC_{cc} = 2.701 \times 10^{-4}$$
$$SPC_{ag} = 4.062 \times 10^{-4}$$
$$SPC_{fp} = 3.890 \times 10^{-5}$$

Multiplying the incident doses by the appropriate SPC's gives a total dose at a position 3 ft above the center of the floor as follows:

$$\text{Neutrons} = (12{,}000 \text{ rads}) \times (5.751 \times 10^{-5}) = 0.69 \text{ rad } (9\%)$$
$$\text{Concrete-capture gamma rays} = (12{,}000 \text{ rads}) \times (2.701 \times 10^{-4}) = 3.24 \text{ rads } (45\%)$$
$$\text{Air-ground gamma rays} = (8{,}000 \text{ rads}) \times (4.062 \times 10^{-4}) = 3.25 \text{ rads } (45\%)$$
$$\text{Fission-product gamma rays} = (1{,}600 \text{ rads}) \times (3.890 \times 10^{-5}) = 0.06 \text{ rad } (1\%)$$
$$\text{Total} = 7.24 \text{ rads}$$

Prob. B

Consider a 20-ft wide and 50-ft long aboveground structure (10-ft height) with a 60-in. wall thickness exposed to the doses given in Table 13 for a range of 1547 m from a 1-megaton weapon (corresponds to a 100-psi overpressure). These doses are:

$$D_n = 3{,}800 \text{ rads}$$
$$D_{ag} = 4{,}800 \text{ rads}$$
$$D_{fp} = 13{,}000 \text{ rads}$$

The SPC values for the structure as obtained from Tables 20-23 are:

$$SPC_n = 4.092 \times 10^{-6}$$
$$SPC_{cc} = 3.872 \times 10^{-5}$$
$$SPC_{ag} = 5.425 \times 10^{-5}$$
$$SPC_{fp} = 3.519 \times 10^{-6}$$

Multiplying the incident doses by the appropriate SPC's gives a total dose at a position 3 ft above the center of the floor as follows:

$$\text{Neutrons} = (3{,}800 \text{ rads}) \times (4.092 \times 10^{-6}) = 0.016 \text{ rad } (3\%)$$

$$\text{Concrete-capture gamma rays} = (3.800 \text{ rads}) \times (3.872 \times 10^{-5}) = 0.147 \text{ rad } (31\%)$$

$$\text{Air-ground gamma rays} = (4.800 \text{ rads}) \times (5.425 \times 10^{-5}) = 0.260 \text{ rad } (56\%)$$

$$\text{Fission-product gamma rays} = (13{,}000 \text{ rads}) \times (3.519 \times 10^{-6}) = 0.045 \text{ rad } (10\%)$$

$$\text{Total} = 0.47 \text{ rad}$$

In both problems the contributions from the secondary gamma rays produced in the concrete and in the air and ground predominate. In Problem A, which is for a 48-in.-thick structure 0.54 mile from a 40-kiloton detonation, the gamma rays produced in the environment surrounding the structure and those produced in the structure itself contribute approximately equally, each comprising 45% of the dose penetrating to the inside of the structure. In Problem B, which is for a 60-in.-thick structure slightly less than a mile from a 1-megaton burst, these two components still contribute a total of approximately 90% of the penetrating dose, but the gamma rays produced in the environmental materials contribute a significantly larger fraction than those produced in the structure itself. These same trends are apparent in Table 24, which gives results from similar calculations for 81 different cases. Only for relatively thin wall thicknesses are any significant contributions made by the neutrons and fission-product gamma rays.

Several other trends can be deduced from Table 24. For the position of interest, the doses in the 10-ft cubical structure are always higher than those in the larger structures. Also, the doses in the structure with the 50-ft length and 20-ft width are higher than those in the structure with the 50-ft width and 20-ft length, which can be attributed to the fact that the length of the structure is facing the burst (see Fig. 21).

While these SPC's for aboveground structures are simple to apply, at present there appears to be no way of assessing their accuracy. The

Table 24. Total Doses Produced in Aboveground Structures by Weapons with Typical Thermonuclear Neutron Emission Spectrum[a]

(Excluding Prompt Gamma-Ray Doses)

Prob. No.	Structure Dimensions			Fractional Contribution[b] to Dose by				Total Dose[c] (rads)
	L (ft)	W (ft)	t (in.)	Neutrons	Concrete-Capture Gamma Rays	Air-Ground Gamma Rays	Fission-Product Gamma Rays	
Case: 40-kiloton Burst at 785-m Height; 15 psi at 1204-m Slant Range								
1a	10	10	18	0.28	0.29	0.40	0.03	1.47(+2)[d]
1b			36	0.12	0.40	0.47	0.01	7.08(0)
1c			60	0.04	0.40	0.55	0.01	1.47(−1)
2a	20	50	18	0.29	0.35	0.32	0.04	9.15(+1)
2b			36	0.12	0.47	0.40	0.01	4.07(0)
2c			60	0.04	0.48	0.48	0.00	8.27(−2)
3a	50	20	18	0.27	0.28	0.39	0.06	1.28(+2)
3b			36	0.13	0.38	0.48	0.01	5.99(0)
3c			60	0.04	0.40	0.56	0.00	1.26(−1)
Case: 40-kiloton Burst at 625-m Height; 30 psi at 879-m Slant Range								
4a	10	10	24	0.25	0.41	0.33	0.01	4.13(+2)
4b			48	0.09	0.49	0.41	0.01	7.63(0)
4c			60	0.05	0.49	0.45	0.01	1.11(0)
5a	20	50	24	0.25	0.48	0.26	0.01	2.54(+2)
5b			48	0.08	0.56	0.35	0.01	4.43(0)
5c			60	0.05	0.57	0.38	0.00	6.40(−1)
6a	50	20	24	0.26	0.39	0.34	0.01	3.49(+2)
6b			48	0.09	0.47	0.43	0.01	6.48(0)
6c			60	0.05	0.49	0.45	0.01	9.53(−1)
Case: 40-kiloton Burst at 410-m Height; 100 psi at 528-m Slant Range								
7a	10	10	36	0.21	0.67	0.12	0.00	1.14(+3)
7b			48	0.13	0.72	0.15	0.00	1.51(+2)
7c			60	0.08	0.76	0.16	0.00	2.11(+1)
8a	20	50	36	0.18	0.72	0.10	0.00	7.22(+2)
8b			48	0.11	0.77	0.12	0.00	9.38(+1)
8c			60	0.07	0.80	0.13	0.00	1.32(+1)
9a	50	20	36	0.21	0.65	0.13	0.01	9.47(+2)
9b			48	0.13	0.71	0.15	0.01	1.26(+2)
9c			60	0.06	0.81	0.13	0.00	2.35(+1)
Case: 300-kiloton Burst at 1530-m Height; 15 psi at 2362-m Slant Range								
10a	10	10	18	0.12	0.13	0.65	0.10	2.75(0)
10b			36	0.05	0.17	0.72	0.06	1.42(−1)
10c			60	0.02	0.16	0.79	0.03	3.15(−3)
11a	20	50	18	0.12	0.15	0.48	0.25	1.85(−1)
11b			36	0.06	0.22	0.68	0.04	7.36(−2)
11c			60	0.02	0.20	0.76	0.02	1.62(−3)
12a	50	20	18	0.10	0.10	0.50	0.30	3.09(0)
12b			36	0.05	0.16	0.73	0.06	1.22(−1)
12c			60	0.02	0.16	0.79	0.03	2.73(−3)
Case: 300-kiloton Burst at 1220-m Height; 30 psi at 1715-m Slant Range								
13a	10	10	24	0.16	0.26	0.50	0.08	2.32(+1)
13b			48	0.05	0.30	0.60	0.05	4.44(−1)
13c			60	0.03	0.30	0.63	0.04	6.57(−2)

Table 24. (continued)

Prob. No.	Structure Dimensions			Fractional Contribution[b] to Dose by				Total Dose[c] (rads)
	L (ft)	W (ft)	t (in.)	Neutrons	Concrete-Capture Gamma Rays	Air-Ground Gamma Rays	Fission-Product Gamma Rays	
14a	20	50	24	0.17	0.34	0.43	0.06	1.30(+1)
14b			48	0.05	0.37	0.55	0.03	2.39(−1)
14c			60	0.03	0.37	0.58	0.02	3.54(−2)
15a	50	20	24	0.16	0.25	0.50	0.09	1.97(+1)
15b			48	0.05	0.29	0.61	0.05	3.80(−1)
15c			60	0.03	0.29	0.64	0.04	5.67(−2)
Case: 300-kiloton Burst at 800-m Height; 100 psi at 1037-m Slant Range								
16a	10	10	36	0.15	0.49	0.31	0.05	1.07(+2)
16b			48	0.09	0.52	0.36	0.03	1.44(+1)
16c			60	0.05	0.53	0.39	0.03	2.08(0)
17a	20	50	36	0.14	0.57	0.26	0.03	6.26(+1)
17b			48	0.09	0.59	0.30	0.02	8.39(0)
17c			60	0.05	0.60	0.33	0.02	1.20(0)
18a	50	20	36	0.16	0.47	0.32	0.05	8.92(+1)
18b			48	0.09	0.50	0.37	0.04	1.23(+1)
18c			60	0.05	0.53	0.39	0.03	1.81(0)
Case: 1-megaton Burst at 2290-m Height; 15 psi at 3525-m Slant Range								
19a	10	10	18	0.24	0.25	0.34	0.17	1.32(−1)
19b			36	0.11	0.36	0.42	0.11	6.07(−3)
19c			60	0.04	0.38	0.51	0.07	1.21(−4)
20a	20	50	18	0.19	0.24	0.21	0.36	1.04(−1)
20b			36	0.11	0.44	0.38	0.07	3.35(−3)
20c			60	0.04	0.46	0.46	0.04	6.63(−5)
21a	50	20	18	0.16	0.16	0.23	0.45	1.68(−1)
21b			36	0.11	0.35	0.43	0.11	5.15(−3)
21c			60	0.04	0.37	0.52	0.07	1.04(−4)
Case: 1-megaton Burst at 1820-m Height; 30 psi at 2560-m Slant Range								
22a	10	10	24	0.05	0.08	0.55	0.32	1.81(0)
22b			48	0.02	0.09	0.70	0.19	3.28(−2)
22c			60	0.01	0.10	0.75	0.14	4.81(−3)
23a	20	50	24	0.06	0.12	0.57	0.25	8.61(−1)
23b			48	0.02	0.13	0.71	0.14	1.58(−2)
23c			60	0.01	0.13	0.75	0.11	2.35(−3)
24a	50	20	24	0.05	0.07	0.55	0.33	1.55(0)
24b			48	0.02	0.09	0.71	0.18	2.83(−2)
24c			60	0.01	0.09	0.76	0.14	4.17(−3)
Case: 1-megaton Burst at 1190-m Height; 100 psi at 1547-m Slant Range								
25a	10	10	36	0.09	0.30	0.45	0.16	2.75(+1)
25b			48	0.06	0.31	0.50	0.13	3.77(0)
25c			60	0.03	0.32	0.55	0.10	5.44(−1)
26a	20	50	36	0.10	0.38	0.41	0.11	1.46(+1)
26b			48	0.06	0.39	0.47	0.08	2.00(0)
26c			60	0.03	0.40	0.50	0.07	2.91(−1)
27a	50	20	36	0.09	0.29	0.46	0.16	2.33(+1)
27b			48	0.06	0.30	0.52	0.12	3.22(0)
27c			60	0.03	0.31	0.56	0.10	4.73(−1)

[a]See Table 12.

[b]Based on free-field doses given in Table 13 and SPC's given in Tables 20–23.

[c]The dose delivered to 1 gram of tissue at a point 3 ft above the center of the floor of the structure. All structures have 10-ft inside height.

[d]Read: 1.47×10^2.

ANISN code used for calculating the transport of the incident radiation through the concrete is considered to be reliable, but ANISN is a one-dimensional code and therefore each wall had to be treated separately and, further, each wall had to be treated as an infinite slab of concrete rather than as a wall with a finite length and a finite width. The results for all the walls were then added, with no consideration given to the interacting effects of the walls, although this probably did not introduce a significant error. Probably the largest error lies in the prediction of the number of secondary gamma rays produced in the concrete. The production cross sections used in the calculations were preliminary and calculations now underway at ORNL indicate that neglecting the gamma rays produced by the neutron inelastic-scattering process may have underestimated this secondary contribution by as much as a factor of 2.

Additional errors may be inherent in the examples given here. The incident doses are based on the air-transport data sets of Straker,[69] and the cross sections he used for nitrogen and oxygen differ somewhat from the latest evaluations (see discussions near the ends of Sections 9.2.1 and 9.3.1). If it develops that the incident neutron doses are too low, then not only would the contribution to the neutron dose be underestimated but also the contribution to the dose due to gamma rays produced by the neutrons in the concrete. Similarly, errors in the incident secondary gamma-ray doses would affect the penetrating dose.

Because of the large number of unknowns, plus the lack of experimental studies to support the calculations, each radiation component calculated in these examples may be greatly underestimated, by as much as a factor of 8 to 12 or more. If, on the other hand, the SPC's are applied to incident doses that are known to be correct, the uncertainty associated with the SPC's probably would be reduced to a factor of 5 to 7, which, of course, is still not good enough and indicates the need for further studies of this type.

10.3. Entranceways (Rectangular Tunnels)

The protection offered against weapons radiation by any structure may be severely compromised by the necessary addition of an accessway. In general the access to the structure will be through a tunnel which will serve to reduce both the overpressure and the amount of radiation that reaches the structure door. But for the tunnel to be effective, it must contain bends, since neutrons or gamma rays traveling through a straight tunnel will undergo little attenuation in the air and radiation "streaming" to the structure door will become a problem. When bends are introduced, the particles must scatter against the nuclei of the tunnel walls and change directions in order to continue their travel through the tunnel. Gamma rays that scatter at large angles suffer so much energy loss that their further travel is improbable. Thus gamma-ray streaming can be greatly reduced simply by introducing a 90-deg bend in the tunnel and gamma-ray streaming is essentially eliminated by the addition of a second bend. Neutron streaming cannot be entirely eliminated, however, since neutrons can scatter at large angles with little or no reduction in energy. Therefore, they not only can negotiate 90-deg bends, they can also produce secondary gamma rays throughout the length of the tunnel by interacting with various nuclei of the walls. Those gamma rays produced in the last leg of the tunnel, not having to negotiate a bend, will contribute to the dose reaching the structure doorway.

For the foregoing reasons, the few studies that have been made of the transmission of radiation in passageways have primarily been of one- and two-legged ducts that consist of straight segments connected at right angles. For doses due to incident neutrons, the most extensive studies have been made by Maerker,[100] who performed Monte Carlo calculations of the neutron transmission and capture-gamma-ray production in concrete-walled ducts that are rectangular in cross section. For incident gamma rays, studies have been performed by Huddleston and Ingold,[101] who developed an empirical formula for gamma-ray transmission through rectangular ducts. Mooney and Wells[83,98] have applied the results from these studies to the design of passageways for the underground and aboveground struc-

tures described in Sections 10.1.1, 10.1.2, and 10.2, and their techniques are described in the following paragraphs. In all cases it is assumed that no barrier is inserted in the duct to attenuate the radiation. This is an unrealistic assumption, since doors (or baffles) no doubt will be necessary to reduce the overpressure to tolerable limits. It is also assumed that no radiation enters through the tunnel walls. This is a good assumption for underground tunnels, but may not be for aboveground tunnels. Certainly in the final analysis the thickness of the tunnel walls must be considered for passageways to aboveground structures.[ll]

Maerker's calculations[100] for neutrons incident on the entrance of two-legged concrete-walled ducts consisted of a parametric study in which the first- and second-leg lengths L_1 and L_2 and the duct height and width were allowed to vary. The composition of the concrete is given in Table 15. The source was assumed to be a plane cosine current source (isotropic flux in the forward half space) having an energy spectrum corresponding to that calculated by Straker[102] for a distance of 1500 m from a point fission source in an infinite medium of air. Such a spectrum is composed of about 16% fast neutrons (>200 keV), 79% intermediate neutrons (0.5 eV to 200 keV), and 5% thermal neutrons (<0.5 eV). For each source energy group, Maerker calculated the multicollision neutron dose and capture gamma-ray dose[mm] at various positions along the axis of the duct and presented the results on the basis of a unit current of neutrons in that energy group. He then fitted the results to empirical expressions.

The empirical expressions can be used for any field of neutrons incident on the entrance of the duct providing that the fraction of the incident neutron current in each of the three source energy groups is known. However, the expressions are quite lengthy and to use them directly would

---

[ll] The remainder of this section is largely quoted from refs. 83 and 98.

[mm] When the position of interest was in the second leg, the capture gamma-ray production in the first leg was neglected.

require considerable computational time. In order to provide design data on two-legged entranceways that would be consistent with the structure SPC's, Mooney and Wells used the expressions to calculate doses that would be produced by specific neutron weapons spectra. A total of 48 duct, or entranceway, configurations were considered. In each case the fraction of the neutron current incident on the duct in a particular source energy range was multiplied by the appropriate dose attenuation expression. The resulting attenuation factors were summed, and the total attenuated dose (rads per unit incident neutron current) was divided by the first-collision dose per unit incident neutron current. The result was an attenuation factor that, when applied to a known incident neutron dose, will give the total neutron-induced dose at a particular point in the duct.

The first set of duct attenuation factors calculated were for doses produced by the high-yield weapon that was assumed to produce the field of neutrons incident on the underground structures described in Section 10.1.1 and 10.1.2. The resulting attenuation factors are published in ref. 83. A second set of attenuation factors for the same duct configurations was calculated for the three neutron energy distributions determined to be incident on the front, sides, and rear of the aboveground structures discussed in Section 10.2.[98] All three spectra were used to account for three possible locations of the entranceway around the structures (see Fig. 24). Note that entranceway (*a*) located on the side of the structure is facing in the direction of the detonation, and thus the incident energy distribution used for this entranceway is the same as that incident on the front of the structure. A comparison of the calculated doses in the three entranceways showed the doses in entranceways (*b*) and (*c*) to be approximately 96% and 92% respectively of that in entranceway (*a*); therefore, the attenuation factors for entranceway (*a*) can easily be corrected for the other entranceways.

The attenuation factors for the various duct configurations are given in Table 25. In each case the attenuation factor is for a position at

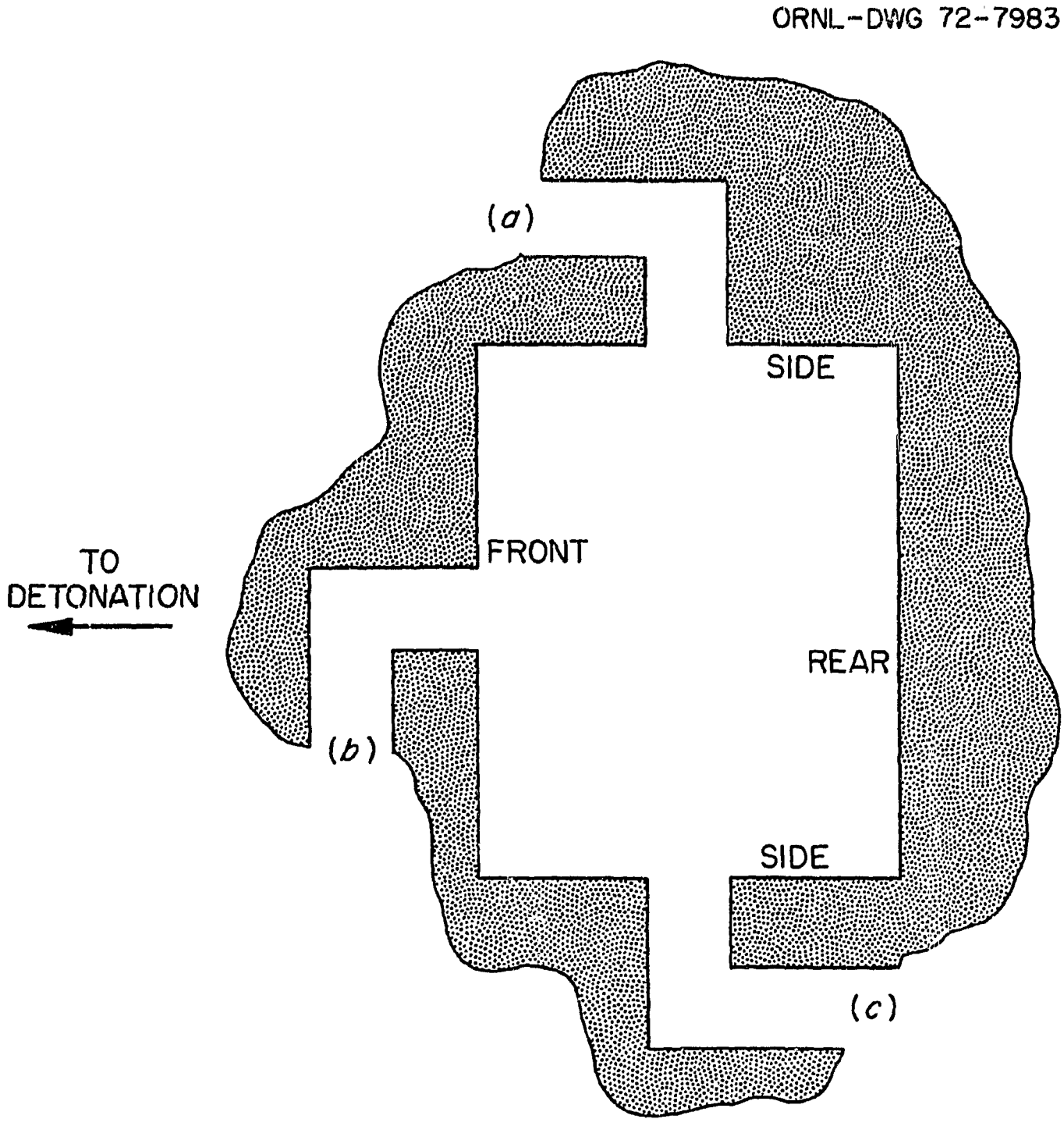

Fig. 24. Three Entranceway Geometries for Aboveground Rectangular Structures.

Table 25. Attenuation Factors for Neutron-Induced Doses in Two-Legged Rectangular Entranceways[a]

[Note: Attenuation factors apply to Entranceway (*a*) in Fig. 24; multiply by 0.96 for Entranceway (*b*) and by 0.92 for Entranceway (*c*).]

Entranceway		First-Leg Length (ft)	Second-Leg Length (ft)	Attenuation Factor[b]
Height (ft)	Width (ft)			
7	3	9	0	5.646(−1)
			9	3.511(−2)
			18	7.949(−3)
			27	2.506(−3)
7	3	15	0	2.091(−1)
			9	1.312(−2)
			18	3.021(−3)
			27	9.463(−4)
7	3	20	0	1.106(−1)
			9	6.593(−3)
			18	1.515(−3)
			27	4.647(−4)
7	3	25	0	6.542(−2)
			9	3.597(−3)
			18	8.184(−4)
			27	2.452(−4)
7	3	30	0	3.626(−2)
			9	2.062(−3)
			18	4.602(−4)
			27	1.337(−4)
7	3	36	0	2.754(−2)
			9	1.284(−3)
			18	2.779(−4)
			27	8.155(−5)
7	6	18	0	3.071(−1)
			18	1.253(−2)
			36	2.302(−3)
			54	6.032(−4)
7	6	25	0	1.536(−1)
			18	6.344(−3)
			36	1.170(−3)
			54	3.073(−4)
7	6	30	0	1.008(−1)
			18	4.130(−3)
			36	7.614(−4)
			54	1.996(−4)
7	6	35	0	6.908(−2)
			18	2.772(−3)
			36	5.097(−4)
			54	1.329(−4)
7	6	40	0	4.906(−2)
			18	1.908(−3)
			36	3.491(−4)
			54	9.020(−5)
7	6	50	0	2.700(−2)
			18	9.689(−4)
			36	1.742(−4)
			54	4.408(−5)

Table 25. (continued)

Entranceway Height (ft)	Entranceway Width (ft)	First-Leg Length (ft)	Second-Leg Length (ft)	Attenuation Factor[b]
12	12	36	0	2.679(−1)
			36	1.026(−2)
			72	1.789(−3)
			108	4.439(−4)
12	12	50	0	1.320(−1)
			36	5.062(−3)
			72	8.858(−4)
			108	2.208(−4)
12	12	75	0	4.861(−2)
			36	1.754(−3)
			72	3.046(−4)
			108	7.528(−5)
12	12	100	0	2.215(−2)
			36	7.111(−4)
			72	1.207(−4)
			108	2.903(−5)

[a]From Mooney and Wells, ref. 98.

[b]Total neutron-induced dose at end of entranceway per unit free-field neutron dose. Note: The free-field neutron dose is the first-collision dose, in rads; the neutron-induced dose in the entranceway includes the multicollision neutron dose and the secondary gamma-ray dose produced by neutron captures in the walls of the last leg of the entranceway, all in rads.

the end of the duct, which corresponds to the door of the structure.[nn] Thus, multiplying the neutron dose incident on the entranceway by the appropriate attenuation factor will give the neutron-induced dose at the door of the structure. To project this doorway dose on into the structure, it is necessary to multiply the dose by an analytical expression developed by Mooney and Wells:

$$F_d = 1 - \cos^4 \theta \quad ,$$

where

$\theta = \tan^{-1} (S_D/X_D)$ (see Fig. 25),

$S_D = \sqrt{HW/\pi}$,

H, W = height and width of entranceway.

The use of this expression is facilitated by a plot of $1 - \cos^4 \theta$ versus S_D/X_D presented in Fig. 26. Projecting the dose by this technique assumes that the dose from the room door can be described by a circular opening having the same area as the actual entrance and that the only location of interest is on the entranceway centerline. Both assumptions have been shown to be reasonable.

As pointed out above, the streaming of gamma rays from the entrance of a tunnel to the door of a structure can usually be neglected if at least one 90-deg bend is introduced in the passageway, and for that reason no studies of the streaming of initial gamma rays in passageways have been undertaken. As a consequence, the only method available for predicting the doses contributed by incident gamma rays is the one developed by Huddleston and Ingold[101] for fallout gamma rays whose energies are not expected to exceed 3.7 MeV. Mooney and Wells[83,98] have adapted the method to initial gamma rays with obvious reservations.

According to the Huddleston-Ingold method, an estimate of the gamma-ray dose attenuation in two-legged rectangular entranceways at a position located at the end of the second leg can be obtained from an empirical formula developed for a point isotropic source located on the centerline

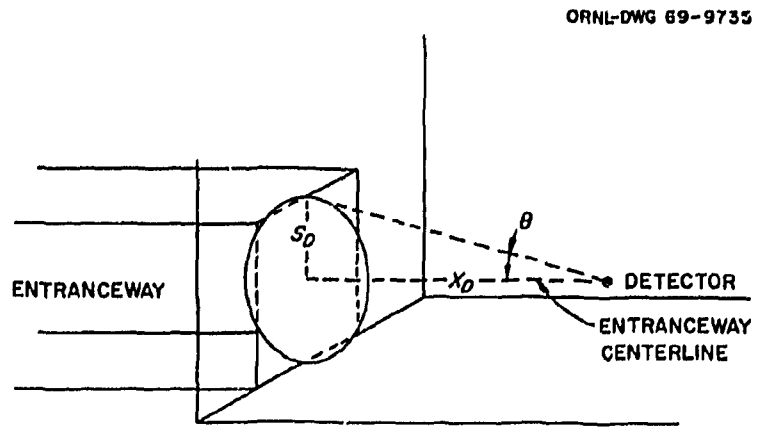

Fig. 25. Geometry for Projecting Entranceway Neutron-Induced Dose into Structure.

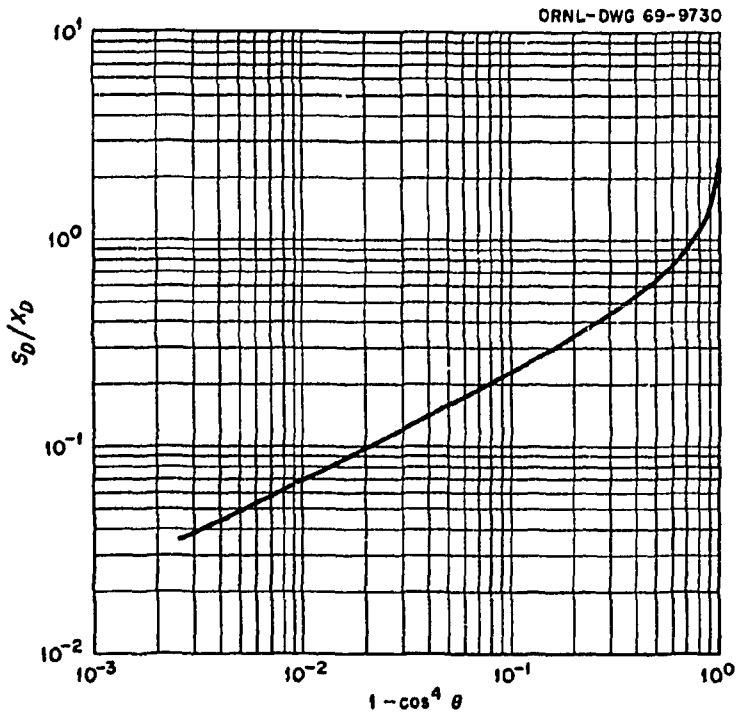

Fig. 26. Dose Attenuation Function ($1 - \cos^4\theta$) as a Function of S_D/X_D. Function used to project neutron-induced dose from structure door to position inside structure. (From Mooney, Wells, and Claiborne, ref. 83.)

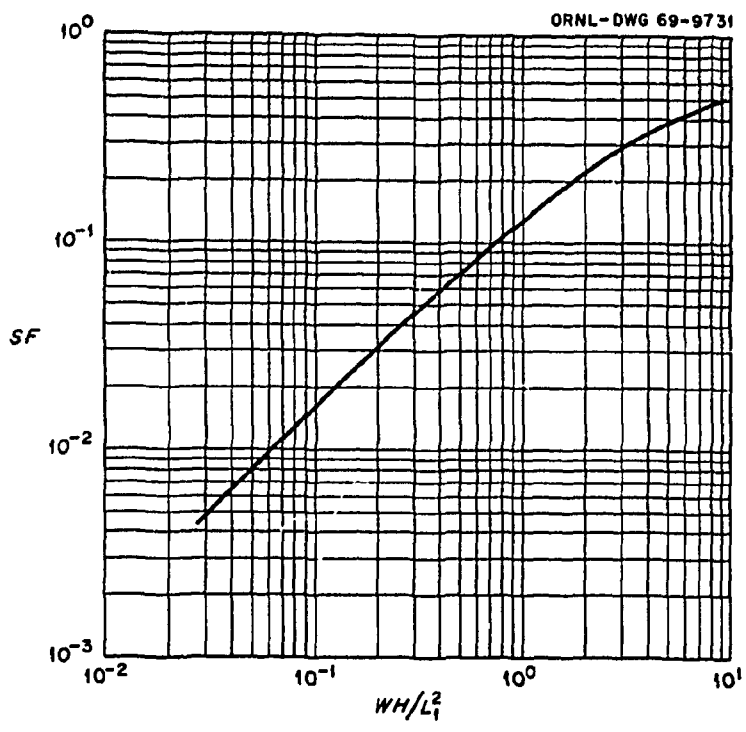

Fig. 27. Source Correction Factor as a Function of WH/L_1^2. Correction factor used in calculating streaming of fission-product or air-capture gamma rays through entranceways. (From Mooney, Wells, and Claiborne, ref. 83.)

axis just outside the entranceway opening. The formula is based on experimental and analytical data and is given as follows:

$$\frac{D_d}{D_0} = \frac{HW^2}{3(L_1L_2)^{2.7}\ E_0^{0.6}} \quad ,$$

where

D_d = dose rate on axis of duct at point of interest,

D_0 = dose rate 1 ft from the source in air,

E_0 = gamma-ray source energy (MeV),

and H, W, L_1, and L_2, all in feet, are defined above.

This formula can be used with 95% certainty that the actual dose rate will not be greater than the dose rate computed from the formula, providing that the following criteria are met:

$$0.3 \text{ MeV} \leq E_0 \leq 3.7 \text{ MeV}$$

$$1.0 \text{ ft} < W < H < 6.0 \text{ ft}$$

$$2.0 \text{ ft} \leq L_1 \leq 24.0 \text{ ft}$$

$$2.0 \text{ ft} \leq L_2 \leq 24.0 \text{ ft}$$

$$L_1/H \leq 6.0$$

$$L_2/H \leq 6.0$$

$$1.0 \leq H/W \leq 2.0$$

Using the formula to calculate the streaming of fission-product and secondary gamma rays through two-legged ducts requires the use of a source correction factor (SF). If it is assumed that the source is isotropic and incident with uniform intensity over the entranceway opening, an estimate of the source correction factor can be made by calculating the fraction of the solid angle subtended by the entranceway opening at a detector located at the end of the first leg. If it is further assumed that the rectangular opening can be represented by a circular opening of the same area, then SF is proportional to $1 - \cos\theta$, where θ is defined as the

angle between the centerline axis of the first leg and a line extending from the detector to the edge of the circular opening.

A graph of the source correction factor *SF* plotted versus WH/L_1^2 is given in Fig. 27. The values of WH/L_1^2 will cover the range of dimension limitations listed above.

Owing to the assumptions described above, the source correction factor can be considered only as a rough approximation at best; however, its use will definitely provide better estimates of the gamma-ray attenuation than would be obtained from the formula without it.

Using the formula for calculating the streaming of fission-product and secondary gamma rays introduces some uncertainty in the accuracy due to the presence of gamma rays with energies above 3.7 MeV. If the gamma rays with higher energies are treated as though they were 3.7-MeV gamma rays, however, the results obtained from the formula should be reasonable.

The application to weapons radiation has been simplified by folding the representative fission-product and secondary gamma-ray energy spectra incident on the three entranceways shown in Fig. 24 into the $E_0^{0.6}$ term. The equation then becomes

$$\frac{D_d}{D_1} = \frac{HW^2 \cdot C(E) \cdot SF}{3(L_1 L_2)^{2.7}} \quad ,$$

where *SF* is the source correction factor from Fig. 27, and $C(E)$ has the following values:

Entranceway	$C(E)$ for Fission-Product Gamma Rays	$C(E)$ for Secondary Gamma Rays
(*a*)	1.657	1.011
(*b*)	1.942	1.076
(*c*)	3.087	2.261

Graphs of the terms $(L_1 \text{ or } L_2)^{2.7}$ versus L_1 or L_2 and $E_0^{0.6}$ versus E_0 shown in Figs. 28 and 29 respectively.

Because of the relative unimportance of fission-product and nitrogen-capture gamma rays in entranceways, no technique is offered for projecting the dose at the door of the room into the underground structure. Rather it is assumed that the dose at the door is the only information required.

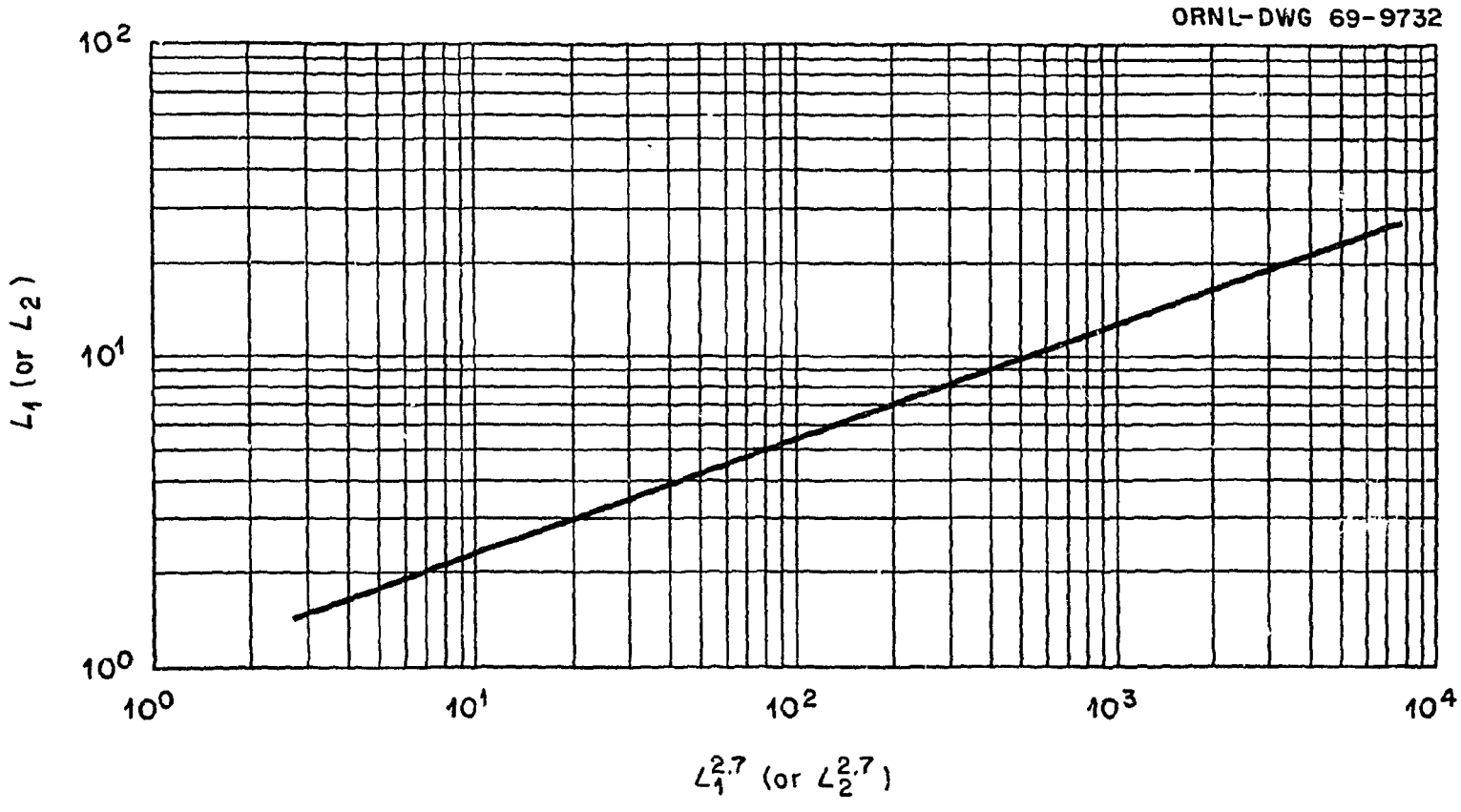

Fig. 28. Graph of L as a Function of $L^{2.7}$. Function used in calculating streaming of fission-product or air-capture gamma rays through entranceways. (From Mooney, Wells, and Claiborne, ref. 83.)

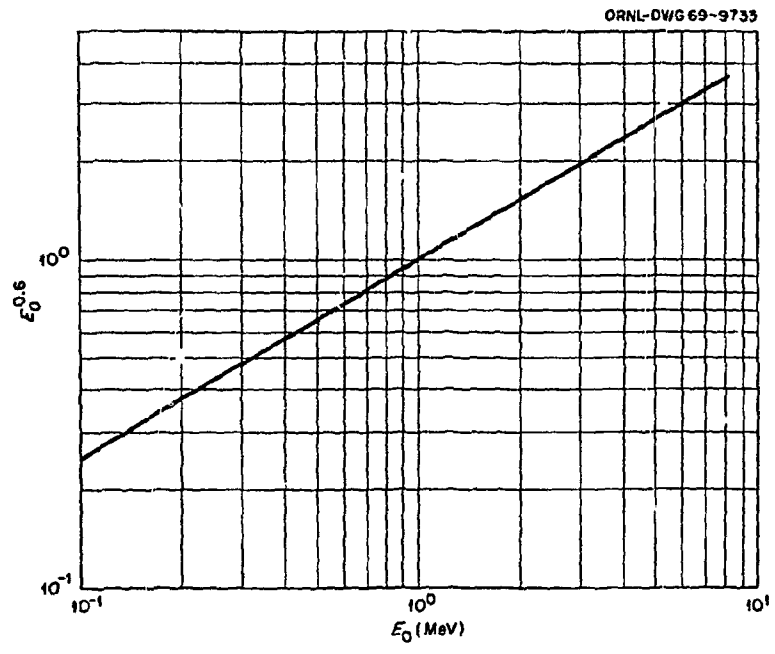

Fig. 29. Graph of E_0 as a Function of $E_0^{0.6}$. Function used in calculating streaming of fission-product or air-capture gamma rays through entranceways. (From Mooney, Wells, and Claiborne, ref. 83.)

11.0 STATUS OF CROSS-SECTION TECHNOLOGY

In the final analysis, the accuracy of any weapons radiation transport calculation depends on the accuracy of the cross sections utilized as input; thus the importance of obtaining detailed sets of cross sections that are reliable over large energy ranges can hardly be overemphasized. It has been pointed out earlier that gamma-ray-interaction cross sections for all materials are relatively well known and easily obtained, but the same statement cannot be made for neutron-interaction cross sections. Even before many large-scale shielding calculations were attempted, the application of computer codes to reactor criticality calculations had pointed out deficiencies in neutron cross sections and created a demand for "best sets" of cross sections for the elements in and around a reactor core. In the early 1960's the Cross Section Evaluation Center, now called the National Neutron Cross Section Center (NNCSC), was established at Brookhaven National Laboratory to serve as a repository and distribution agency for nuclear interaction data. Neutron cross sections are released from the Center in a format (called the ENDF format, for *E*valuated *N*uclear *D*ata *F*iles)[103-105] that can be computer processed for use in radiation transport calculations. The criteria for an evaluated set of cross sections are that an evaluator or a team of evaluators will have analyzed all available experimental data, combined the results with values predicted from nuclear model calculations, and attempted to extract the true values of the cross sections over the range of energy specified. The evaluations are approved by a group of evaluators who form a Cross Section Evaluation Working Group (CSEWG).

Although ENDF data have consistently been used in shielding studies, it has been increasingly apparent that insofar as shielding transport calculations are concerned, much has been lacking in the measured and evaluated data deposited in NNCSC. In particular, CSEWG has concentrated on neutron data for materials in reactor cores, and the group has not considered secondary gamma-ray data. Also, little experimental neutron data have been available on which to evaluate cross sections for energy regions in which the probability of interaction is low, and these regions,

referred to as cross-section minima regions, are of utmost importance in neutron penetration calculations. In order to fill the hiatus, shielding research programs have been expanded to include cross-section studies, several of which have been referred to in this chapter. Also, in 1967 a Shielding Subcommittee of CSEWG was formed and in 1971 a Defense Nuclear Agency Working Cross Section Library[106] was established at the ORNL Radiation Shielding Information Center.

Two key features of the DNA Working Cross Section Library are that the data undergo frequent revision and are maintained in ENDF format. The first feature ensures that for the elements of particular interest to DNA an up-to-date record will be kept of those cross sections that are in a rapid state of change. The second feature ensures that the DNA data will be usable in any computer program which processes the ENDF library and further that the DNA data can eventually be deposited with the NNCSC. Evaluations for elements of interest to DNA that are not in a state of rapid change presumably will be directly available from the NNCSC.

Responsibility for each element in the DNA Library is assigned to a team of evaluators, who consider new data that become available and authorize changes. RSIC serves as a clearinghouse. It receives data from and forwards data to the evaluators, coordinates reviews, processes the cross sections through checking codes, etc., and finally packages each data set for distribution. The data sets, which include both neutron cross sections and secondary gamma-ray production cross sections, are identified by a scheme that indicates whether they have been approved by CSEWG.

The evaluators participating in the DNA Library are individuals who have been prominent in cross-section studies and/or evaluations. As of this writing (October 1972), the elements included in the Library and the corresponding evaluators are as follows:

Elements	Evaluators
Nitrogen, oxygen, aluminum	P. G. Young and D. G. Foster Los Alamos Scientific Laboratory
Lead, calcium	C. Y. Fu and F. G. Perey Oak Ridge National Laboratory
Hydrogen	L. Stewart, R. J. LeBauve, and P. G. Young Los Alamos Scientific Laboratory
Silicon	C. Y. Fu, D. Larson, and F. G. Perey[oo] Oak Ridge National Laboratory
Beryllium	R. J. Howerton and S. T. Perkins Lawrence Livermore Laboratory
Sodium	N. C. Paik and T. A. Pitterle Westinghouse Advanced Reactors Division F. G. Perey Oak Ridge National Laboratory
Tantalum	R. J. Howerton, S. T. Perkins and M. MacGregor Lawrence Livermore Laboratory
Iron	S. K. Penny, W. E. Kinney, R. W. Wright, F. G. Perey, and C. Y. Fu Oak Ridge National Laboratory

A comparison of the above list of elements with those comprising the materials most frequently used in weapons radiation transport calculations (see Table 17) shows that most of the important elements are being "worked on." Others, notably carbon, will be added in the near future.

In the opinion of F. G. Perey,[107] who has the primary responsibility for the ORNL evaluations placed in the DNA Library, the status of the cross-section sets for elements important for weapons initial radiation transport calculations can be summarized as presented in the next several paragraphs. It is to be emphasized, however, that Perey's analysis is predicated on the assumption that the cross sections will be used in

---

[oo] Before July 1, 1972, the evaluation for silicon was performed by M. K. Drake and R. R. Kinsey, Brookhaven National Laboratory.

weapons shielding calculations and that the same analysis will not always apply to reactor shield calculations.

Of all the cross-section sets available, only the neutron-interaction cross sections for hydrogen are at a precision level which transcends the need for radiation transport calculations. The errors in the cross sections for this element are so small (less than 1%) that the set can be considered to be a standard against which other sets can be tested. Therefore, any further work on this element will be done only to improve the standard and not for any effect that changes in the cross sections would have on transport calculations.

With the latest evaluations of Young and Foster, the neutron-interaction cross sections for nitrogen and oxygen are probably adequate for calculating neutron transport through the atmosphere; similarly the oxygen cross sections are adequate for treating neutron transport in the ground and in concrete.

The neutron-interaction cross sections for lead and sodium also are probably sufficiently accurate for weapons radiation transport calculations. Conversely, those for aluminum, calcium, and silicon are not well enough known.

The neutron-interaction cross sections available for carbon are adequate only for neutron energies up to 2 MeV. Those for energies between 2 and 5 MeV are fair, and those above 5 MeV are completely inadequate. An evaluation of carbon cross sections currently being performed at ORNL by Claire Perey is expected to yield good neutron-interaction cross sections for energies up to 10 MeV. Above 10 MeV the cross sections will remain inadequate for some time.

More data are available on iron than on any of the other elements in the DNA Library, but it cannot yet be said that a good evaluation of the neutron-interaction cross sections exists. This can be attributed

to the fact that the cross sections for iron vary rapidly with the neutron energy. An intensive recent review of the data below 2 MeV (as of July 1972) has shown that "windows" exist at several energies in the cross sections for this element, whereas heretofore the only window that had been firmly established as being important was a well-known one at 24 keV The presence of a window in a cross section means that neutrons having the same energy as that of the window will stream through the material with a very small probability of interaction; that is, the neutrons will have very long mean free paths.

The current status of neutron-interaction cross sections thus can be summarized as follows: The cross sections for nitrogen, oxygen, lead, and sodium are adequate; those for carbon are adequate up to 2 MeV and should be good up to 10 MeV within the next several months; those for aluminum, calcium, and silicon are not well enough known; and those for iron are in an undetermined state. It is pointed out, however, that as a result of a large-scale program supported by DNA during the last two or three years, techniques for measuring neutron-interaction cross sections have improved and moreover the measurements are being limited to those cross sections which sensitivity studies have shown to be the most likely to influence calculated quantities such as dose, silicon ionization, etc. (As mentioned in Section 6.6.2, sensitivity studies are calculations of the transport of neutrons and the production and transport of secondary gamma rays in which the effects of varying specific cross sections are studied.)

The status of the cross sections for secondary gamma-ray production is at present not as good as that for neutron-interaction cross sections, but dramatic improvements appear to be imminent. Until the DNA program was undertaken, essentially all the data available on secondary gamma rays were limited to those produced by the capture of thermal neutrons. Now the production of secondary gamma rays by the inelastic scattering of high-energy neutrons is being investigated intensively, and the data should be available for all the elements of interest to the military by the end of June 1973. Additional experiments to accumulate data on the

production of secondary gamma rays by the capture of epithermal neutrons will require another two or three years. Thus sufficient data should be available within the next few years on which to base secondary-production cross sections over wide energy ranges for the important elements.

Relative to the situation that has existed over the years, the preceding paragraphs offer an optimistic view of the status of the cross-section technology. It must be recognized, however, that with the exception of the neutron-interaction cross sections for hydrogen, all cross sections have been obtained from experiments or calculations based on several approximations. As a result, all evaluations lack realistic error estimates that must be available before the magnitude of the errors associated with transport calculations can be determined precisely.

12.0 SUMMARY AND DISCUSSION

Shield evaluation, rather than shield design, would more properly describe the responsibility of the engineer who must ensure that the initial nuclear radiations penetrating into a structure are reduced to specified levels. In all probability his work will begin only after a number of other design parameters have been formulated, particularly the requirements for the blast shield. Since the blast shield will form part of the radiation shield -- perhaps all of it -- the first task will be to evaluate the blast shield with respect to its radiation-attenuating characteristics. The preceding discussion has shown that shields are usually evaluated through a series of "transport" calculations that consider each of the different types of incident radiation. Another approach is to apply SPC's (*S*tructure *P*rotection *C*oeffi·ients) that have been derived from earlier transport calculations. Performing the transport calculations for a specific structure with the latest methods and the best sets of cross sections available will give the most accurate answers possible with the current state of the art; however, at present such calculations are very time consuming and expensive and can be performed only by persons familiar with the techniques. Applying SPC's, which are simply ratios of the penetrated dose to the incident dose, requires considerably less effort and less expertise, but the available SPC's are limited to particular structure types and can be used to determine only the total amount of radiation penetrating to specific locations in the structures (as opposed to the rates of arrival). Even if the design of the structure of interest corresponds to one for which SPC's are available, this technique should not be relied on for a refined shield evaluation or design because of the large errors associated with the answers. On the other hand, SPC's will be useful in preliminary studies to investigate trends and to get a "feel" for the problem.

In both the most sophisticated and the most elementary techniques for evaluating a shield, it is first necessary to describe the incident field of each of the initial radiation sources (the free-field environment). If a full-scale shield-penetration calculation is to be performed,

the incident particles must be described in terms of their energies and angles of incidence, and when peak radiation pulses are of interest they must also be described in terms of the times that they arrive at the structure. To facilitate the calculation, the incident energy, angle, and time distributions are usually normalized to one incident particle, and the total number of particles delivered to the outside of the structure is not considered until after the penetration of the normalized distribution into the structure has been determined. If the SPC technique is to be used, then the incident field for each type of radiation must be converted to total dose, in which case it is assumed that the energy and angular distributions of the incident radiations contributing to that total dose are the same as those used in calculating the SPC's.

The different types of radiations whose incident fields must be determined are described in detail in Sections 2.0 and 3.0. They consist of the fission and fusion neutrons emitted directly from the weapon, the prompt gamma rays emitted directly from the weapon (including the fission gamma rays), the fission-product gamma rays emitted from the debris cloud, and the secondary gamma rays produced by neutron interactions in the air and ground. As has been pointed out repeatedly, not all these radiation sources need be considered in every case. For example, if the structure is an underground building, if the detonation occurs at some distance away (that is, not overhead), and if the radiation response of interest inside the structure is proportional to the total amount of radiation penetrating into the structure, then all of the incident gamma rays can usually be disregarded. If, however, the structure is aboveground or if peak pulses of radiation are the concern, then all sources must be considered.

The character of each of the radiation sources incident on the structure depends on the design of the weapon, which determines the numbers, energies, and directions of the radiations it emits. (The description of the weapon output is one of the greatest uncertainties associated with weapons shielding studies.) The incident radiation fields are also influenced by the height of the detonation, by the ground range distance from the structure, and by the compositions and densities of the air and

ground, since these parameters determine which of the neutron and gamma-ray interactions described in Sections 4.0 and 5.0 will occur between the weapon and the structure location. Through these interactions some of the radiations will be scattered both toward and away from the structure, others will be absorbed in the environment, and still others will be produced at locations between the weapon and the structure. Thus the incident field of radiation must always be determined for a specific set of burst conditions.

The two calculational methods most frequently used for determining weapons initial radiation free-field environments are the Monte Carlo and discrete ordinates transport methods described briefly in Section 6.0. Both these methods are very powerful, but neither has yet been developed to the extent that a real problem can be described in complete detail. In particular, a number of simplifying assumptions are always necessary to describe the weapon as a radiation source, as is pointed out in Section 7.0. In general, discrete ordinates calculations are more economical, but they are limited to problems that can be described in two space dimensions, whereas Monte Carlo calculations are not. The choice of the method must be determined by an examination of the problem, with the response functions that are to be applied to the transport results being one of the determining factors. For example, if time-dependent quantities are needed, such as ionization or displacement rates (see Section 8.0), and if the problem description requires more than one space dimension, then the discrete ordinates method cannot be used. If, however, only time-integrated quantities are needed and the problem can be described in one or two space dimensions, then the discrete ordinates method can be used.

Typical results from free-field calculations for each of the different types of incident radiations are described in Section 9.0. Some of these calculations are for specific weapons radiation energy spectra, and if the assumption is made that one of these spectra is sufficiently similar to the neutron or gamma-ray emission spectrum of the weapon of interest, then these results can be used as the incident environment. Other calculations discussed in Section 9.0 give results for monoenergetic

sources of different energies (referred to as transport data sets), and these results can be folded and weighted to construct a free-field environment for a specific weapons spectrum. With either approach, however, the environment arrived at is for the particular set of burst conditions for which the original calculations were made. Converting the results to a different air density is relatively simple (see Section 7.0), but rather elaborate techniques, which are still under development, are required to correct for other differences in the burst conditions. These correction techniques are referred to in Section 9.0. It is not recommended that such radiation environments be constructed, however, if the best possible answer is being sought. Rather, a full-scale transport calculation should be performed to determine the free-field environment.

As pointed out above, if SPC's are to be applied to the structure, then each free-field environment must be given in terms of total dose, which when multiplied by the appropriate SPC yields the corresponding dose inside the structure. The structures for which SPC's are available are described in Sections 10.1 and 10.2. They include belowground and aboveground single-compartment concrete structures with rectangular cross sections and flat roofs. They also include cylindrical underground structures with concrete covers and dome- and arch-type structures covered with soil. In each case it is assumed that the structure has no irregularities in any of its surfaces, so that any additional radiation that might penetrate into the structure through an accessway or gap must be determined separately. Attenuation factors that can be used to estimate radiation penetration through entranceways that are rectangular in cross section are discussed in Section 10.3.

If the SPC technique is not to be used and a full-scale shield-penetration calculation is planned, then the energy, angular, and time distributions of the incident radiations are tailored, either during the free-field calculations or subsequently, for use as input in the shield penetration calculation. The shield penetration calculation will probably be performed with a combination of different discrete ordinates and Monte Carlo computer transport codes, with each selected to handle the different

parts of the problem in the simplest geometry possible. The calculations will be performed in succession, with the output from one used as input for the next. Examples of this technique are illustrated by the two sets of silo calculations described in Sections 10.1.3 and 10.1.4. It will be noted that the second silo does not have a symmetrical design and that low-density areas extend from the outside to the inside of the structure. These low-density areas represent regions through which radiation, particularly neutrons, might stream into the structure, and this part of the problem must be investigated in detail, possibly by more than one technique, whereas simpler calculations may be adequate for other regions. These two sets of silo calculations have demonstrated that coupling various techniques greatly increases the efficiency of structure penetration calculations and that intercomparing techniques gives insight into the reliability of the methods.

But as Section 11.0 points out, the reliability of the results obtained in any of the transport calculations depends on the accuracy of the cross sections used as input. Gamma-ray interaction cross sections are well established, and calculations based on gamma-ray interactions alone can be assumed to be accurate. During the last two or three years, the neutron-interaction cross sections for a number of materials have become available within an acceptable accuracy, but there are notable exceptions. In particular, the neutron interaction cross sections for iron are not yet sufficiently well known, primarily because they exhibit large fluctuations within relatively narrow energy intervals. Also minima (or windows) in the cross sections are being identified and neutrons with energies corresponding to these windows can effectively stream through iron, which means that iron structural components extending from the outside to the inside of a structure may constitute a weakness in the radiation shield.

Cross sections that describe the production of secondary gamma rays by the interactions of neutrons are largely unknown for neutrons with epithermal energies and are not well established for neutrons with thermal energies. This represents a hiatus in the cross-section technology

since the secondary gamma rays produced in thick shields contribute a major fraction of the radiation that penetrates into a structure cavity. It is ironic that the dense materials that are most effective in attenuating the gamma rays incident on the outside of the shield are the materials that are most prolific in producing the secondary gamma rays. Mixing the dense materials with lighter materials, such as boron, may suppress secondary gamma-ray production. Also, including a material that will "moderate" the energies of the neutrons in the outer edges of the shield may shift the birth sites of most of the secondary gamma rays to the outer regions of the shield where they can still be attenuated. In general, however, it is assumed that the radiation shield materials will be the same as the blast shield materials (reinforced concrete) and that the optimum thickness must be determined.

Because of the uncertainties associated with cross-section evaluations for a number of materials that enter into weapons radiation transport calculations, cross-section studies are currently receiving considerable emphasis, and the outlook for improving the status of the cross-section technology is optimistic. A recent important development in this area is the cross-section sensitivity study, which is a transport calculation designed to identify energy regions and reactions that particularly affect the response of interest. Sensitivity studies serve both to limit cross-section investigations to those that are most important and to identify the cross sections that should be input into a calculation in the greatest detail.

With the expected improvement in the cross sections and the continued development of calculational methods, there is reason to believe that the large uncertainties now associated with shield design will soon be greatly reduced. Still each type of structure proposed for actual construction is sufficiently complicated to require special adaptation of the calculational methods, and this precludes any predictions as to when a comprehensive engineering method of general applicability may be developed.

REFERENCES

1. *The Effects of Nuclear Weapons*, Samuel Glasstone, Editor, U.S. Atomic Energy Commission, p. 15, April 1962 (Revised February 1964).

2. *Nuclear Weapons Blast Phenomena, Vol. I. Source and Development of Blast Waves in Air*, Compiled by P. A. Ellis, D. C. Sachs, F. H. Shelton, and J. F. Moulton, Defense Atomic Support Agency, DASA-1200-1 (March 1971) (SRD).

3. V. I. Kukhtevich, I. V. Goryachev, and L. A. Trykov, *Protection from Penetrating Radiation of a Nuclear Explosion*, Atomizdat Press, Moscow, 1970; Translated by Joint Publications Research Service, Washington, D.C., as JPRS-53498, 1971.

4. A. Protopopov and B. Shiryaev, "Investigation of γ-Rays Emitted in the Fission of U^{235} Induced by 2.8 and 14.7 MeV Neutrons," *Zh. Eksperim. i. Teor. Fiz* 34, 331 (1958).

5. R. S. Booth and F. J. Muckenthaler, *The Total Gamma-Ray Energy Spectrum Above 1 MeV from Neutron Interactions in ^{235}U and ^{238}U*, Oak Ridge National Laboratory, ORNL-4691 (1971).

6. R. W. Peelle and F. C. Maienschein, *The Absolute Spectrum of Photons Emitted in Coincidence with Thermal-Neutron Fission of Uranium-235*, Oak Ridge National Laboratory, ORNL-4457 (1970).

7. J. W. Motz, "Gamma-Ray Spectra of the Los Alamos Reactors," *Phys. Rev.* 86, 753 (1952).

8. V. J. Orphan and C. G. Hoot, *Measurement of Gamma Ray Production Cross Sections for Nitrogen and Oxygen*, Gulf General Atomic, GA-8006 (DASA 2267) (1969).

9. J. K. Dickens and F. G. Perey, "The $^{14}N(n,x\gamma)$ Reaction for $6.7 \leq E_n \leq 11$ MeV," *Nucl. Sci. Eng.* 36, 280 (1969).

10. J. K. Dickens and F. G. Perey, "The $^{16}O(n,x\gamma)$ Reaction for $6.7 \leq E_n \leq 11$ MeV," *Nucl. Sci. Eng.* 40, 283 (1970).

11. J. K. Dickens, "$^{28-30}Si(n,x\gamma)$ Reactions for $5.3 \leq E_n \leq 9.0$ MeV," *Phys. Rev.* C 2(3), 990 (1970).

12. J. K. Dickens, "$Al(n,x\gamma)$ Reactions for $5.3 \leq E_n \leq 9.0$ MeV," *Phys. Rev. C* 5(1), 100 (1972).

13. J. K. Dickens, Oak Ridge National Laboratory, private communication on iron measurements.

14. J. K. Dickens, "The Neutron-Induced Gamma-Ray Reactions in Sodium-23 in Energy Range $4.85 \leq E_n \leq 7.5$ MeV," *Nucl. Sci. Eng.* 50, 98 (1973).

15. R. E. Maerker and F. J. Muckenthaler, *Gamma-Ray Spectra Arising from Fast-Neutron Interactions in Elements Found in Soils, Concretes, and Structural Materials*, Oak Ridge National Laboratory, ORNL-4475 (April 1970).

16. R. E. Maerker and F. J. Muckenthaler, *Gamma-Ray Spectra Arising from Thermal-Neutron Capture in Elements Found in Soils, Concretes, and Structural Materials*, Oak Ridge National Laboratory, ORNL-4382 (August 1969).

17. K. J. Yost and M. Solomito, *Sensitivity of Gamma-Ray Dose Calculations to the Energy Dependence of Gamma-Ray Production Cross Sections*, Oak Ridge National Laboratory, ORNL-TM-2209 (May 24, 1968); this paper was also presented at the Conference on Neutron Cross Sections and Technology, Washington, D.C., March 4-7, 1968.

18. G. R. Crocker and M. A. Conners, *Gamma-Emission Data for the Calculation of Exposure Rates from Nuclear Debris. Vol. I. Fission Products*, U.S. Naval Radiological Defense Laboratory, USNRDL-TR-876 (June 10, 1965).

19. L. B. Engle and P. C. Fisher, *Energy and Time Dependence of Delayed Gammas from Fission*, Los Alamos Scientific Laboratory, LAMS-2642 (July 1962).

20. Thomas Jaeger, *Principles of Radiation Protection Engineering*, Translated by Lawrence Dresner, McGraw-Hill Book Co., Inc., 1965 (German edition published by Springer-Verlag, 1960).

21. J. R. Stehn and E. F. Clancy, "Fission-Product Radioactivity and Heat Generation," *Proc. 2nd U.N. Int. Conf. PUAE* 13 (1958) 13.

22. F. C. Maienschein, R. W. Peelle, W. Zobel, and T. A. Love, "Gamma Rays Associated with Fission," *Proc. 2nd U.N. Int. Conf. PUAE* 15 (1958) 366.

23. W. Zobel and T. A. Love, "Short Lived Fission Product Gamma Radiation," paper presented at the Symposium on the Shorter-Term Biological Hazards of a Fallout Field, Dec. 12-14, 1956, Washington, D.C.

24. G. R. Crocker and D. T. Wong, *Gamma-Emission Data for the Calculation of Exposure Rates from Nuclear Debris. Vol. II. Induced Activities*, U.S. Naval Radiological Defense Laboratory, USNRDL-TR-888 (August 1965).

25. P. N. Stevens and D. K. Trubey, "Methods for Calculating Neutron and Gamma-Ray Attenuation," Chapter 3 of *Weapons Radiation Shielding Handbook*, edited by L. S. Abbott, H. C. Claiborne, and C. E. Clifford, Defense Nuclear Agency, DNA-1892-3, Rev. 1 (formerly DASA-1892-3) (March 1972).

26. C. Eisenhauer, *An Engineering Method for Calculating the Protection Afforded by Structures Against Fallout Radiation*, National Bureau of Standards, NBS Monograph 76 (July 1964).

27. W. R. Kumel, Editor, *Radiation Shielding: Analysis and Design Principles as Applied to Nuclear Defense Planning*, Office of Civil Defense and Kansas State University, TR-40 (November 1966).

28. D. Spielberg, *Penetration of Neutrons from a Point Fission Source in Air; Moments Method Calculation*, United Nuclear Corporation, NDA 2106-10 (April 1961).

29. J. V. Pace, III, F. R. Mynatt, and L. S. Abbott, *A Study of the Overlap Conditions Required in Sequential Discrete Ordinates Transport Calculations for a 14-MeV Neutron Source in a 5000-m Radius Cylinder of Air*, Oak Ridge National Laboratory, ORNL-TM-3269 (June 1971).

30. N. M. Greene and C. W. Craven, Jr., *XSDRN: A Discrete Ordinates Spectral Averaging Code*, Oak Ridge National Laboratory, ORNL-TM-2500 (1969).

31. R. Q. Wright, J. L. Lucius, N. M. Greene, and C. W. Craven, Jr., *SUPERTOG: A Program to Generate Fine Group Constants and P_n Scattering Matrices from ENDF/B*, Oak Ridge National Laboratory, ORNL-TM-2679 (1969).

32. See, for example, J. R. Knight and F. R. Mynatt, *MUG: A Program for Generating Multigroup Photon Cross Sections*, Computing Technology Center, Union Carbide Nuclear Division, CTC-17 (1970).

33. K. D. Lathrop, *GAMLEG -- A FORTRAN Code to Produce Multigroup Cross Sections for Photon Transport Calculations*, Los Alamos Scientific Laboratory, LA-3267 (1965).

34. W. E. Ford, III, and D. H. Wallace, *POPOP4 -- A Code for Converting Gamma-Ray Spectra to Secondary Gamma-Ray Production Cross Sections*, Computing Technology Center, Union Carbide Nuclear Division, CTC-12 (1969).

35. W. E. Ford, III, and J. S. Gillen, "App. B. A Sample Coupling Code," in *The Testing of ^{238}U Secondary Gamma-Ray Production Data Sets from the POPOP4 Library*, Oak Ridge National Laboratory, ORNL-TM-3482 (1972).

36. N. M. Greene, W. E. Ford, III, J. L. Lucius, J. E. White, and R. Q. Wright, "AMPX: Multigroup Coupled Neutron-Gamma Cross-Section Generator," paper in *Neutron Phys. Div. Ann. Prog. Rep. May 31, 1972*, Oak Ridge National Laboratory, ORNL-4800, p. 30.

37. G. C. Wick, "Uver Ebene Diffusions probleme," *Z. Phys.* 121, 702 (1943).

38. S. Chandrasekhar, *Astrophys. J.* 100, 76 (1944).

39. B. G. Carlson, *Solution of the Transport Equation by the S_n Method*, Los Alamos Scientific Laboratory, LA-1891 (1955).

40. See, for example, F. R. Mynatt, F. J. Muckenthaler, and P. N. Stevens, *Development of Two-Dimensional Discrete Ordinates Transport Theory for Radiation Shielding*, Computing Technology Center, Union Carbide Nuclear Division, CTC-INF-952 (1969).

41. K. D. Lathrop, *DTF-IV, A FORTRAN-IV Program for Solving the Multigroup Transport Equation with Anisotropic Scattering*, Los Alamos Scientific Laboratory, LA-3373 (1965).

42. K. D. Lathrop and F. W. Binkley, *Theory and Use of the General-Geometry TWOTRAN Program*, Los Alamos Scientific Laboratory, LA-4432 (1970).

43. W. W. Engle, Jr., *A User's Manual for ANISN, A One-Dimensional Discrete Ordinates Transport Code with Anisotropic Scattering*, Computing Technology Center, Union Carbide Nuclear Division, K-1693 (1967).

44. F. R. Mynatt, *A User's Manual for DOT, A Two-Dimensional Discrete Ordinates Transport Code with Anisotropic Scattering*, informal notes included in Computer Code Collection CCC-89 of Radiation Shielding Information Center, Oak Ridge National Laboratory.

45. S. A. Dupree, H. A. Sandmeier, G. E. Hansen, W. W. Engle, Jr., and F. R. Mynatt, *Time-Dependent Neutron and Photon Transport Calculations Using the Method of Discrete Ordinates*, Los Alamos Scientific Laboratory, LA-4557; Oak Ridge National Laboratory, ORNL-4662 (1971).

46. D. C. Irving, R. M. Freestone, Jr., and F.B.K. Kam, *05R, A General-Purpose Monte Carlo Neutron Transport Code*, Oak Ridge National Laboratory, ORNL-3622 (1965).

47. S. K. Penny, D. K. Trubey, and M. B. Emmett, *OGRE, A Monte Carlo System for Gamma-Ray Transport Studies, Including an Example (OGRE-P1) for Laminated Slabs*, Oak Ridge National Laboratory, ORNL-3805 (1966).

48. B. Eisenman and F. R. Nakache, *UNC-SAM: A FORTRAN Monte Carlo System for the Evaluation of Neutron or Gamma-Ray Transport in Three-Dimensional Geometry*, United Nuclear Corporation, UNC-5093 (1964); E. S. Troubetzkoy, *UNC-SAM-2: A FORTRAN Monte Carlo Program Treating Time-Dependent Neutron and Photon Transport Through Matter*, UNC-5157 (1966); and E. S. Troubetzkoy, *Modification of UNC-SAM-2 to UNC-SAM-3*, Defense Atomic Support Agency, DASA-3338 (UNC-5157 Supplement) (1970).

49. E. A. Straker, P. N. Stevens, D. C. Irving, and V. R. Cain, *The MORSE Code -- A Multigroup Neutron and Gamma-Ray Monte Carlo Transport Code*, Oak Ridge National Laboratory, ORNL-4585 (1970).

50. M. B. Emmett, C. E. Burgart, and T. J. Hoffman, *DOMINO, A General Purpose Code for Coupling Discrete Ordinates and Monte Carlo Radiation Transport Calculations*, Oak Ridge National Laboratory, ORNL-4853 (1973).

51. Duaine Lindstrom, *Technical Report and User's Manual [of] DASH -- FORTRAN IV Void Tracing and S_n-Monte Carlo Bridging Code*, Aerojet General, SRT-TRM01-W393-4C (1970).

52. See, for example, *A Review of Calculations of Radiation Transport in Air -- Theory, Techniques, and Computer Codes (Proceedings of a Seminar, November 15-17, 1971)*, Compiled by D. K. Trubey and H. E. Comolander, Oak Ridge National Laboratory, ORNL-RSIC-13 (1972).

53. B. J. McGregor and E. A. Straker, *A Study of the Effects of Source Asymmetry on Time-Dependent Neutron and Secondary Gamma-Ray Transport in Air*, Oak Ridge National Laboratory, ORNL-4741 (1972).

54. P. N. Stevens and H. C. Claiborne, "Basic Concepts of Radiation Shielding Analysis," Chapter 2 of *Weapons Radiation Shielding Handbook*, L. S. Abbott, H. C. Claiborne, and C. E. Clifford, Editors, Defense Nuclear Agency, DASA-1892-5 (1970).

55. L. V. Spencer and U. Fano, *Phys. Rev.* 81, 464 (1950).

56. L. V. Spencer and U. Fano, *J. Res. Natl. Bur. Std.* 46, 446 (1951).

57. H. Goldstein and J. E. Wilkins, *Calculations of the Penetration of Gamma Rays, Final Report*, Nuclear Development Associates, Inc., NYO-3075 (1954).

58. L. M. Contreras, B. W. Mar, and R. P. Moshofsky, *A Study of Radiation Phenomena from Nuclear Weapons at Close-In Distances*, Air Force Special Weapons Center, Kirtland Air Force Base, AFSWC-TDR-620-130, Vols. I and II (1963) (SRD).

59. Francis H. Clark, "Gamma-Ray Buildup Factors for Sand, Air, and Wood (Cellulose)," *Nuclear Applications* 6, 588 (1969).

60. M. B. Wells, *Radiation Resistant Combat Vehicle Investigation -- Final Report. Vol. II: Transport of Initial Radiation from Nuclear Weapons*, General Dynamics/Fort Worth, FZK-134-2 (1961) (SRD).

61. J. D. Marshall and M. B. Wells, *The Effect of Cutoff Energy on Monte Carlo Calculated Gamma-Ray Dose Rates in Air*, Radiation Research Laboratory, RRA-M67 (1966).

62. G. Butler, Jr., L. M. Contreras, and R. P. Moshofsky, *Procedures for Calculating Nuclear Radiation Dose and Dose Rates from Nuclear Weapons Detonated in the Lower Atmosphere*, Kirtland Air Force Base, AFSWC-TDR-61-106, Vols. I and II (1961) (SRD).

63. W. E. Selph and M. B. Wells, "Methods for Predicting Radiation Fields Produced by Nuclear Weapons," Chapter 6 of *Weapons Radiation Shielding Handbook*, edited by L. S. Abbott, H. C. Claiborne, and C. E. Clifford, Defense Nuclear Agency, DASA-1892-4 (1969) (SRD).

64. See, for example, Nancy N. Gibson and John H. McNeilly, Volume 3 of *Sourcebook for Free-Field Nuclear-Environment Data. The Free-Field Neutron and Gamma-Ray Environment*, BRL-R-1494, Vol. 3 (AD-514231L) (RRD-23-72) (February 1971) (SRD).

65. A. A. O'Dell, *Moments Method Calculation of the Scattered Angular Energy Flux for Point Isotropic Gamma Sources in an Infinite Homogeneous Air Medium*, EG & G, Inc., Santa Barbara Division, UC-34 (EFF 1183-2285) (1971).

66. H. C. Claiborne and W. W. Engle, Jr., "Bracketing the Peak Primary Gamma-Ray Dose from Nuclear Devices by Steady-State Transport Calculations," *Nucl. Tech.* 13, 209 (1972).

67. E. A. Straker, "Neutron Spectrum from Point Fission and 14-MeV Sources in Infinite Air," Problem 3.0 in *Shielding Benchmark Problems*, Oak Ridge National Laboratory, ORNL-RSIC-25 (ANS-SD-9) (1969).

68. E. A. Straker, *Status of Neutron Transport in the Atmosphere*, Oak Ridge National Laboratory, ORNL-TM-3065 (1970).

69. E. A. Straker, *Time-Dependent Neutron and Secondary Gamma-Ray Transport in an Air-Over-Ground Geometry. Vol. II. Tabulated Data*, Oak Ridge National Laboratory, ORNL-4289 (1968).

70. E. A. Straker and M. L. Gritzner, *Neutron and Secondary Gamma-Ray Transport in Infinite Homogeneous Air*, Oak Ridge National Laboratory, ORNL-4464 (1969).

71. E. A. Straker, "The Effect of the Ground on the Steady-State and Time-Dependent Transport of Neutrons and Secondary Gamma Rays in the Atmosphere," *Nucl. Sci. Eng.* 46, 334 (1971); reprinted at Oak Ridge National Laboratory as ORNL-TM-3754 (1972).

72. L. G. Mooney and M. B. Wells, *The Shielding Effectiveness of Single Compartment Concrete Underground Structures Against Neutrons from Nuclear Weapons*, Radiation Research Associates, RRA-T64 (1967) (SRD).

73. R. H. Ritchie and V. E. Anderson, *Some Monte Carlo Results on the Penetration of Neutrons from Weapons in an Air-Over-Ground Geometry*, Oak Ridge National Laboratory, ORNL-3116 (1962) (SRD).

74. R. J. Harris, Jr., J. A. Lonergan, and L. Huszar, "Models of Radiation Transport in Air -- The ATR Code," paper 23 (p. 451) in ref. 51 (ORNL-RSIC-13) (1972).

75. L. G. Mooney and R. L. French, *Improved Models for Predicting Nuclear Weapon Initial Radiation Environments*, Radiation Research Associates, DASA-2615 (RRA-T93) (Dec. 31, 1969) (SRD).

76. R. L. French, "A First-Last Collision Model of the Air/Ground Interface Effects on Fast-Neutron Distributions," *Nucl. Sci. Eng.* 19, 151 (1964).

77. R. L. French and L. G. Mooney, "Prediction of Nuclear Weapon Neutron-Radiation Environments," *Nucl. Tech.* 10, 348 (1971).

78. J. A. Auxier, Z. G. Burson, R. L. French, F. F. Haywood, L. G. Mooney, and E. A. Straker, *Nuclear Weapons Free-Field Environment Recommended for Initial Radiation Shielding Calculations*, Oak Ridge National Laboratory, ORNL-TM-3396 (1972).

79. E. A. Straker, *Investigation of the Adequacy of Nitrogen Cross-Section Sets: Comparison of Neutron and Gamma-Ray Transport Calculations with Integral Experiments*, Oak Ridge National Laboratory, ORNL-TM-3768 (1972).

80. W. W. Engle, Jr., and F. R. Mynatt, *Time-Dependent Neutron and Secondary Gamma-Ray Transport in Infinite Homogeneous Air -- Comparison of Two Cross-Section Sets*, Oak Ridge National Laboratory, ORNL-TM-3932 (1972).

81. The Evaluated Nuclear Data File is maintained by the National Neutron Cross Section Center at Brookhaven National Laboratory, Upton, N.Y.

82. P. G. Young and D. G. Foster, Jr., *An Evaluation of the Neutron and Secondary Gamma-Ray Production Cross Sections for Nitrogen*, Los Alamos Scientific Laboratory, LA-4725 (to be published); *An Evaluation of the Neutron and Secondary Gamma-Ray Production Cross Sections for Oxygen*, LA-4780 (to be published).

83. L. G. Mooney, M. B. Wells, and H. C. Claiborne, "Engineering Method for Designing Initial Radiation Shields for Blast-Hardened Underground Structures," Chapter 7 of *Weapons Radiation Shielding Handbook*, L. S. Abbott, H. C. Claiborne, and C. E. Clifford, Editors, Defense Nuclear Agency, DASA-1892-6 (1970) (SRD).

84. A. D. Anderson, "A Theory for Close-In Fallout from Land-Surface Bursts," *J. Meteorol.* 18, 431 (1961).

85. E. W. York et al., *A Computational Model to Determine Nuclear Radiation Environment from Prompt Weapon and Fission Product Gammas and Fast Neutrons*, Air Force Weapons Laboratory WL TDR-64-85, Vol. I (1964) (SRD).

86. W. E. Loewe, J. W. Mandler, T. G. Stinchcomb, and W. E. Zagotta, *Study of Initial Gamma Dose and Dose Rate Measurements*, U.S. Army Nuclear Defense Laboratory, NDL-TR-75 (IITRI-A6082-19) (1966) (SRD).

87. L. G. Mooney and R. L. French, "A New Look at the Fission-Product Gamma-Ray Component of Nuclear Weapon Initial Radiation," paper 13 (p. 251) in ref. 51 (ORNL-RSIC-33) (1972).

88. F. F. Haywood, "Spatial Dose Distribution in Air-Over-Ground Geometry," *Health Phys.* 11, 185 (1965).

89. P. I. Richards, *Prompt Doses and Dose Rates from Nuclear Weapons*, Air Force Special Weapons Center, AFSWD-TR-58-13 (1958) (SRD).

90. J. D. Marshall and M. B. Wells, *Simplified Method for Calculating Nitrogen-Capture and Fission-Product Gamma-Ray Doses Inside Underground Concrete Structures*, Radiation Research Associates, Inc., RRA-M71A (June 11, 1967; revised April 21, 1969).

91. R. E. Maerker, Oak Ridge National Laboratory, unpublished calculations privately communicated to L. G. Mooney and M. B. Wells, Radiation Research Associates, Inc.

92. L. G. Mooney and M. B. Wells, *Effects of Neutron Energy Spectrum in Air on the Neutron-Induced Dose in Concrete Underground Structures*, Radiation Research Associates, Inc., RRA-M65 (1966).

93. R. H. Karcher and J. H. Wilson, *Structural and Shielding Considerations in the Design of Hardened Facilities*, Holmes and Narver, Inc., HN-183 (June 30, 1965).

94. These methods, mentioned briefly in the introduction to Section 6.6, are described in ref. 25.

95. E. A. Straker, J. V. Pace, III, F. R. Mynatt, M. B. Emmett, W. W. Engle, Jr., L. R. Williams, and L. S. Abbott, *Penetration into a Missile Silo of Neutrons and Secondary Gamma Rays Produced by Point Isotropic Neutron Sources*, Oak Ridge National Laboratory, ORNL-TM-3599 (Dec. 20, 1971) (SRD).

96. Developed by J. Ching, E. M. Oblow, and H. Goldstein, and described in ORNL-TM-4235, *Application of Discrete-Energy Technique to Discrete-Ordinates S_n Method for Studying Neutron Transport in Iron* (to be published).

97. F. R. Mynatt, T. J. Hoffman, J. V. Pace, III, C. E. Burgart, and L. S. Abbott, *Calculations of the Penetration of Nuclear Weapons Radiation into a Missile Silo*, Oak Ridge National Laboratory, ORNL-TM-4021 (1973).

98. L. G. Mooney and M. B. Wells, "Engineering Method for Designing Initial Radiation Shields for Aboveground Structures," Chapter 8 of *Weapons Radiation Shielding Handbook*, Defense Nuclear Agency, to be issued as one of the DNA-1892 series (SRD).

99. L. G. Mooney, *Calculations of Weapons Radiation Doses in Single-Compartment Above-Ground Concrete Structures*, Radiation Research Associates, Inc., RRA-M93 (November 26, 1969).

100. R. E. Maerker, "Semiempirical Equations for Neutron-Induced Doses within Rectangular Concrete Ducts," in *Neutron Phys. Div. Ann. Prog. Rep. May 31, 1968*, ORNL-4280, p. 83.

101. C. M. Huddleston and W. C. Ingold, *A Revised Formula for the Calculation of Gamma-Ray Shielding Properties of Shelter Entranceways*, (DASA 11.058) Technical Note N-843, U.S. Naval Civil Engineering Laboratory (October 1966).

102. E. A. Straker, *Calculations of the Transport of Neutrons from Fission and 14-MeV Point Sources in an Infinite Medium of Air*, Oak Ridge National Laboratory, ORNL-TM-1547 (1966).

103. H. C. Honeck, "ENDF -- Evaluated Nuclear Data File Description and Specifications," Brookhaven National Laboratory, BNL-8381 (1964).

104. H. C. Honeck, "ENDF/B -- Specifications for an Evaluated Nuclear Data File for Reactor Applications," Brookhaven National Laboratory, BNL-50066 (1966, rev. 1967).

105. M. K. Drake, Editor, "Data Formats and Procedures for the ENDF Neutron Cross Section Library," Brookhaven National Laboratory, BNL-50274 (T-601) (1970).

106. R. W. Roussin, "Defense Nuclear Agency Working Cross Section Library: Description and Contents," Oak Ridge National Laboratory, RSIC-34 (1972).

107. Private communication to L. S. Abbott.